2014

Mechanism for compaction and densification of large stover modules

Ann Klein
Iowa State University

Mechanism for compaction and densification of large stover modules

by

Ann Klein

A thesis submitted to the graduate faculty

in partial fulfillment of the requirements for the degree of

MASTER OF SCIENCE

Major: Agricultural and Biosystems Engineering

Program of Study Committee:
Stuart Birrell, Major Professor
Brian Steward
Steven Hoff

Iowa State University

Ames, Iowa

2014

TABLE OF CONTENTS

LIST OF FIGURES

LIST OF TABLES

ACKNOWLEDGEMENT

I would like to start by expressing my sincere thanks to Dr. Stuart Birrell, first of all for giving me the opportunity to continue my studies. Also, his guidance and knowledge throughout the duration of this project have served as a great asset and helped prepare me for my future not only as an engineer but in my personal life as well. I appreciate his encouragement and patience, especially during the long hours and stressful times.

I would also like to thank my committee members, Dr. Brian Steward and Dr. Steven Hoff, for supporting me with their guidance and expertise throughout the project. They served as great mentors not only during this research, but also in the classroom.

Thank you to John Deere, for providing not only the funding to complete this project, but all of the assistance along the way. More specifically, I would like to thank Kevin Ehrecke and Aaron Bruns for providing me with very useful resources and feedback.

This project could not have been completed without the help of many of my colleagues. Thank you to Luke Hodnefield, Brian McEvoy, Kevin Muell, and the numerous undergraduate students who all spent many hours helping me with fabrication and testing. I'd also like to thank the employees of the Agricultural Engineering and Agronomy Farm for all of their assistance.

Lastly, I would like to thank my family and friends. Their unwavering encouragement and patience with me during this time has been invaluable. Thank you to my fiancé, Nick Jaques, for your love and understanding. Also to Amy and Shane Wright, for your support and advice. Finally, to my parents, Stan and Sandra Klein, thank you for all of your help always and instilling in me the drive to complete this project.

ABSTRACT

With a growing push towards independence from foreign oil, research has turned to alternative feedstocks for biofuels. One of these feedstocks is corn stover, which is mostly a by-product of corn grain production. Studies show that a main issue with the corn stover supply chain for biofuels is the logistical and handling costs. Currently, transporting large square bales of stover by truck is the most common system. A main factor in the handling and transportation cost is the density and size of the package of corn stover. Research has shown that creating a larger package considerably reduces these costs.

A machine was proposed to compact and, if possible, package the material in an anaerobic state to prevent deterioration. The machine produced a module approximately 2.4 m by 2.4 m and could have variable length. Three horizontal plungers slid forward and backward inside the compression chamber to compact the stover. At the rear of the chamber, a two-paired door system provided back and sidewall pressure to densify the module. A pressure distribution model created for the compaction chamber predicted that angling these doors results in nearly zero back pressure at the rear of the chamber.

Structural, hydraulic, electrical, and control systems were included in development and fabrication of a working prototype large module builder. This prototype was tested for achievable density and pressure distribution inside the compaction chamber. Compaction capabilities were comparable to other commonly used methods, with an average density of 151 kg/m^3 when the doors were held at an angle, which was 25% greater than the density with the doors fully open. In addition, the predictions for pressure within the compaction chamber nearly followed a one-to-one relationship with calculated pressures from test data. A regression line for the data produced a slope of 1.12 and an R-squared of 0.82.

CHAPTER 1: INTRODUCTION

Due to the growing demand for fuel as well as the rising costs of those fuels, the United States Department of Energy has developed a number of goals to achieve independence from foreign oil. The Energy Independence and Security Act of 2007, Renewable Fuels Standard mandates that by the year 2022, 136 billion liters of biofuels will be blended into traditional fuels (U.S. Environmental Protection Agency, 2007). With this increased demand for biofuels, researchers have turned to renewable feedstocks in order to provide options for these fuel sources.

Biofuels are manufactured from biomass substances, or living organisms. Currently, the dominant feedstock used for biofuel production is corn-based ethanol, with over 47 billion liters of ethanol produced per year (U.S. Department of Energy, 2013). However, the use of corn to produce liquid fuels has been criticized since the production of corn-based ethanol fuel competes with food production. Therefore, there is a need to develop other non-food feedstock sources for processing in order to obtain fuels. In particular, a number of cellulosic feedstocks including forest biomass and wood from logging residues; agricultural residues from corn, wheat, sugarcane, and sorghum production; and various types dedicated energy crops such as miscanthus, energy canes, and annual and perennial grasses, are being studied for their biofuel production capabilities (U.S. Billion Ton Update, 2011). However, corn stover will be an important cellulosic feedstock. Currently, it is the most viable and immediate cellulosic feedstock option as it is readily available and is a co-product of high value grain production.

1.1 Overview of Corn Stover and Biofuels

Corn stover consists of all plant residues, including the stalks, leaves and cobs left in the field after harvest of the grain, and is mostly a by-product of corn grain production. Corn stover is a biomass used for ethanol production, and has few competing uses, with the exception of relatively small use in animal feedstocks. With corn production relatively constant each year, the supply of corn stover is also constant. The Billion-Ton Study (2005), evaluates the possibility of replacing 30% of U.S. petroleum consumption with biofuels by the year 2030. This study proposes meeting this goal by producing at least one billion dry tons of sustainable biomass each year. An update to this study was published in 2011 with additional research included for costs and sustainability. In this study, corn stover is shown as the fastest growing potential biofuel source in the next eighteen years, with the possibility for 149 million dry metric tons per year by 2030 (U.S. Billion ton Update, 2011).

Iowa has a strong history in the biofuel market, as the leading producer of ethanol. Iowa is the leading corn producer in the US. Therefore, it has the largest amount of corn stover available and is expected to produce up to 24% of the nation's available corn stover (Tyndall et. al., 2011). Other Midwestern states of Minnesota, Illinois, Nebraska, and Indiana represent the remaining top corn production states. Overall, these five states make up over 60% of the nation's stover harvest (Graham et. al., 2007). This evidence reinforces the idea that the growth potential for corn stover harvesting is very large, also making the Midwest a prime candidate for biomass collection and densification applications. In addition, there are possibilities for corn stover harvesting and packaging equipment to be used on other biomass crops as well, further expanding the reach of this project.

CHAPTER 2: REVIEW OF LITERATURE

2.1 Current Methods for Harvesting and Densification of Corn Stover

Presently, corn stover can be harvested in multi-pass harvest operations or in a single-pass harvest operation. In multi-pass stover harvest operations, grain is harvested, and the stover is left in the field. In multiple operations after grain harvest, the stover is chopped, windrowed, and then baled. However, the multi-pass operations significantly increase contamination of the stover material with soil and other debris that is picked up and packaged with the stover. The contamination can causing major issue during processing at bio-refineries. Alternatively, some methods utilize a single pass system that takes in both grain and stover during the corn harvesting process and divides them into two separate output streams (Shinners et al., 2007). In addition, it is important that corn stover is harvested in a sustainable manner that protects soils and the environment. Therefore, a number of studies have been conducted on the maximum amount of stover that can be collected versus material left in the field to protect soil and water resources (Karlen et al., 2011; Huggins et al., 2011).

After harvest, the focus turns to storage of the stover. To ensure a sustainable feedstock supply chain, and convince producers to harvest stover, the costs within the system must be minimized. The density of the stover material is the most significant factor in optimizing the feedstock supply chain and reduce storage costs. Transporting and storage of loose bulk stover is both inefficient and costly. The bulk density of chopped corn stover can range anywhere from about 32-64 kg/m^3 for raw chopped stover, with bulk densities up to 128 kg/m^3 depending size of the stover particles and degree of grinding (Mani et al., 2004). This rather large range in density can be due to particle size, moisture content, or plant type

(Zhou et al., 2008). In order to combat this, many different efforts have been made to increase the density of the feedstock. The most common methods used are pelletizing and baling.

Pelletizing or cubing corn stover involves a process that starts with hauling the harvested stover out of the field and to a pre-processing facility where the densification is completed. There, the biomass is first ground, and then fed through a press system creating small cubes or pellets. With this process, very high densities of the stover can be reached, ranging from 961 to 1,121 kg/m^3 for a single pellet and nearly 7.5 kg/m^3 for bulk density (Sokhansanj & Turhollow, 2004). This is a very significant increase from the loose bulk density; however this process is very intensive with large, specialized equipment. In addition, pelletizing stover incurs more cost than baling stover, with estimates that place this method ten dollars more expensive than baling per dry ton of stover (Sokhansanj & Turhollow, 2004).

Overall, the most common form of biomass densification is baling. As stated before, it is common for a second pass operation to follow the corn harvest, where either square or round balers are used to collect and bale the stover windrow. Estimated ranges of bulk densities of bales are very wide. The low end of the range is about 80 kg/m^3, while some studies boast densities upwards of 240 kg/m^3, with an average overall somewhere in the 160 to 192 kg/m^3 range (Sokhnsanj et al., 2002; Prewitt et al., 2007; Lizotte & Savoie, 2011). This very wide range is dependent on many factors included in baling. Shinners et al., (2007) have shown that the moisture content of the stover when baled can significantly affect dry bulk density, with an average difference of 27.9 kg/m^3 between wet and dry bales.

Numerous different types of balers have been used from large and small square balers to round balers. In many cases, some aspects of the baler are modified in order to be robust enough to handle the tough corn stalks. One study outfitted a John Deere round baler with a shredding attachment to chop the material into more manageable pieces (Glassner et al., 1998). Another approach used utilizes the single-pass system of harvesting grain and corn stover simultaneously. With this approach, a baler is pulled directly behind the combine (Webster, 2011). If the corn is harvested at high moisture contents, the single-pass system can result in high moisture content bales, but also eliminates the need for multiple passes though the field, making the process more efficient.

2.2 Logistical Concerns and Models

The success of the harvesting corn stover as a biomass hinges on a cost-effective and efficient solution to storing and transporting the stover. In order for producers to become comfortable with the idea of harvesting corn stover, they must have a profitable outcome including all harvest, packaging, transportation, and any other costs. Many studies have been conducted on the feasibility of collecting and transporting corn stover. The logistic models used focus directly on the transportation of the stover from the field to the bio-refinery.

Corn stover is generally harvested between late summer and fall, so the window for collecting the crop is approximately 60 calendar days for Iowa (National Agricultural Statistics Service, 2013). Refineries, however, need a constant supply of stover all year round. Therefore the distribution and size of the biomass storage locations must be considered. In general, most systems include local storage sites within approximately two to nine miles of a field site, with the bio-refineries placed anywhere from about 32 to 97

kilometers away from any given local storage area (Morey et al., 2010). This distance is dependent on the size of the refinery and the geographic location. During storage, the material must be protected to prevent excessive dry matter loss and prevent deterioration in the quality of the material.

A variety of transportation methods have been analyzed for moving corn stover from the local storage locations to the refinery itself. Many of these systems are optimized for the densification method used during harvest. For example, common solutions to baling or pelletizing operations include hauling by over-the-road trucks or by rail cars. An option of using slurry to transport bulk stover through pipelines is set forth by Suh et al (2011).

Most of the discussion comes not from finding a new way to transport the material, but which is the most economical and environmentally friendly option. A Minnesota study by Suh et al., (2011) claimed that the lowest cost option for transporting the stover is a pipeline system, and the highest cost system is transportation by rail. However, pipeline systems were found to generate the most carbon dioxide emissions while the rail system generated the least carbon dioxide emissions. Truck transportation fell in the middle of the spectrum. A possible issue with pipeline systems is the fact that they have a very large initial cost to set up the line and the entire infrastructure related to it. In addition, pipeline systems can be difficult to adjust for changing conditions once they are created. Provisions for truck or rail systems are already in place in almost all areas where bio-refineries would be located, making them more available and immediate options.

In general, transportation of stover bales is the most common logistical method, and in some cases, further pre-processing such as pelletization occurs to increase density. The best economic option is dependent on the size of the bio-refinery. Suh and Suh (2010)

present that transportation of pellets by truck, as compared to standard bales (340 kg), can decrease logistical costs for refineries producing 276 million liters per year or more. However, they also simulated the logistical cost model for a larger bale size of 540 kilograms, and found that regardless of the size of the refinery, the large bale transportation option resulted in the least cost, by at least five dollars per dry ton (Suh & Suh, 2010). Sultana and Kumar, (2011) have found baling to be the least expensive option to deliver the stover, due to the higher fixed cost of the production of pellets. Other studies found the total delivery cost of bales to be between about 40 and 50 dollars per dry ton, depending on the size of the bio-refinery (Perlack & Turhollow, 2002). Overall, pelletizing incurs higher equipment costs that would be difficult for individual farmers to employ. With all of this data, the most feasible option in the short term is to produce bales of stover and transport them to the refineries by trucking systems. Even in the long term, this option allows for improvements to the logistic system. In addition, as technology increases, and the densification of the matter becomes more effective, the bale option becomes even more valuable.

2.3 Large Module Type Systems

Recently, some research has been conducted on the use of larger module type packages for collection and transportation of biomass. This research utilizes a modified cotton module builder to create a module of sorghum about 2.4 m by 2.4 m and about 5.5 m long (Searcy, et al., 2014). In order to package these modules, a plastic bag is designed to fit inside the cotton module builder and the material is packed into the machine. The cotton module builder is then pulled off, and a top plastic cover is manually placed on in an attempt

to seal the module from air. In addition to the machine system, a logistical cost model is created that takes into account formation, field and road transportation, and unload operations. With all of these factors, the simulated module system results in approximately 30% lower logistics cost as compared to conventional baling (Searcy, et al., 2014). Issues with creating this form of module include the fact that a specialized plastic bag must be made for the modified cotton module builder, and the top of the bag must be sealed manually. Also, the poor sealing on the bags allowed for degradation of the biomass (Searcy, et al., 2014).

The previous studies suggest large module-type systems for harvesting and densification of corn stover could significantly reduce feedstock supply costs. The cost incentives can be further exploited by the possibility of densification, packaging, and sealing in a single machine without manual effort.

2.4 Densification Models for Corn Stover

The previous studies show that large, dense bales and/or modules have the potential to be the most cost effective and attainable transportation method for corn stover. Therefore, the properties of stover as well as the densification behavior of materials must be understood in more detail.

2.4.1 Densification Models for Pressure and Volume Change

When examining densification equations, most of the data refers to the compaction of powders or ground matter. Some common models found for these compaction characteristics include those derived by Heckel (1961), Walker (1923), Cooper and Eaton (1962), and

Kawakita and Ludde (1971). These models have been applied to biomass materials such as straw, switchgrass, and corn stover (Mani et al., 2004; Chevanan et al., 2010).

In trying to explain compaction behaviors of many different types of biomass, many researchers turn to the compression equations for powder set forth by Kawakita and Ludde (1969). These equations relate the volume reduction in the powder to the pressure applied.

$$C = \frac{V_0 - V}{V_0} \qquad \text{Equation 2.1}$$

$$\frac{P}{C} = \frac{1}{ab} + \frac{P}{a} \qquad \text{Equation 2.2}$$

In these equations, C represents the degree of volume reduction, V_0 is the initial volume, and V represents the volume under the applied pressure, P. The other two factors, a and 1/b, are constants which are derived from characteristics of each specific powder.

More recently, Chevanan et al., (2010) relates the Kawakita-Ludde compression equations to larger particles. The larger particles used are knife mill chopped switchgrass, wheat straw, and corn stover. The study contains data from four different particle sizes approximately 3, 5, 9, and 13 mm. The bulk density of each particle size is measured. Then, the values for the factors of a and 1/b constants are found experimentally using a tapping procedure and measuring the change in volume. These values for bulk density, a, and 1/b for corn stover allow a model of change in volume based on applied pressure for a given particle size to be constructed.

2.4.2 Pressure Distribution Model for Inside Module Chamber

In order to understand the magnitude of the forces required to compress corn stover, information must also be found on the effect of the compression on the sidewalls as well as at

the back of the module. Many models exist for explaining these pressures, however one of the most useful pressure models, the equation developed by Afzalinia & Roberge (2008). The study focuses on building an analytical model for the pressure distribution throughout the bale chamber of a large square baler. The materials used in this study include wheat and barley straw, for a the large square baler with an approximately 0.9 m by 1.2 m and 5.5 m long bale chamber.

Factors in the model include material properties of modulus of elasticity and Poisson's ratio. The geometry of the chamber consists of a top angled down wall and two angled side walls as shown to the right.

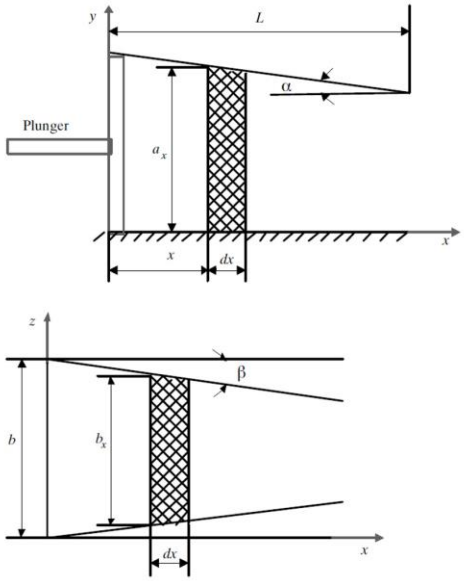

Figure 2.1: Side view (upper) and top view (lower) of the compression chamber

The model is derived to produce two equations, one for back pressure on the module, P_x, and two for sidewall pressure, P_y and P_z. In the following equations, the lowercase a and b represent dimensional values as seen in the figure. The distance along the module chamber in the x-direction is shown as x, and the α and β are the angles of the top and side doors respectively.

$$P_x = P_p e^{-Ax} + \frac{B}{A^2}(1 - Ax - e^{-Ax}) \qquad \textbf{Equation 2.3}$$

$$P_y = \frac{\nu}{1-\nu}\left[P_p e^{-Ax} + \frac{B}{A^2}(1 - Ax - e^{-Ax})\right] + E\left[\frac{b\alpha + 2a\nu\beta}{ab(1-\nu^2)}\right]x \qquad \textbf{Equation 2.4}$$

$$P_z = \frac{\nu}{1-\nu}\left[P_p e^{-Ax} + \frac{B}{A^2}(1 - Ax - e^{-Ax})\right] + E\left[\frac{2a\beta + b\nu\alpha}{ab(1-\nu^2)}\right]x \quad \text{Equation 2.5}$$

The uppercase letters A and B are constants derived from the model and include material and chamber properties. Poisson's ratio and the coefficient of friction are represented by ν and μ respectively.

$$A = \frac{\nu}{1-\nu}\left[\frac{\alpha + 2\mu}{a_m} + \frac{2(\mu+\beta)}{b_m}\right] \quad \text{Equation 2.6}$$

$$B = E\{[b_m(\alpha + 2\mu)(\alpha b + 2\beta\nu a + 2a_m(\beta + \mu)(\alpha\nu b + 2\beta a)] \div [aba_m b_m(1-\nu^2)]\} \quad \text{Equation 2.7}$$

Where:

$$a_x \approx a_m = a - \alpha\left(\frac{L}{2}\right) \quad \text{Equation 2.8}$$

$$b_x \approx b_m = b - 2\beta\left(\frac{L}{2}\right) \quad \text{Equation 2.9}$$

The results of the analytical model when compared to experimental data prove to be about 97.5% accurate in the x-direction (Afzalinia & Roberge, 2008). For the y and z-directions, the analytical model seems to overestimate the sidewall pressures at small distances, but correlates with the model more closely at larger distances, roughly 1.5 m or more (Afzalinia & Roberge, 2008). The amount the model appears to overestimate is approximately four times the measured experimental pressure in both the y and z-directions, however this overestimate appears to be somewhat consistent over the range of distances.

These results provide equations that are suitable for estimating pressures in a large square module chamber. This model may also predict the pressure distribution in a larger

chamber, like that of the large module builder proposed here, and provides a basis for governing calculations for the design of the machine.

CHAPTER 3: OBJECTIVES

The goal of this research was to design and fabricate a machine to compact and package corn stover or other biomass in a single step, utilizing a large module approach. The eventual goal of large modules reduces logistical and handling costs in the feedstock supply chain. In order to accomplish this goal, two main objectives were set forth as follows:

- Objective #1: Determine the achievable density of a large square corn stover module which is the size of approximately four large square bales. Tasks supporting this objective include:
    - Design and build a machine to produce a large square module of corn stover.
    - Test the machine to determine achievable density capabilities and corresponding system pressures
    - Compare the densities to current square baling methods
    - Compare the system pressures to the model created from the Afzalinia & Roberge Pressure Distribution Model
- Objective #2: Address the issue of compacting and protecting the module in a single step. Tasks supporting this objective include:
    - Explore options of traditional bale wrap and twine, as well as alternative methods
    - Derive a complete machine system to be used in conjunction with the single-pass harvesting system for corn

- Develop a system that can produce a comparatively dense large module of corn stover and also package the module without having to handle it more than once.

The long term focus of this research was to create opportunities to improve logistics and feedstock supply chain costs by moving to larger square modules.

CHAPTER 4: INITIAL LARGE MODULE BUILDER DEVELOPMENT

In order to take the advantages of the large module cost models set forth above by Searcy et al, (2014) some issues need to be addressed. It requires the design of machines capable of compacting corn stover or other biomass to a desirable density at least comparable to conventional baling methods, and if possible packages the material in an anaerobic state to prevent deterioration of higher moisture stover materials. The present machine under development will be used to study the implications of making such a large module in one solid form. Currently, little is known about how the biomass will hold together, if it will compact uniformly, or how the biological parameters of the material affect the densification process.

After densification, the machine must be able to package the stover in such a way that is feasible to both store and transport the stover, without significant loss. Aspects to consider include whether or not the packaging material is readily available, easy to use, and acceptable for bio-refineries. If the package can be sealed tightly enough for anaerobic storage, the quality and stability of the biomass can be greatly improved during extended storage of the material.

The goals of this research include designing and fabricating the machine in order to eventually test and address these issues. Development of the machine encompassed the design methods and supporting calculations for the various machine systems, including the structural integrity, hydraulic capacity, controls, and overall flow of the material through the machine. Finally, some initial testing was completed to determine achievable density of the

material, as well as validate the pressure models that have been scaled up to a module of this size.

The first stage of the design process involved high-level decisions about sizing and materials to use. Conventional large square balers use a flywheel system for stover compaction; however a module of this larger size was not conducive to this method. Therefore, for an easily fabricated test machine, hydraulic plungers were used for the main compaction process, with the hydraulic system driven from the Power-Take-Off (PTO) shaft of a tractor. For the packaging of the module, a silage bag was chosen to encase the compacted stover. Some benefits of a silage bag include its ability to fit around a square module and resistance to tearing or puncture. In addition, the silage bag created only two places for sealing (one on each end of the module). If a roll type wrap is used, multiple layers of wrap would be required, and sealing the ends of the package could be more of a challenge. Finally, silage bags were readily available and come in many different sizes.

4.1 Initial Sizing and Harvest Capabilities

To begin the design process some general information was determined. First of all, the capacity of the machine and size of module were major design constraints. Other factors considered included in-field use of the module builder with single-pass harvest systems, and transportation by over-the-road trucks. The following assumptions were made:

Table 4.1: Assumptions for harvest capabilities to size large module builder prototype

Parameter	Value	Unit
Harvest speed	8	kph
Combine corn head capacity	12	rows
Corn row spacing	76	cm
Material pickup rate from combine	2.7	metric tons/acre
Mass flow rate from combine	49.4	metric ton/hr
Bulk density of loose stover	48	kg/m^3
Desired compacted module density	160	kg/m^3
Semi-trailer width	2.4	m
Semi-trailer length	16	m

The assumptions for the harvest speed and material pickup rate were chosen to be on the high side of the range of values commonly used for single-pass harvest systems. A target density of 160 kg/m^3 was desired. Since trucking is the most common and feasible method of transport, semi-trailers were chosen for the sizing calculations as well. With these parameters, the height and width of a finished module were chosen to be 2.4 m by 2.4 m. This would easily fit on top of a flatbed trailer without needing an oversized load permit. Table 4.2 shows the relationship of possible module lengths to trailer space. Assuming 16 m trailer length from above, three different module lengths were proposed.

Table 4.2: Module size optimization for different tractor trailer lengths

	Full Module Length		
	2.4 m	3.0 m	3.7 m
Integer # modules/trailer	6	5	4
Wasted trailer length (m)	1.6	1.0	1.2

With this information, the best module size for fully utilizing the trailer would be three meter long modules. The one meter of wasted trailer length would be most likely filled by the extra length created from whichever sealing method is used. Other than trailer size, waste can also come from the stock lengths of the silage bags used to package the material.

If the module is 2.4 m tall and 2.4 m wide, it can be assumed that each end of the module will need another 1.2 m of silage bag to completely cover the ends of the module. An additional two foot allowance was added for sealing. If a 3 m long module is chosen, the full length of silage bag needed for that module would be 6 m. The following table shows how this length of module also minimizes the waste of the silage bag as well.

Table 4.3: Module size optimization for different silage bag stock lengths

	Common Silage Bag Length (m)				
	45.7	**61.0**	**76.2**	**91.4**	**106.7**
Integer # modules/bag	7	10	12	15	17
Wasted silage bag length (m)	3	0	3	0	3

A ten foot diameter silage bag was chosen as the perimeter is 9.58 m. With an eight-by-eight module, the perimeter of the finished module would be 9.75 m. If the compaction chamber is made slightly smaller than this finished size, this would allow for some stretch in the silage bag. Also, this is the closest available silage bag size to the necessary module dimensions.

With the module size determined, the harvest rate parameters were used to calculate the volume pickup rate of stover under these conditions using the following equation.

$$\frac{2.7\frac{metric\ tons}{acre} * \frac{1000\ kg}{metric\ ton}}{48\frac{kg}{m^3}} = 56\frac{m^3}{acre} \qquad \textbf{Equation 4.1}$$

At a speed of 8 kph, using a twelve row head (width of 9.1 m), the harvest rate of the combine was calculated.

$$8\frac{km}{hr} * 9.1\ m * \frac{acre}{4046.9\ m^3} = 18.18\frac{acres}{hr} \qquad \textbf{Equation 4.2}$$

At a pickup rate of 56 cubic meters per acre, the combine would be taking in 17 cubic meters of loose stover per minute. If the combine is travelling at 8 kph, the loose stover pickup rate can be found by using the following equation:

$$\frac{17\frac{m^3}{min} * \frac{60\ min}{hr}}{8\frac{km}{hr} * \frac{1000\ m}{km}} = 0.039\frac{m^3\ loose\ stover}{m\ travelled} \qquad \textbf{Equation 4.3}$$

With the mass constant before and after compaction, the change in volume is a ratio of the loose and compacted density. Volume and density are represented by "V" and "D," respectively, in the following equations.

$$\frac{V_{initial}}{V_{final}} = \frac{D_{final}}{D_{initial}} \qquad \textbf{Equation 4.4}$$

The final volume of the compacted 2.4x2.4x3 meter module would be equal to 18.1 cubic meters. Therefore, the volume needing to be picked up to complete one module is:

$$V_{initial} = \frac{160\frac{kg}{m^3}}{48\frac{kg}{m^3}} * 18.1\ m^3 = 60.4\ m^3 \qquad \textbf{Equation 4.5}$$

At the rate found in Equation 4.5, the travel distance to complete one full module would be 0.47 km.

$$Distance\ to\ complete\ one\ module$$

$$= 0.039 \frac{m^3\ loose\ stover}{m\ travelled} * 60.4\ m^3 \qquad \text{Equation 4.6}$$

$$= 472\ m = 0.472\ km$$

In order to make the most out of all aspects of this type of large module builder machine, it would be optimal for the machine to be able to place completed modules at the ends of the fields for quicker pickup. Some type of carrying system may need to be employed to be able to bring the finished module to the edge of the field while another module is starting to be formed. It should be noted that this distance would be greatly affected by the single-pass harvest system parameters, and therefore would be examined further in the future.

4.1.1 Determining Maximum Module Face Pressure

With the module size determined, another main design constraint was setting a maximum pressure to apply to the module face. In order to do this, the chopped biomass version of the Kawakita-Ludde model from Chevanan et al, (2010) was used to apply to the larger particle size commonly found in single pass harvesting. The experimental data set from the Chevanan et al (2010) study was used to compute the material property coefficients a and 1/b used in the Kawakita-Ludde model. Across all chopped particle sizes, the average values of a and 1/b were calculated for chopped corn stover and found to be 0.63 and 9.97 respectively. Next, the average loose bulk density was found for each particle size and then averaged over all particle sizes. The average bulk density of chopped corn stover was 54.3 kg/m^3 (Chevanan et al, 2010). From here, the volume terms of the model were translated to a density basis, where D_0 and D_p are the bulk loose and compressed densities, V_0 and V_p are

the initial and final volumes, respectively, for a constant mass m, contained within the module.

$$m = D_0 V_0 = D_p V_p \qquad \text{Equation 4.7}$$

Therefore, the equation for the change in volume, C, can be rewritten as:

$$C = \frac{V_0 - \frac{D_0 V_0}{D_p}}{V_0} = \frac{D_p - D_0}{D_p} \qquad \text{Equation 4.8}$$

The equation relating to pressure can be rearranged as follows:

$$C = \frac{Pa}{\left(\frac{1}{b} + P\right)} \qquad \text{Equation 4.9}$$

Now, inputting the equation for the volume change as a function of density:

$$\frac{D_p - D_0}{D_p} = \frac{Pa}{\left(\frac{1}{b} + P\right)} \qquad \text{Equation 4.10}$$

$$\frac{D_0}{D_p} = 1 - \frac{Pa}{\left(\frac{1}{b} + P\right)} \qquad \text{Equation 4.11}$$

Finally, solving for the final density provided an equation to predict the density of the module at any given pressure applied, utilizing the average values for D_0, a, and 1/b computed from the experimental data of Chevanan et al, (2010).

$$D_p = \frac{D_o\left(\frac{1}{b} + P\right)}{\frac{1}{b} + P(1 - a)}$$

The final density of the module was graphed against possible face pressures applied. The results are seen in Figure 4.1. As can be seen on the graph, the density quickly rises from the loose bulk density of was 54.3 kg/m^3 as the applied pressure increases. After

approximately 414 kPa applied pressure, the density of the module was not predicted to increase very rapidly. For this reason, 414 kPa was chosen as the maximum applied module face pressure to design all subsequent components to.

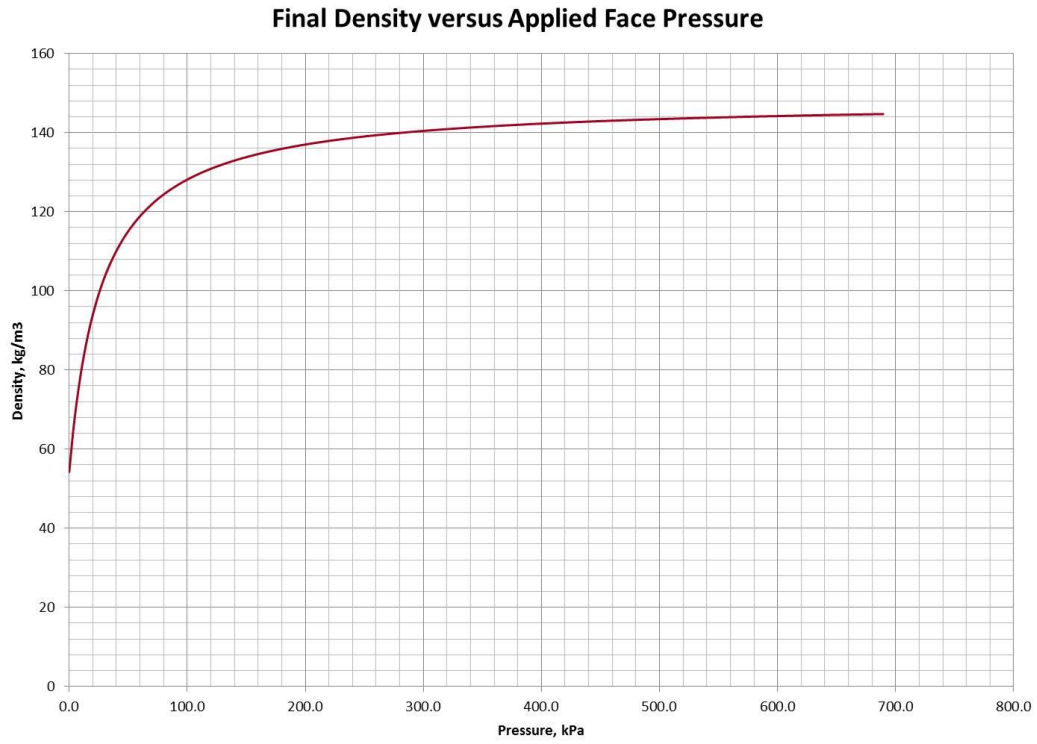

Figure 4.1: Graph of final module density prediction for a given applied module face pressure

At 414 kPa pressure, the full force on the compaction face of the module would be 250,818 kg. With this large of an overall force, and to make the system more manageable, the plunger to compact the stover was broken up into three equal parts, each producing a maximum force of 83,606 kg. The plunger sections were designed horizontally. There is a top, a middle, and a bottom plunger. Each plunger is approximately 2.4 m wide and 0.8 m tall.

4.3 Overall Machine Layout and Methods

Material flow through the machine must be continuous in order to keep the equipment moving quickly through the field. Also, the packaging and sealing portion must be able to be completed either very quickly or simultaneous to compaction. Beginning at the simplest case, the easiest way to bring material into the test machine was from the top with the use of a hopper and feed conveyors. For compacted material to easily be pushed through the compaction chamber the movement of the compaction cylinders was proposed to be horizontal.

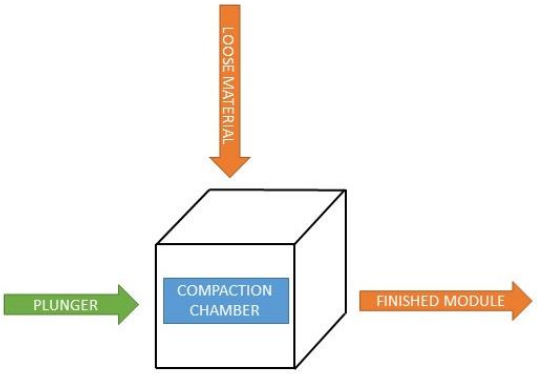

Figure 4.2: Initial compaction chamber design

4.3.1 Angled Door Design Concept

Utilizing the information from the reviewed literature for pressure at the back of the compaction chamber as well as the sidewalls, a sequential door design was developed. Four doors, one on each side, were placed at the rear of the chamber. If the doors could be held at a given angle, the compaction forces could be transferred almost completely into the chamber structure, therefore compacting the module while also keeping it inside the chamber with no additional wall at the back of the chamber. Ideally, this eliminates the need for a backing bale as used conventional square balers.

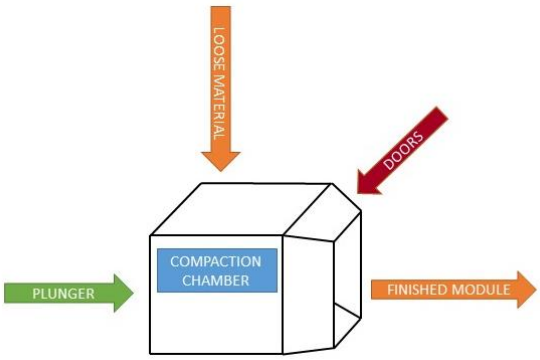

Figure 4.3: Initial compaction chamber and door design

The equations developed by Afzalinia and Roberge (2008) were used to approximate the back pressure and sidewall pressures within the compaction chamber of the large module builder, using equations 2.3, 2.4, and 2.5 derived in Chapter 2. In order to apply the model to this design, the calculations were completed in two separate steps. The first step determined the pressures in the initial square section of the module chamber (before the doors). The angles on the walls were set to zero. In the second step, the pressure gradients within the door section were calculated with angles α and β. The dimensional characteristics for these two sections is shown in Table 4.4.

Table 4.4: Constant size and dimensional factors for application of pressure distribution model inside compaction chamber

Stationary Section		
a	2.3	m
b	2.3	m
L	1.0	m
α	0	deg
β	0	deg
Door Section		
a	2.3	m
B	2.3	m
L	1.2	m
α	7	deg
β	7	deg

The model was used exactly as shown in the literature review for the determination of the back pressure, P_x. However, as noted, the predicted pressures for the sidewalls, P_y and P_z, was reduced by a factor of four for this large module model to correlate more closely with the experimental data from the literature review. The modulus of elasticity for stover was estimated at 40 Pa, and Poisson's ration was estimated at 0.4. To begin, the model was created with a coefficient of friction of 0.6 between the walls of the chamber and the stover. With these parameters and a module face pressure from the plungers of 414 kPa, the back pressure, P_x, at the rear of the chamber was predicted to be 69 kPa. Assuming the high value of the compaction pressure (414 kPa) will not be reached, it was deemed reasonable to develop the machine with the door design.

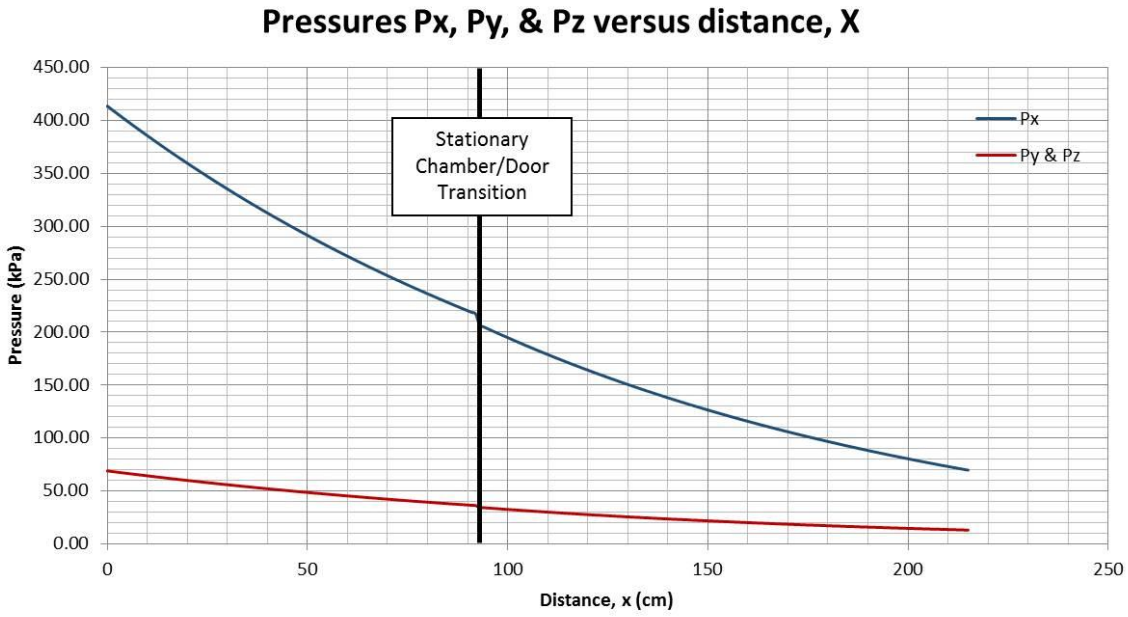

Figure 4.4: Graph of the predicted back pressure, Px, and sidewall pressures, Py and Pz, for full compaction chamber of large module builder based on 414 kPa face pressure applied

Upon starting a new module, the doors were closed at the back of the compaction chamber. The two pairs of doors' hinges were offset so that the top and bottom doors were closed on the inside, with the side doors closed on the outside. In this way, when the doors were opened to a compaction angle as shown in Figure 4.3, the full perimeter of the module was covered.

4.3.2 Module Packaging Concept

A silage bag is sold as a ring of plastic folded upon itself. The overall width of the ring is about 0.6 m long. With the two sets of doors at the rear of the compaction chamber, the packaging material, or silage bag, could be placed around the doors (Figure 4.5). This way, as the module was being formed, it could be directly pushed into the protective covering. As the module was pushed through the compaction chamber, the silage bag could simply unfold similar to how they do when placed on a silage bagging machine. Also, with the compaction chamber able to have an open rear side and the module extruded into the silage bag, the overall length of the module could be varied as needed. This concept eliminated the need for specialized wrapping material and allowed the package to be created and sealed without the need for an operator to revisit the module once it is complete and dropped from the machine.

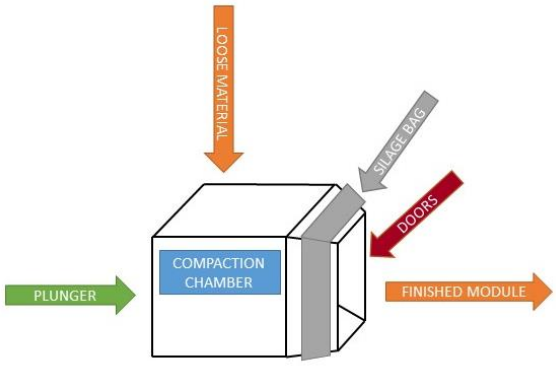

Figure 4.5: Compaction chamber with silage bag

In order to seal the bag, a square frame holded the bag outside of the doors. A hoop structure was attached to the square frame to allow the entire hoop and bag to rotate. This twisted the bag and provides a tightly wound section where the bag can be tied off and sealed.

4.3.3 Large Module Builder Operation Modes

This concept provided a nearly seamless way to move material through the machine. Module compaction, formation, packaging, and sealing can nearly be done simultaneously (Figure 4.6). Three different operational modes categorize the machine concept: compaction mode, extrude mode, and rotate mode. In compaction mode, the doors are held closed as loose material is fed into the compaction chamber. The plunger compresses an initial small module. When this initial section is full of compacted stover, the doors open, starting with the side doors (outside pair). The doors open to the angle specified by the pressure models derived above. The top and bottom doors open second. The top door follows the same angle criteria as the side doors. The bottom door opens completely, so the floor of the entire chamber is flat. The feed system fills the chamber with additional loose material and the plungers continue to cycle out and back, compacting the module. The bag and hoop sit stationary around the doors while they are angled open and in compaction mode.

When a module is determined to be complete, the system enters extrude mode. In this mode, all doors open completely. Once the doors are open, the plunger extends to full stroke, just beyond the rear edges of the doors. The finished module is now completely out of the compaction chamber, and has been pushed into the tied end of the silage bag.

With the module extruded from the chamber, the doors close once again. When the doors are closed, the hoop is free to rotate in the space previously occupied by the open doors. This is classified as rotate mode. The hoop rotates which twists the bag. Then, the bag is tied off and the finished module is cut away from the machine. Meanwhile, the compaction chamber, with its closed doors, starts over in compaction mode, producing another initial module in the chamber.

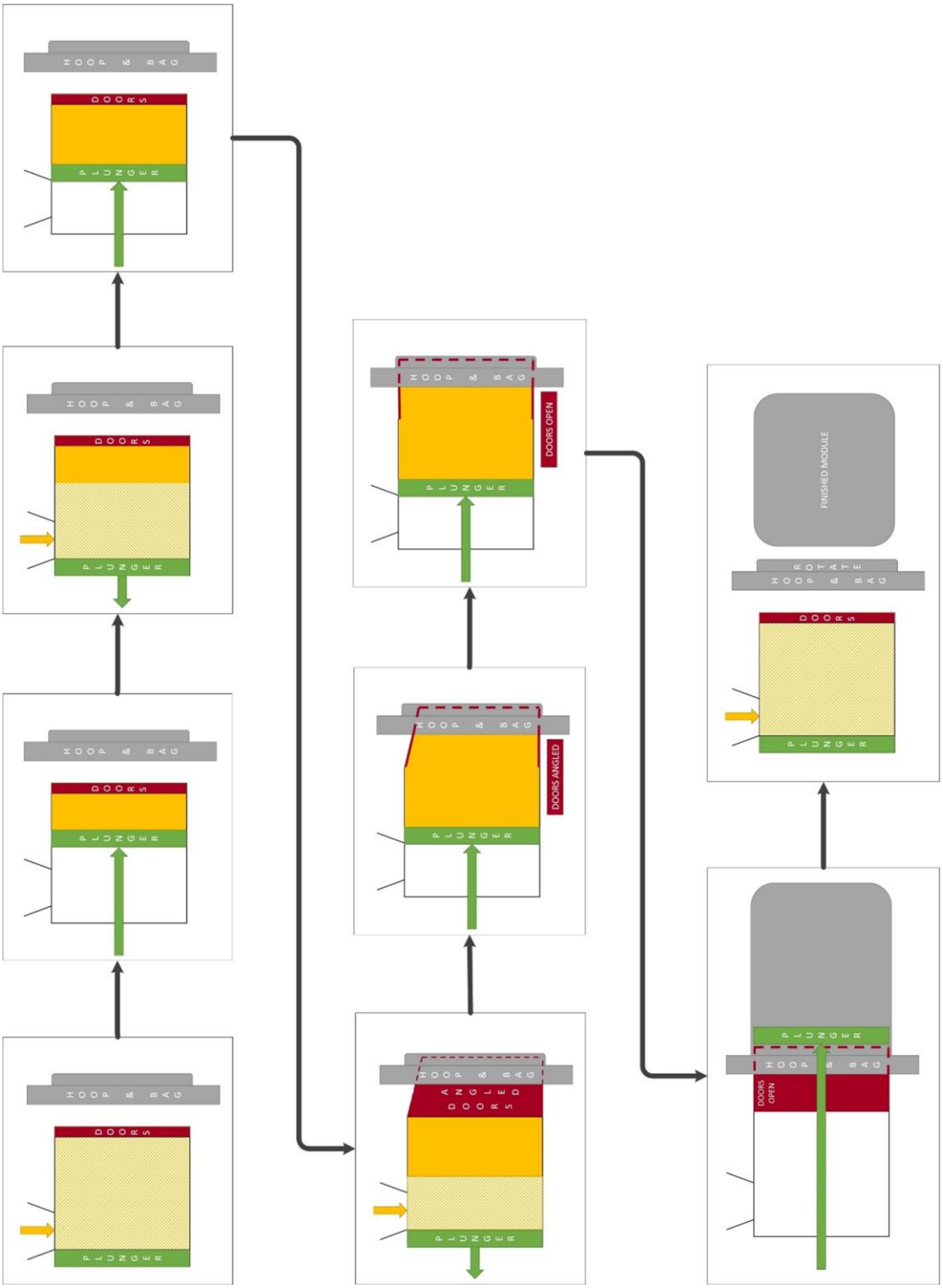

Figure 4.6: Step-by-step large module builder operational modes including compaction, extrusion, and rotation

4.4 Small Scale Test Stand

The overall aim of the small test stand was to characterize the control of the plunging system. A main goal of the machine was to create a module which had uniform density throughout, while still creating an even module face. Therefore, two different options to control the plungers existed. First, the pressure in the hydraulic cylinders was measured. In addition, due to differences in stover or other factors, each section may not travel equal distances to create uniform density. Therefore, the test stand also measured the distance travelled during each cylinder plunge. With these two factors, the small scale model was used to understand the implications of using a three section compaction design and then move forward to create a control system for this type of machine.

4.4.1 Physical Small Scale Test Stand Overview

The three plunger model was created from a steel frame with three hydraulic cylinders. For this scaled test stand, the small module size was 45.7 cm by 45.7 cm. The stand used three Prince Wolverine 6.35 cm bore, 1.5 m stroke cylinders (Prince Hydraulics, Sioux City, SD). An 20 cm opening in the compaction chamber allowed stover to enter, leaving about 40 cm of total compressed length. The compression chamber included tracks for each of the three plungers to travel in a straight horizontal line. A solidly mounted backing board was placed at the output

Figure 4.7: Overall setup of scaled down module builder test stand

end of the chamber. Also the sides, top, and bottom of the chamber were fitted with 6.3 mm thick clear plastic. The hydraulic cylinders were controlled by solenoid actuated Prince Model SV stack valves (Prince Hydraulics, Sioux City, SD) located on the top of the apparatus. A stand-alone hydraulic power pack was used to supply flow to the valve.

Control components included three types of sensors. The first of these was a SHARP GP2D12 infrared distance sensor (Sharp Corporation, Osaka, Japan). These sensors were used as level sensors to trip the cylinders only when each bin is full. Next, Bourns 3590 potentiometers were used to measure the distance of the cylinder stroke. The apparatus was designed with a pulley on the potentiometer shaft, a string attached to the plunger, and a weight. This string, when pulled, spins the pulley forward or backward. Lastly, there were three Omega PX309-3KGSV pressure transducers placed directly in-line with each cylinder (Omega Engineering, Stamford, CT).

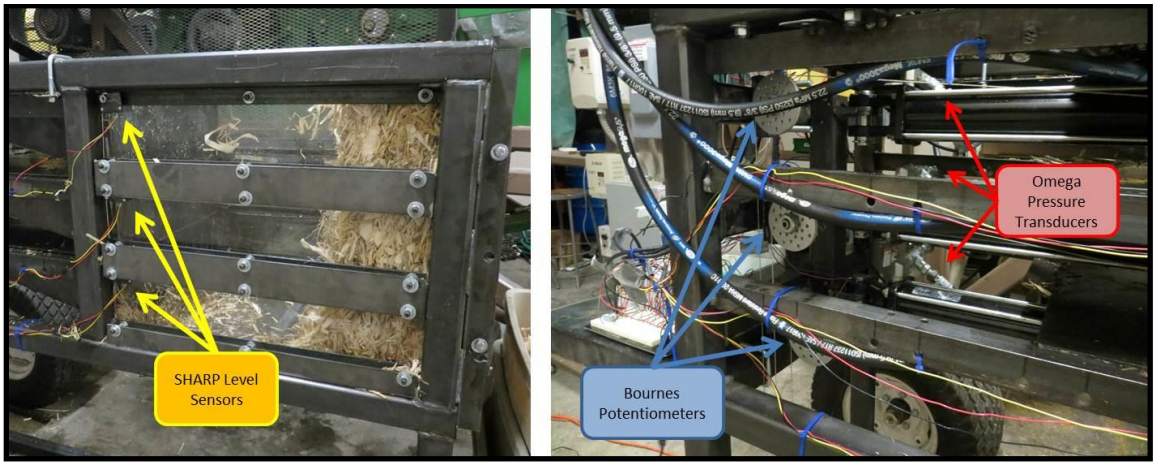

Figure 4.8: Sensor placement on scaled down module builder test stand

4.4.2 Sensor Reading and Control Logic

In order to coordinate with the test stand as well as all of the hardware, a VBA program was written to read the sensor values and send the proper control signals to the hydraulics. Two different control programs stopped the stroke of the hydraulic plungers. The main process was started by retracting all plungers to the zero point. Next, the program waited for the first level sensor to trigger, and the corresponding plunger was activated and extended. The process was ended once the in-line pressure within the hydraulic cylinder exceeded the corresponding pressure that was specified in the interface. This process was repeated for the middle and top plungers before repeating the loop, and retracting all plungers. Alternatively, the other program option still stopped the bottom plunger at the threshold pressure, and then used the recorded distance travelled to match the other two levels for an even module face.

4.4.3 Small Scale Test Stand Observations

Some challenges with the small scale test stand included using the infrared distance sensors to trigger the plungers. These sensors reacted in a somewhat erratic manner and were susceptible to false readings due to the falling stover. Also, the potentiometer readings for distance worked relatively well in this application, however, would be difficult to translate to the large machine.

From the control program side of the testing, the pressure controlled system appeared to work well. The distance travelled by each plunger was nearly the same when the valves were shut off by the pressure threshold. When the chamber was opened after the mini-module was complete, there did not appear to be definitive differences between each of the

three plunged sections. The conclusions from the small scale test stand were that the pressure controlled program logic will most likely work well for the larger scale machine and provide the best option for creating a uniform module. However, much care would need to be taken to ensure even filling of the chamber to accomplish this. Also, when retracting the plungers, the module face stayed much more even when the bottom plunger was pulled first. This seemed to minimize spring-back of the material, possibly due to dwell time of the plunger. Conversely, if the top plunger was retracted first, the subsequent plunger almost pulled part of the module face with it when it retracted next, and so forth. These observations were taken into account and directly applied towards the design of the full scale machine.

CHAPTER 5: COMPACTION CHAMBER STRUCTURAL DESIGN

With the information from the initial calculations and the small scale test stand, focus shifted to the full-size machine design. The next step in the development of the machine was designing the structure of the compaction chamber. The process included a steel framework to house the hydraulic plunging cylinders, a box for the stover to be compressed inside of, and the door structure and hinges. The compaction chamber also housed a truss system to counteract the forces produced by the hydraulic plungers. 3D CAD modeling was completed using the PTC/Creo Parametric program. Structural simulations were completed though Finite Element Analysis, or FEA, with PTC/Creo Simulate. This section details the design process for these components.

The simplest form of the compaction chamber consisted of a steel framework of four individual sides (Figure 5.1). The top frame contained an opening for material to enter the machine. The bottom frame was placed on standoffs since the machine was mounted on top of a deck-over trailer. The side frames of the chamber were designed with c-channel tracks to allow the three individual plungers to slide forward and backward within the chamber. These c-channels were located on both the top and bottom of each of the three sections. In between the c-channel tracks,

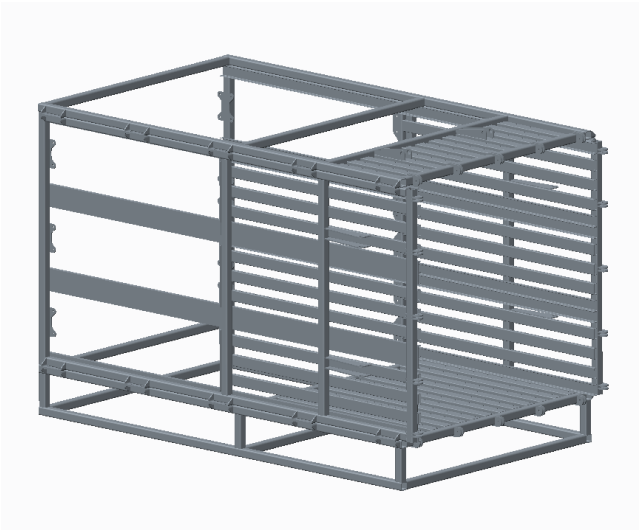

Figure 5.1: Four-sided compaction chamber frame

rectangle tubing was placed with 7.6 cm gaps all around to serve as the compaction chamber surface framework, but still allowed for air to move in and out of the chamber. These rectangle slats provided a strong framework without placing large, heavy sheets of steel inside the entire chamber. All four sides of the chamber were welded separately and then bolted together for ease of fabrication.

5.1 Design and Analysis of Plungers and Trusses

Each of the three plunging sections were driven by two hydraulic cylinders. More information on the sizing and selection of these cylinders is included in the Hydraulic System Design chapter. The large forces in the system drove the need for a substantial truss system to mount the cylinders within (Figure 5.2). Initially, the design explored building a large truss system in one piece that would bolt onto the front of the compaction chamber framework. However, FEA proved that this method was not feasible without heavy steel

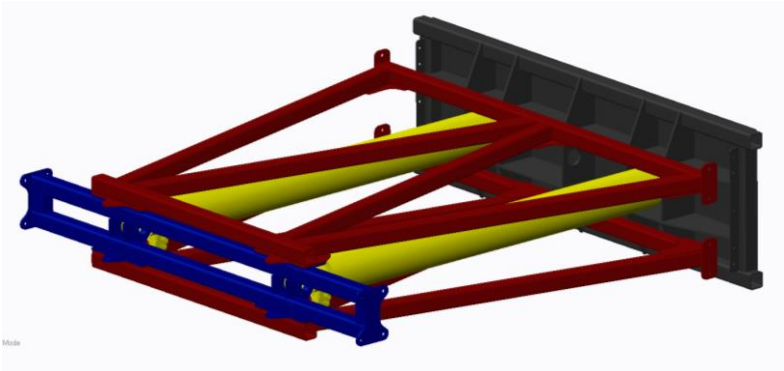

Figure 5.2: CAD model of telescoping compaction cylinders, trusses, front cross-members, and plunger

reinforcement. Therefore, another design approach was taken with the truss system tucked in around the plungers. The trusses were welded as two separate flat frames, one bolted on top of the cylinders and one bolted on the bottom.

The plunger structure itself was designed to minimally deform under the pressure at the module compression face, as well as the force from the hydraulic cylinders. For ease of use throughout the design and achieve satisfactory FEA analysis results, the best possible steel size to use was a 7.6x7.6 cm square tube with a 6.3 mm wall thickness. The plunger frame was reinforced with steel plate webbing to reduce the tube frame required. One final frame member provided structure at the front end of the hydraulic cylinders, between the two side frames of the compaction chamber.

Figure 5.3 shows the results of the FEA analysis for the trusses. The forces input into the FEA program were found dividing the overall hydraulic cylinder compaction force for

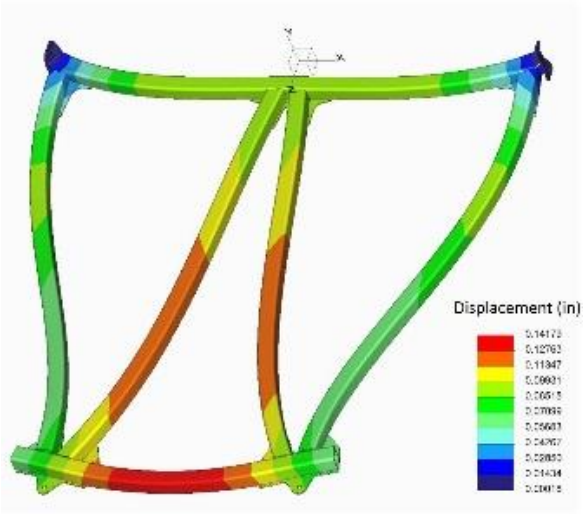

Figure 5.3: FEA analysis of displacement of truss structure under maximum loading

one individual plunger between the two trusses. Then those forces were distributed as bearing loads over each of the bolt locations. The results show the maximum deflection in the framework was held to 3.6 mm (0.142 in) in the front cross member.

A similar FEA process was followed for the plunger framework. Assuming the truss system supports the hydraulic cylinders, a static analysis could be conducted by fixing the pin holes of the hydraulic cylinders and applying the distributed load produced by the

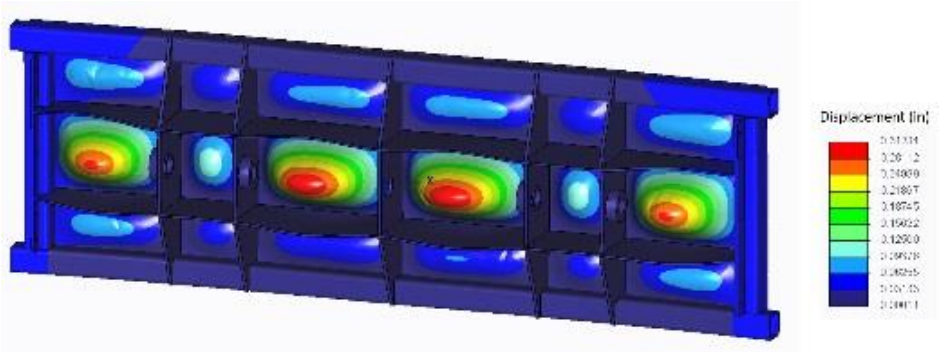

Figure 5.4: FEA analysis of displacement of plunger under maximum loading

compaction forces on the face of the plunger. Results of the simulation proved the structure would support the given forces with a maximum deflection of 7.92 mm (0.312 in). This largest deflection was located in thin steel plunger sheet face. The simulation showed the actual framework only deflecting 0.79 mm (0.031 in) at the outer edges.

The stresses caused by the compaction forces are designed to be taken through the truss system, so the front cross-brace frame does not require any FEA analysis. The plungers slid forward and backward in the compaction chamber, and in extrude mode, they extended into the door section. In order to travel smoothly and cross the threshold of the door hinges,

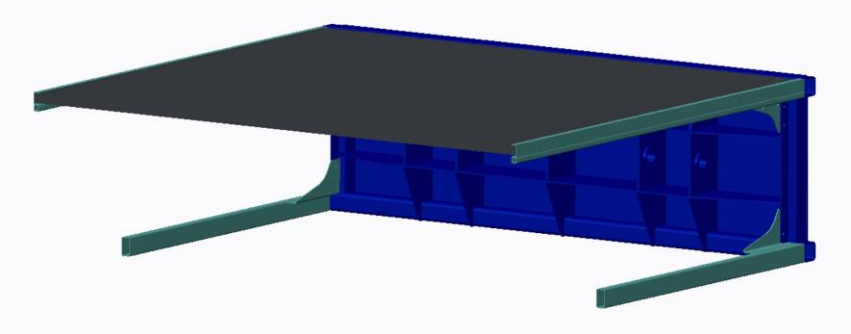

Figure 5.5: Plunger structure with sliding tracks and flooring

track systems were bolted to each corner of the plunger and rode in the same c-channel as the plunger itself (Figure 5.5.). The top set of tracks extended back about two meters from the plunger. Since the plungers actuated sequentially, grain bin flooring was used between the two upper tracks to provide a floor for the loose stover being fed into the compaction chamber. The lower set of tracks extended back about 1.5 m from the plunger. This way, the rear part of all four tracks on each plunger were still located in the initial compaction chamber section when the plungers fully extended.

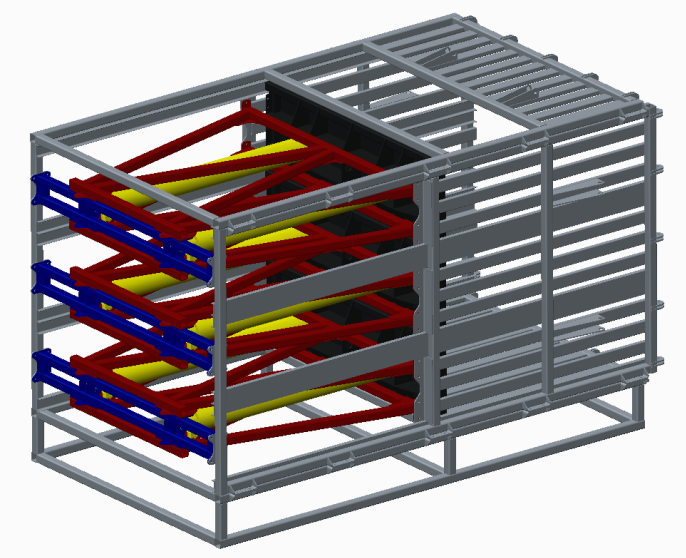

Figure 5.6: Full initial compaction chamber CAD model

The stresses caused by the compaction forces were designed to be taken through the truss system, so the front cross-brace frame did not require any FEA analysis. With all of the plungers in the machine, the front portion of the compaction chamber is seen in Figure 5.6.

5.2 Design of Compaction Door Hinges

Moving towards the exit of the machine, the next component for design was the door chamber. The door chamber serveed three purposes. First, the doors closed completely to close off the initial module chamber and allow the silage bag hoop to rotate. Then the doors

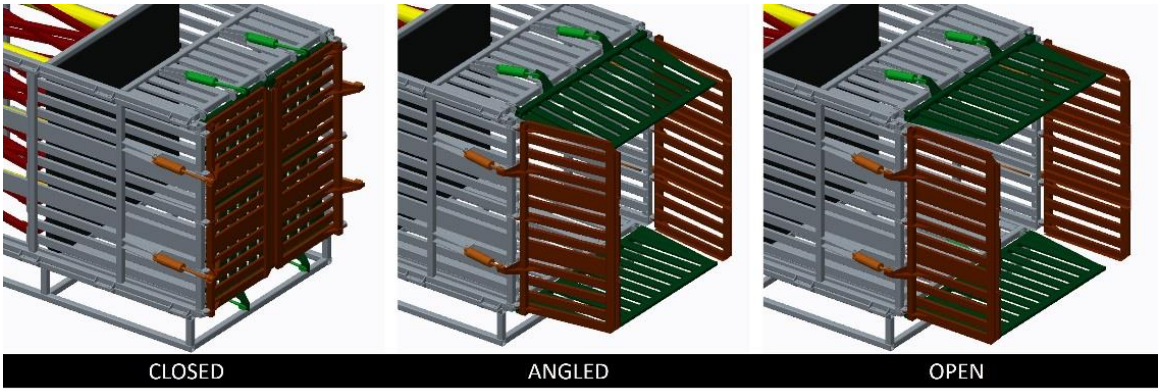

Figure 5.7: Three different operational door positions: fully closed, angled to specified compaction angles, or fully open

opened to a specified angle while the module is continually formed. Finally, the doors opened to a full angle that is in line with the initial module chamber. This allowed the plungers to travel to their full stroke and extrude the module from the compaction chamber.

The door chamber consisted of two sets of doors (Figure 5.7). The first set hinged on the top and bottom of the main compaction chamber, and extended approximately 1.2 m each. These doors functioned as the inside set, and provided the first contact to the compressed module. When closed, they completely covered the back side of the module chamber, and were comprised of rectangle tubing slats similar to the main chamber. The second set of doors mounted to the left and right sides of the main chamber. These doors closed on the outside of the top and bottom doors, and also functioned as tracks for the plungers when open completely. The outside door framework provided tracks made from c-channels in line with the channels located in the main compaction chamber frame. The rectangle tubing slats also provided the same structure for the doors as in the main chamber. Angled edges on the top and bottom door allowed the left and right door to also sit at an angle, creating the compaction parameters found through the compaction chamber pressure model. The thin design of the doors allowed the packaging system to fit closely to the compressed module.

Two hydraulic cylinders actuated each door at the hinges, pushing on a lever arm welded to the door frame. This allowed the cylinders to be tucked in close to the main compaction chamber, yet have enough stroke to fully actuate the door. The hinge for each door contained five pivot points. 1.6 cm shank shoulder bolts functioned as hinge pins. Analysis for the hinge design included shear analysis of the bolts, bearing strength of the hinge mount, and tear out strength of the hinge mount.

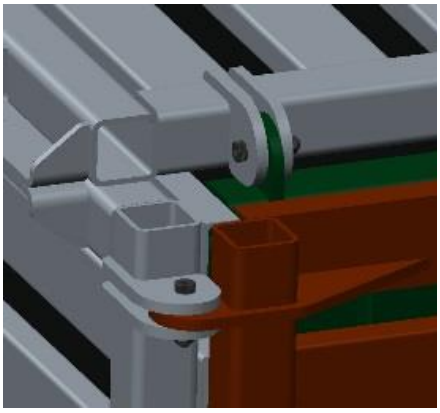

Figure 5.8: Close up view of door hinge pins

To simplify the hinge design analysis, the full module force was assumed to act evenly on every hinge bolt, with 20 bolts total. This led to a force of 12,542 kg on each bolt at the design parameter of 414 kPa at the module face. Two, 12.7 mm thick plates on the compaction chamber formed a clevis around one 12.7 mm thick plate on the door to comprise the hinge. The dimensions of the bolts and design of hinge plates allowed for the first mode of failure to be shear of the shoulder bolt (pin). This design was chosen so that if failure occurs, the repair can be completed with a replaceable part, rather than fixing the welded frame of the doors. However, it should be noted that this value was very close to the next possible failure mode of bearing deformation, so this would also be possible.

Table 5.1: Failure modes of door hinge design

Failure Mode	Force	Unit
Double shear of bolt	13,448	kg
Bearing deformation of hinge plate	13,732	kg
Tear out of hinge plate	21,573	kg
Force applied by module compaction, per bolt	**12,541**	**kg**

CHAPTER 6: FEED AND PACKAGING SYSTEM DESIGN

With the development of the compaction chamber complete, focus shifted to feeding the system and packaging a module of this size. Although the packaging portion of the machine was not tested at this time, the concepts were still developed and fabricated for this research.

6.1 Feed System

Material flow through the machine started with the hopper. A 0.6 m tall, rectangular hopper sat on top of the compaction chamber (Figure 6.1). The front face of the hopper was angled forward to allow for easier filling of the machine if using a single-pass harvest system. The bed of the hopper contained two 1 m wide flat PVC belt conveyors. The conveyors were placed side-by-side, with a 10 cm gap down the center to leave room for bearings on the pulleys. Two conveyors were needed due to the length to width ratio. One single conveyor would shift from side to side on the rollers and also be difficult to turn. The conveyors covered the entire distance of the floor of the hopper, and left a throat opening on the top compaction chamber frame of 0.9 m by 2.3 m.

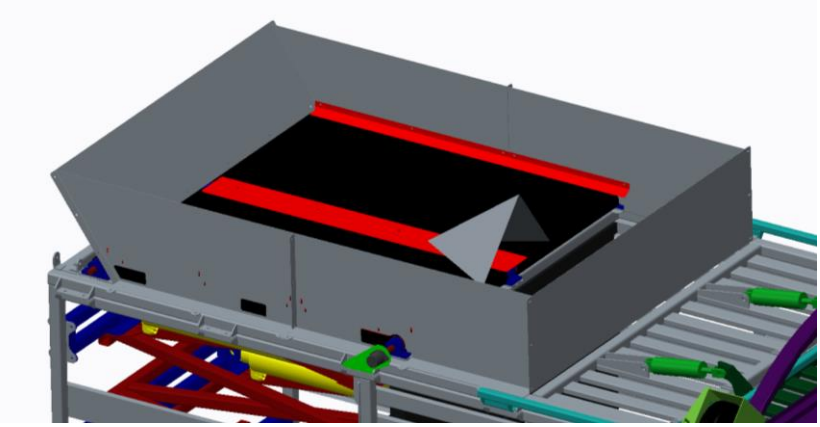

Figure 6.1: Feed System Hopper and conveyors

Each side of the hopper had cover plates, as well as a strip down the center split to keep material from falling down on the sides of the belting. A triangle shaped diverter split the material flow between the two sides of the compaction chamber for more even filling. A sheet metal false floor sat directly below the top surface of the conveyors to keep from sagging. Two hydraulic motors in series were used to drive the conveyors from the throat end. Each conveyor was tensioned at the front side of the machine.

6.2 Rotating Hoop Packaging Concept

As shown, currently large square bales are tied with twine and then sometimes wrapped in plastic for protection. This could require multiple steps to actually free the stover when the bales are needed for use. The approach taken was to eliminate twine from the packaging process and wrap the modules in a single step. For this initial machine design, the silage bag proved to be the simplest option.

Multiple options were explored to mount and seal the silage bag. One of these options included a stationary square frame with sliding doors at the rear of the chamber. These sliding doors would act like a guillotine, pinching the bag together with a seam at the center. This seam could then be sealed for anaerobic conditions. For an initial machine, this design was deemed somewhat complicated due to the guillotine door structure as well as a method to seal the long seam. An alternative option explored involved the use of a hoop with a square frame mounted in the middle. This hoop rotated, twisting the bag and providing a tightly sealed section where the bag could be tied off. This design was the easiest to both design and fabricate.

6.2.2 Rotating Silage Bag Hoop Frame

The silage bag hoop frame consisted of a rolled rectangular tubing frame for the circular driving surface (Figure 6.2). For ease of fabrication and assembly, the hoop frame was split in two halves. The outside of the rolled tubing was lined with expanded metal to provide traction for the pneumatic wheel drive system. Inside the main hoop, c-channels provided structure for the square portion. A round tube structure extended from the c-channels, making a large square frame to hold the round silage bag in the shape of the square module. This frame was covered by lightweight sheet metal with rounded corners to prevent tearing of the bag.

As mentioned previously, the hoop frame was designed to fit a ten foot diameter silage bag. This hoop fit around the outside of the doors when the doors were fully open, and therefore was kept as thin as possible. This way, the bag sat as close as possible around the exterior of the compressed module upon extrusion.

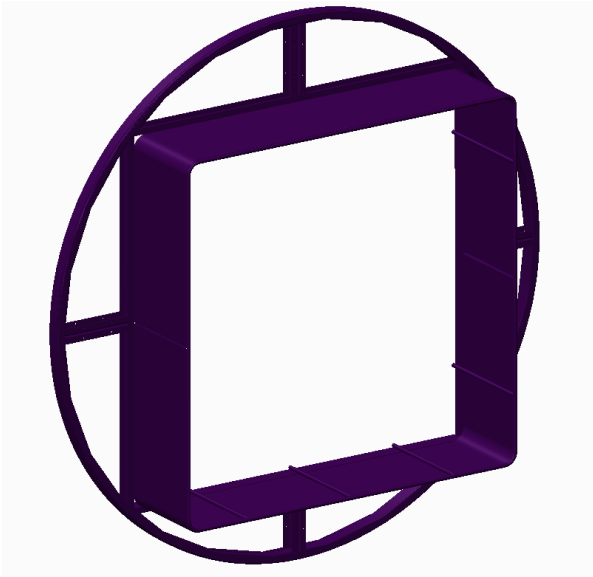

Figure 6.2: Rotating silage bag hoop frame

6.2.1 Rotating Silage Bag Hoop Drive System

Pneumatic rubber tires driven by hydraulic wheel motors powered the hoop rotation. Steel frames attached to each corner of the compaction chamber held tire assemblies in line with the rolled hoop frame, about one third of the way out on the doors when they were open.

These frames were mounted solidly to the compaction chamber and tied together with a strap on each side (Figure 6.3). The location of the hoop placed the end of the frame just in front of the back edge of the doors when the module was extruded from the chamber.

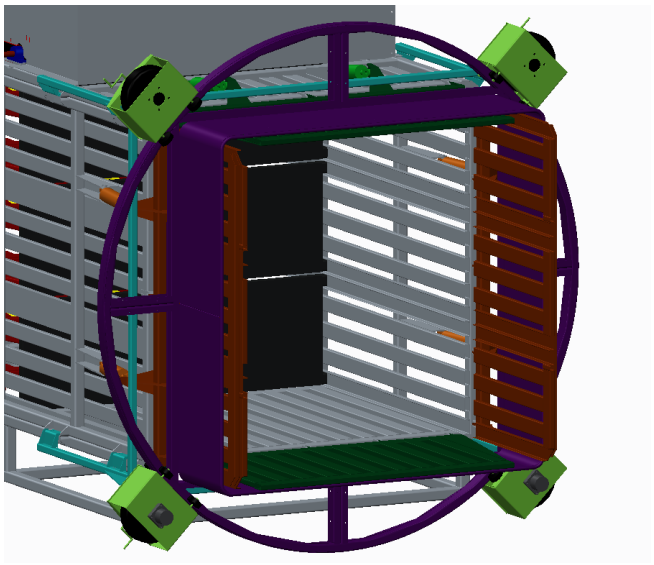

Figure 6.3: Rotating hoop and drive system assembly mounted on compaction chamber

Each tire assembly consisted of a box frame with slots on the front face. These slots provided adjustment in the direction of a line through the center of the hoop circle. This way, each corner drive assembly could be adjusted in or out to center the hoop around the doors. Each frame had a crank adjustment for fine tuning. To hold the hoop in place in the front to back direction, each frame had four solid rubber wheels, two on each side of the rolled tubing frame (Figure 6.4). The side walls of the rolled frame rode on the tread of the small rubber wheels, creating a channel for the hoop to rotate in. A pneumatic tire sat tangent to the outer edge of the rolled tubing frame. For the top two assemblies, this tire acted as an idler to keep the hoop in place. The bottom two assemblies were driven by Parker TL series hydraulic wheel motors in series (Parker Hannifin, Cleveland, Ohio).

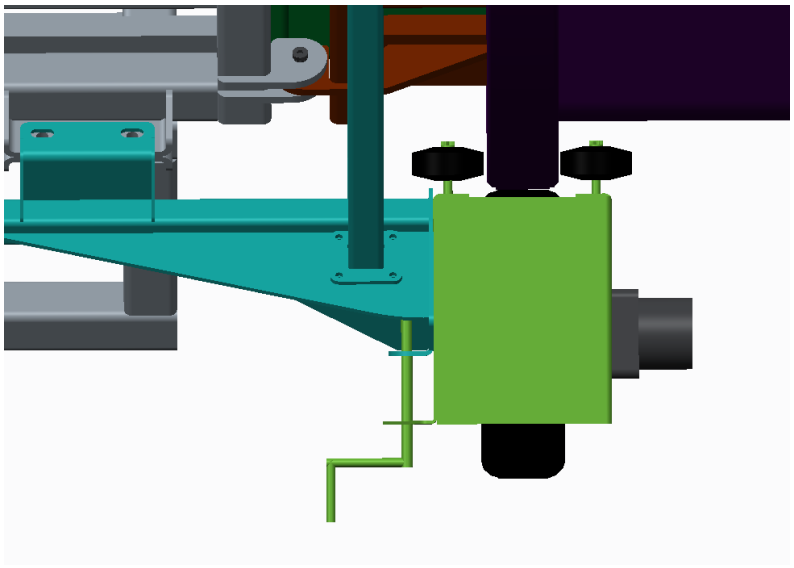

Figure 6.4: Close up view of hoop drive system rollers and drive wheel

CHAPTER 7: HYDRAULIC SYSTEM DESIGN

The main structure and functionality of the large module builder had been developed. Hydraulic power was the main driving force used to actuate all the different components of the system. Hydraulic cylinders moved the plungers, doors, and finished module platform. Hydraulic motors turned the feed conveyors as well as the rotating bag hoop. Initially, using the auxiliary hydraulic outputs from the tractor to power the hydraulic control valves was considered. However, the large internal volume of the compaction cylinders required too much hydraulic oil to function off of the tractor reservoir. Therefore, the hydraulic system was designed as a stand-alone hydraulic drive system powered by the Power Take Off (PTO) shaft of the tractor. A full hydraulic schematic is shown in Figure 7.1.

7.1 Compaction Chamber Hydraulic Component Selection

The component selection for the compaction chamber consisted of the large compaction cylinders and the door actuation cylinders. The design was based on the forces required to provide the necessary compaction pressures on both the module face, as well as the sidewall pressures from the derived model.

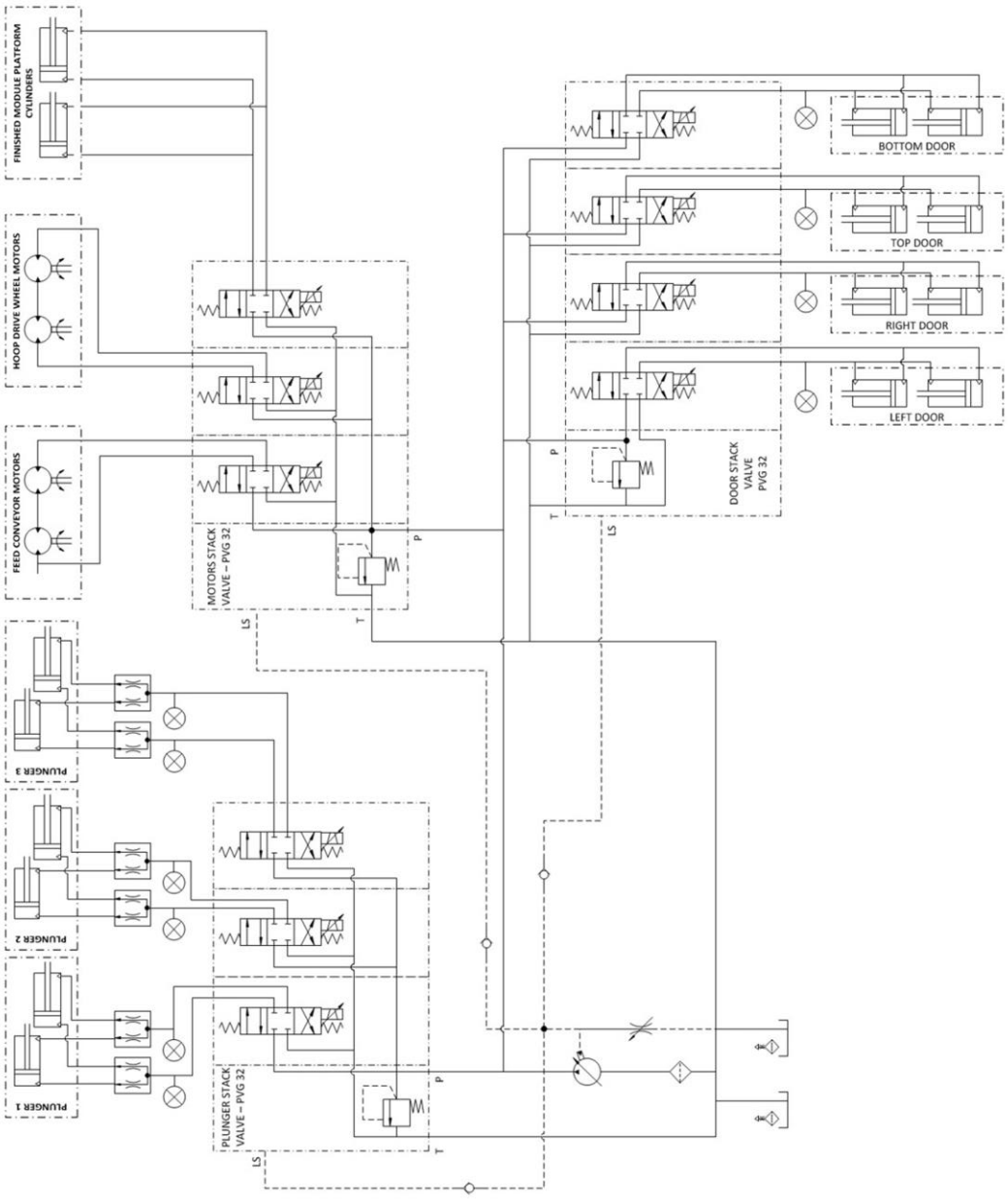

Figure 7.1: Full hydraulic schematic for large module builder prototype machine

7.1.1 Telescoping Compaction Cylinder Sizing and Selection

First, the main hydraulic compaction cylinders were selected. The forces estimated by the pressure and density models in previous chapters led to a compaction force of 83,606 kg on each plunger. With the rectangular shape of the plunger and the force requirements, the decision was made to actuate each plunger with two hydraulic cylinders. The compaction cycles only required a stroke length of about 1.5 m. However, the extrusion process must clear the outside edge of the open doors. Therefore, the full stroke of the compaction cylinders had to be about 3.4 m. In order to keep the test machine as simple as possible, the choice was made to complete both compaction and extrusion with a single hydraulic cylinder system. This decision led to double-acting telescopic cylinders. The cylinders used were made by Prince and have the part number of PMC54-1310-TGCT (Prince Hydraulics, Sioux City, SD). They have a 17.1 cm bore in stage one, a 14.0 cm bore in stage two, and a full stroke length of 3.3 m. The rod end fitting has a tang option, and the base end fitting has a welded cross-tube. These cylinders are very large, but they are rated to provide the necessary amount of force if the machine would be capable of the 414 kPa threshold compaction pressure.

Figure 7.2: Double-acting telescopic hydraulic cylinder to actuate plunger

7.1.2 Compaction Door Cylinder Sizing and Selection

Two hydraulic cylinders actuated each of the doors. The doors were not designed to take the full compaction pressure when they were in their closed state. When the doors were closed, the compaction force by the plunger cylinders was limited. Therefore, the door cylinder sizing took place at the compaction angle of seven degrees (from fully open). Each door was assumed to have equal sidewall pressure from the derived model. The model predicted a pressure of about 13.8 kPa over the face of each door when the module was fully formed. This was utilized as the design point. This method was acceptable because although the highest sidewall pressure was produced towards the front of the doors, the resultant force on the door was quite close to the hinge, causing the torque to be small. The door hinge lever arm dimensions were designed in conjunction with the cylinder sizing based on available hydraulic cylinders and stroke length using an iterative process. The pressure load was resolved to a force located halfway out on the door face. The area of the each door was found below.

$$A_{door} = L_{door} * W_{door} = 2.29\ m * 1.19\ in = 2.73\ m^2 \quad \text{Equation 7.1}$$

If the sidewall pressure is assumed to be 13.8 kPa, the resultant force was found by:

$$F_{sidewall} = P_{sidewall} * A_{door} = 13.8\ kPa * 2.73\ m^2 = 3{,}837\ kg \quad \text{Equation 7.2}$$

A free body diagram of a door is found in Figure 7.3. Values for the variables are found in Table 7.1.

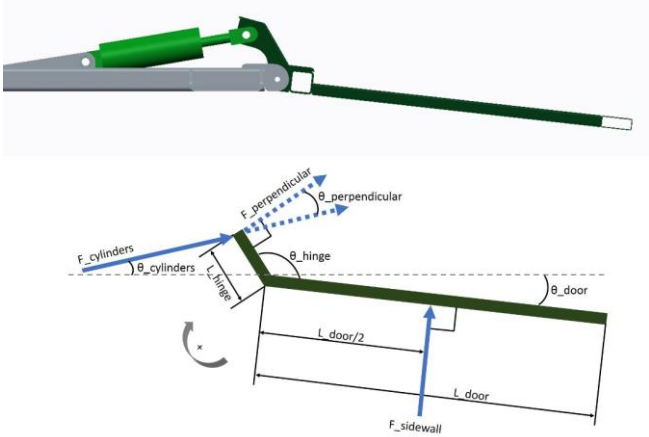

Figure 7.3: Free-body diagram of door to determine hydraulic cylinder size

Table 7.1: Force and dimensional data for door geometry to determine cylinder size

Variable	Value	Unit
F_sidewall	3,837	kg
L_door	1.19	m
L_hinge	17.8	cm
θ_door	7	degrees
θ_cylinders	9.5	degrees
θ_hinge	131.4	degrees

In order to determine the full cylinder force, first the required perpendicular force supplied by the cylinders was calculated. Taking the sum of moments about the hinge results in:

$$\sum T_{hinge} = 0 = \left(F_{sidewall} * \frac{L_{door}}{2}\right) - \left(F_{perpendicular} * L_{hinge}\right) \quad \text{Equation 7.3}$$

$$F_{perpendicular} = \frac{F_{sidewall} * L_{door}}{2 * L_{hinge}} = \frac{3{,}837\ kg * 1.19\ m}{2 * 17.8\ cm * \frac{1\ m}{100\ cm}} \quad \text{Equation 7.4}$$

$$= 12{,}883\ kg$$

From here, geometry was used to find the angle between the perpendicular cylinder force and the full cylinder force. This angle is shown as θ_perpendicular and was found to be 24.9 degrees.

$$F_{cylinders} = \frac{F_{perpendicular}}{\cos\left(\theta_{perpendicular}\right)} = \frac{12{,}883\ kg}{\cos(24.9\ deg)} \quad \text{Equation 7.5}$$

$$= 14{,}204\ kg$$

Through this calculation, the cylinders must supply over 14,000 kg of force to keep the doors at their compression angles. Therefore, each cylinder must provide half of that (there are two per door). The final cylinder force used for sizing was as follows.

$$F_{doorcylinder} = \frac{F_{cylinders}}{2} = \frac{14{,}204\ kg}{2} = 7{,}102\ kg \qquad \text{Equation 7.6}$$

As mentioned, the structural frame of the doors was not designed to withhold the high compaction forces when closed. To help combat the higher pressures seen when the door angle was ninety degrees and the length of material in the chamber was low, the sizing of the door cylinders was increased. Through a process of reasonably sizing the cylinders for the space constraints, this factor was found to be two times the force found above. Also, with the geometry defined, a stroke length of exactly 25.4 cm (10 inches) provided the correct range of motion for the doors. With all of these factors, Lion Hydraulics Lynx 40LH10-150 cylinders were chosen (Monarch Industries, Winnipeg, Canada). The cylinders have a 10.2 cm diameter bore, 3.8 cm diameter rod, and 25.4 cm stroke.

7.2 Hydraulic Valve Components

Next, valves had to be selected to control the hydraulic cylinder and motor components. Danfoss PVG-32 stack valves were chosen (Danfoss, Ames, IA). Each valve section was a three position, four way valve with a closed center. An inlet relief was set at 17,237 kPa. The valve sections were electrically actuated using PVHC (high current) control modules. PVHC modules used two current signals to vary the spool position of the valve and therefore control the flow to each component.

The stack valves were separated into three different valve assemblies (Figure 7.4). One assembly controlled the three plungers. Another controlled the four doors. A final

assembly contained spools designed for use with hydraulic motors and anti-cavitation valves to help with over-running loads. This assembly was used for the feed conveyor motors as well as the hoop drive wheel motors. Two open valve sections on this valve provided room for expansion of the system, and eventually, one of the two open sections was used to actuate the finished module platform cylinders.

Load sense ports on each valve were used to report the highest pressure provided by the work functions that that valve is used for. The three load sense lines from the valves were plumbed together. After all load sense lines were combined, a bleed valve was placed in the line to return the load sense flow to the reservoirs (there was no load sense drain in the main drive pump).

Furthermore, for the three plunger sections, each section contained two telescopic hydraulic cylinders. In order for the machine to function properly and not bind during operation, it was imperative that these two cylinders travel equally. Flow divider valves were used for this function. A flow divider valve was placed on both the extension and retraction sides of the circuit. The valves used were Brand Hydraulics B100AB-3/4 flow divider valves rated at 114 lpm (Brand Hydraulics, Omaha, Nebraska). These allow for free reverse flow, which is necessary because the flow was divided on both

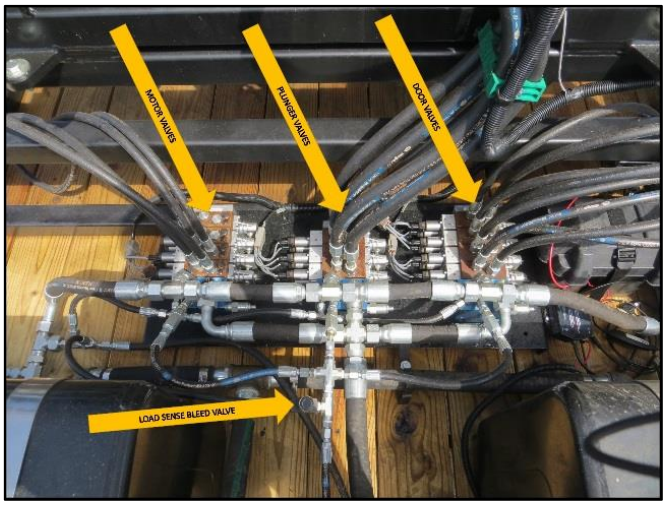

Figure 7.4: Three Danfoss PVG-32 valve assemblies for plungers, doors, and hydraulic motors with load sense bleed valve

the extension and retraction sides of the cylinders. Also, the AB distinction means that the two outlet flows are pressure compensating. This way, if the pressure differential between the cylinders gets too high, the valve allows for cross-flow between the two. This is essential in letting both cylinders reach the full end of stroke and full retraction. Since the door cylinders were mechanically linked and their operation was not as precise, the decision was made to simply tee the two lines together without using a valve to divide the flow.

7.3 Hydraulic Drive System

All of these hydraulic components needed to be driven by some kind of power pack. A tractor served as this power source. A telescoping PTO driveline allowed for quick hookup and removal to the tractor (Figure 7.5). This drove an E-frame Series 45 Danfoss axial piston pump (Danfoss, Ames, IA). The pumps displacement is 130 cubic centimeters per revolution, and outputs 114 lpm at approximately 900 rpm. As stated before, the pump was equipped with load sense. This functionality allowed the pump to have fully variable pressure and flow dependent on the system's needs, and the single pump could be used to supply the multiple work function circuits. The PTO pump was mounted to an overhung

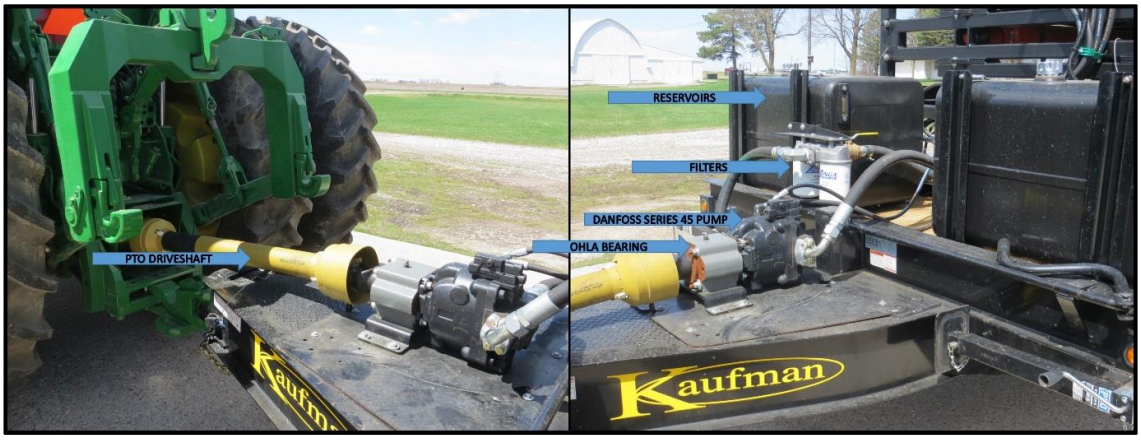

Figure 7.5: Full hydraulic drive system

load adapter (OHLA) bearing. This bearing was mounted directly to the trailer and provided support for the input shaft of the pump. This way, the pump was not directly coupled to the driveshaft connected to the tractor PTO.

Two 265 liter hydraulic reservoirs were mounted on the deck of the trailer at the front. The size of these reservoirs ensured that if all of the telescopic cylinders were fully extended, the system would have enough fluid that the pump would not starve. Finally, a side by side two filter assembly was located between the reservoirs and the pump. Figure 7.6 shows the full and final CAD model with the structural and hydraulic components.

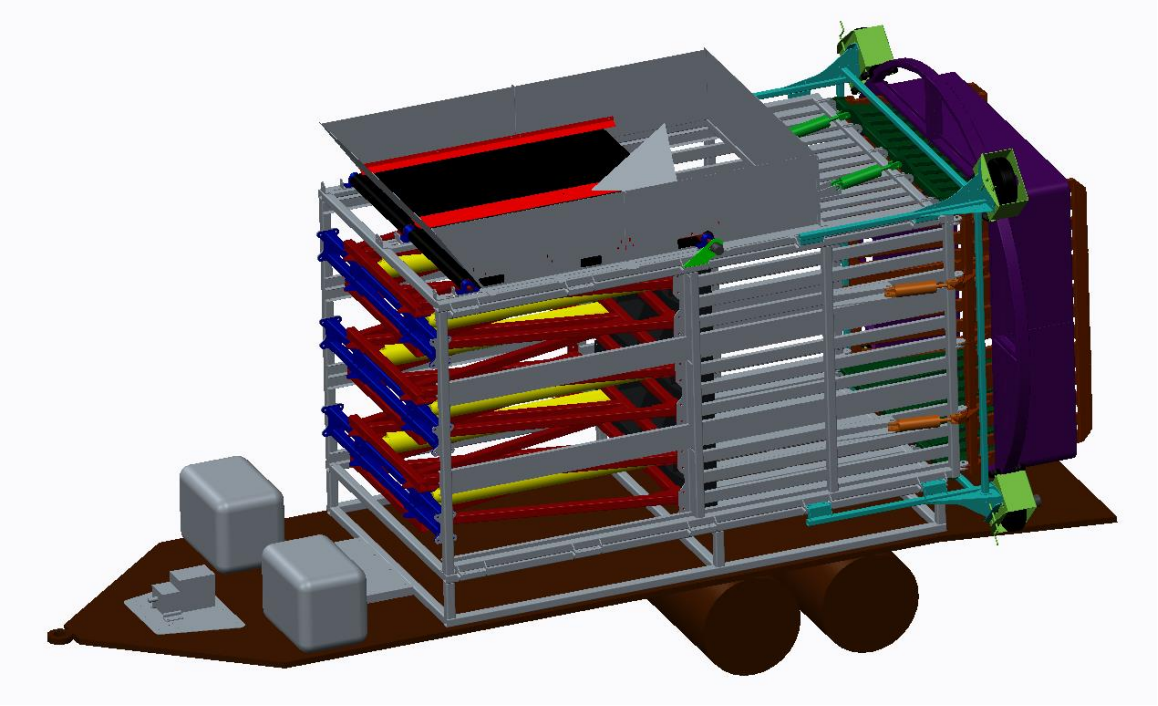

Figure 7.6: Complete CAD model for all structural and hydraulic components

CHAPTER 8: ELECTRICAL AND CONTROL DEVELOPMENT

Various sensors were used to control the large module builder system. These sensors sent their readings to two Danfoss PLUS+1 microcontrollers which were programmed to supply output signals to the valves (Danfoss, Ames, IA). The controllers were programmed using the PLUS+1 language. A simplified schematic of the full system is seen in Figure 8.1. A 12 volt, deep-cycle battery provided the power, and was recharged by the tractor. Next, the electrical system was protected by the fuses in the fuse panel. From here, the two PLUS+1 microcontrollers received the power and distribute it to all of the sensors. The microcontrollers read and interpreted the sensor readings, then made decisions on control of

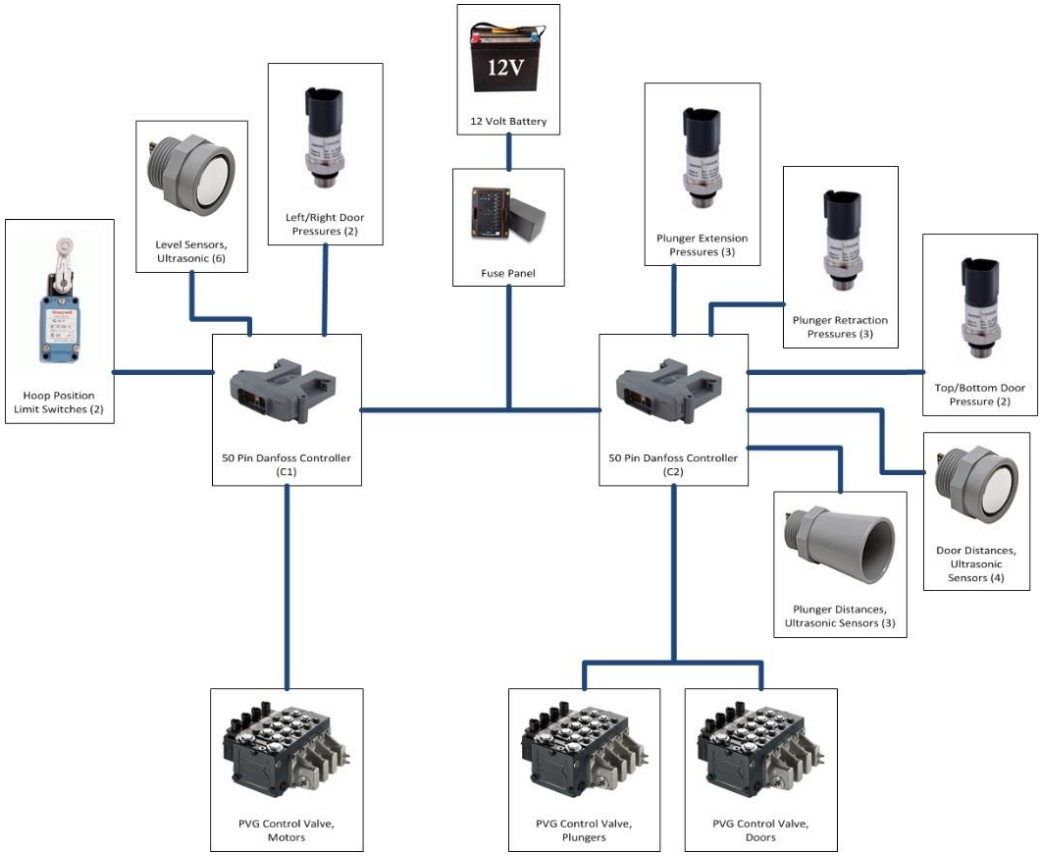

Figure 8.1: Simplified electrical schematic for large module builder electrical and control systems

the PVG valves. The microcontrollers sent out an electrical signal of varying current depending on the required flow from each valve section.

The PLUS+1 Service Tool program provided diagnostic capabilities for the machine control. In order for the two microcontrollers to communicate with the each other as well as the Service Tool, a CAN bus system was used. In addition to the microcontrollers, a HEM Data J1939 Mini Logger was also wired into the CAN bus (HEM Data, Southfield, MI). This allowed not only for diagnostics during operation through the Service Tool, but also data logging for reference afterward. Figure 8.2 shows an overview of the CAN bus.

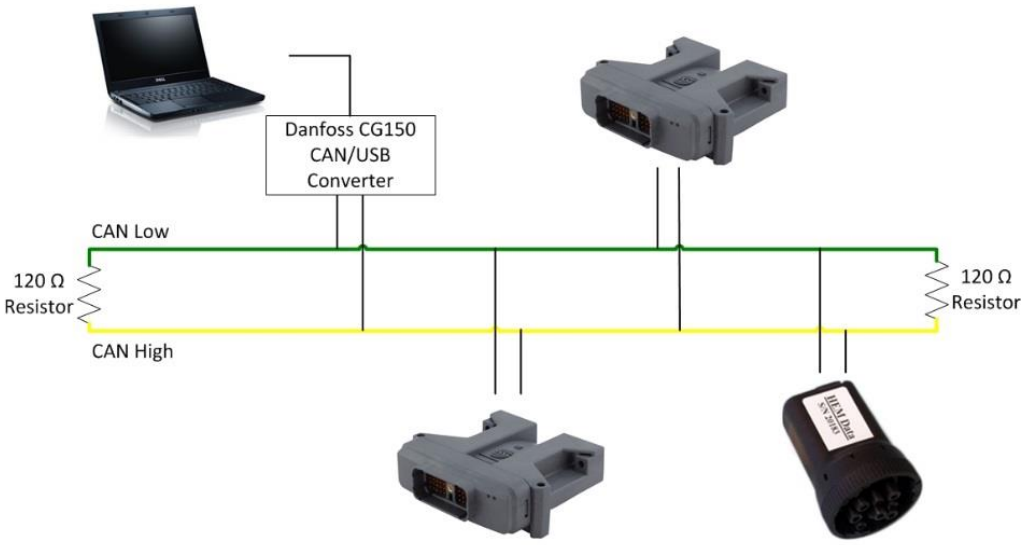

Figure 8.2: Large module builder CAN network

The microcontrollers, fuse panel, and sensor power and ground distribution busses were all placed inside an electrical box. The box was mounted on the deck of the trailer behind the hydraulic reservoirs and right next to battery and main control valves. Short harnesses brought all of the wires outside of the box. This way, all of the machine harnesses could be disconnected and the box could be isolated or removed if necessary. The electrical

box contained a diagnostic port for the HEM Data Mini Logger so that the box did not need to be opened to utilize the logger. Also, a switch box provided manual operation or override of the system. The switch box was connected to an eight foot harness for mobility.

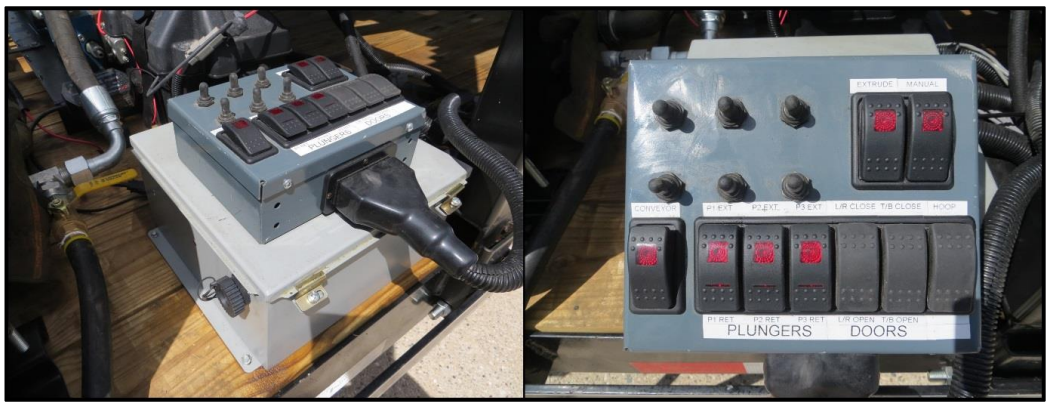

Figure 8.3: Electrical box and switch panel

8.1 Sensor Selection and Implementation

Various sensors were needed to understand exactly what was happening during operation and make decisions on how to actuate the work functions. The sensor control setup of the full scale machine closely resembled the small scale test stand as presented earlier. The level of loose material in the chamber, distance travelled by the plungers, position of the doors and hoop, and hydraulic pressure in the plunger cylinders and doors were recorded.

8.1.1 Material Level Sensors

Ultrasonic distance sensors replaced the infrared sensors used in the small scale machine. The sensors are MaxBotix MB7367 Compact MaxSonar sensors (MaxBotix Inc., Brainerd, MN). They operated on a 5V power supply and produce an analog voltage signal. The sensors read a range of distances up to 5 meters with a resolution of 5 mm. The resolution of the sensor and the distance measured can be found by:

$$R = \frac{V_{supply}}{5120} * 5 = \frac{5}{5120} * 5 = 4.885\ mV\ per\ 5\ mm \qquad \text{Equation 8.1}$$

$$D = \frac{V_{reading}\ [mV]}{R\ \left[\frac{mV}{5mm}\right]} * 5 = 1.0235\left[\frac{mm}{mV}\right] * V_{reading}[mV] \qquad \text{Equation 8.2}$$

Two sensors were placed per plunger, approximately 25 cm above the top of the plunger, for a total of six sensors. The sensors were located directly under the throat opening in the top of the machine on the left side and spaced approximately 46 cm apart. By placing the sensors above the top of the plunger and mounting two sensors per level, this design ensured that the level was completely full of loose material before the sensors triggered the plunger. The wiring and control program were built to support twelve sensors in case future work would require level sensors on both the left and right sides of the machine.

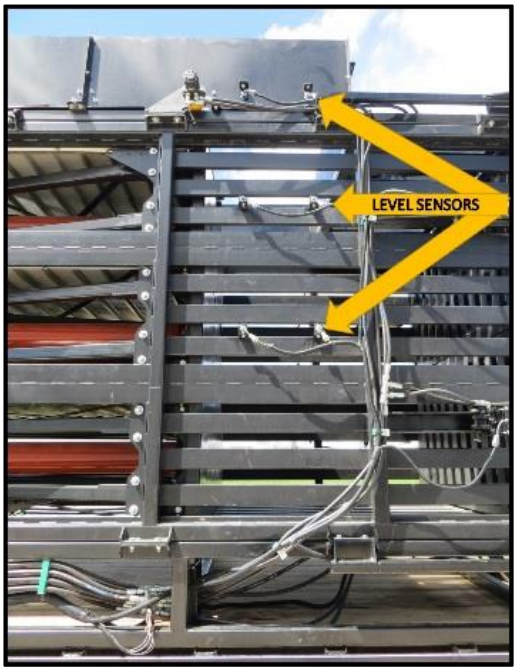

Figure 8.4: Ultrasonic distance sensors used for fill level determination

8.1.2 Distance Sensing

The distance that the plungers travel and the position of the doors must be monitored and used for machine control as well. The doors utilized the same MaxBotix MB7637 sensors to read the stroke length of the hydraulic cylinders that actuate the doors. The sensors were mounted on an adjustable plate to the cylinder base, with a steel target attached

to the rod end clevis. The target included a steel plate with a tube welded to it. The tube provided an allowance for slight misalignment between the sensor and the target. With the geometry of the door hinge and lever, the angle of the door could be calculated from this stroke measurement. Sensors were placed on one of the two cylinders that actuate each door.

A similar sensor measured the plunger distance (Figure 8.5). MaxBotix MB7369 MaxSonar sensors mounted to the truss systems remained stationary as the plunges extended and retracted (MaxBotix Inc., Brainerd, MN). The sensor was located in such a position that the center web on the plunger structure serves as the target. The MB7369 sensors are larger in size and include a cone around the sensor to reduce interference and also includes a stability filter within it to choose the best target. The resolution and distance measurement is the same as the MB7367 sensors.

Figure 8.5: Ultrasonic distance sensor used for plunger and door cylinder stroke length measurement

8.1.3 Hydraulic Pressure Transmitters

Another piece of the control program involved the pressures seen by the hydraulic cylinders for the plungers. These pressures were used to measure the force with which the material was compacted, and also the pressure placed on the full module face. Danfoss MB1250 Heavy Duty Pressure Transmitters were placed in the hydraulic lines just before the

flow divider valves (Danfoss, Ames, IA). Two pressure transmitters were used on each plunger, one for extension and one for retraction. The transmitters output a voltage signal to the PLUS+1 microcontrollers. The PLUS+1 programming provided a component block that converted this voltage directly to a pressure reading that could be used in the control program.

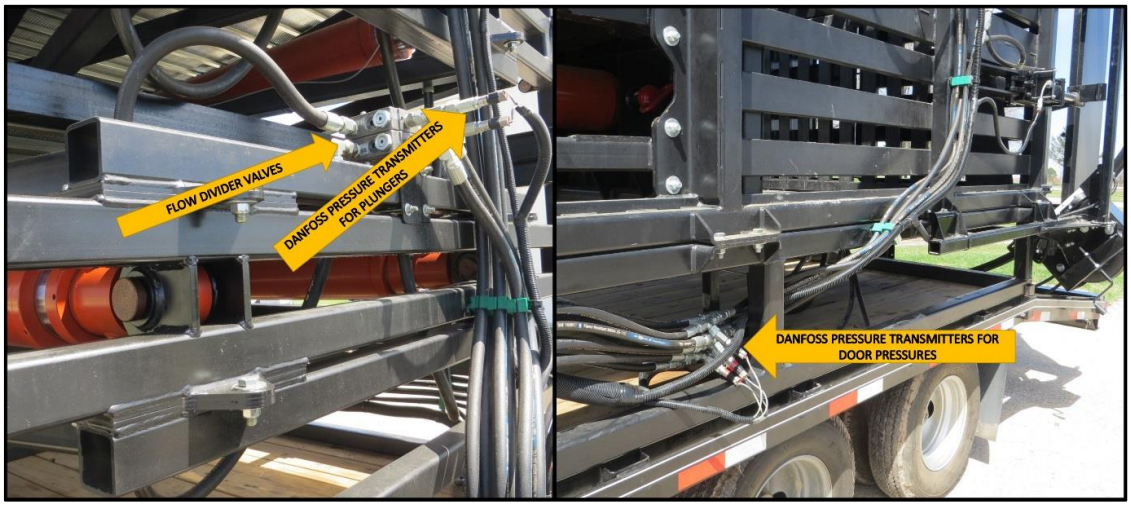

Figure 8.6: Danfoss pressure transmitters used to measure plunger and door pressures

Additional MB1250 pressure transmitters were place in the door cylinder lines. These transmitters measured the pressure on the extension side of the cylinders. This pressure was not part of the control program, but it was recorded and eventually used to verify the compaction chamber pressure models.

8.1.4 Locating the Bag Hoop

Finally, the rotating silage bag hoop had to be located in order to control the door status. It was imperative that the hoop be in the squared position any time the doors opened, and would only spin when the doors were closed. Therefore, a robust design for locating the "home" position on the hoop was developed. Two Honeywell SZL-WL series limit switches

provided this positioning (Honeywell, Morristown, NJ). The switches were mounted to the hoop drive assembly which remained stationary during rotation (Figure 8.7). On the hoop, UHMW plastic was used to make a track system mounted to the outside ring of the hoop. The track system served as a trigger for the two limit switches.

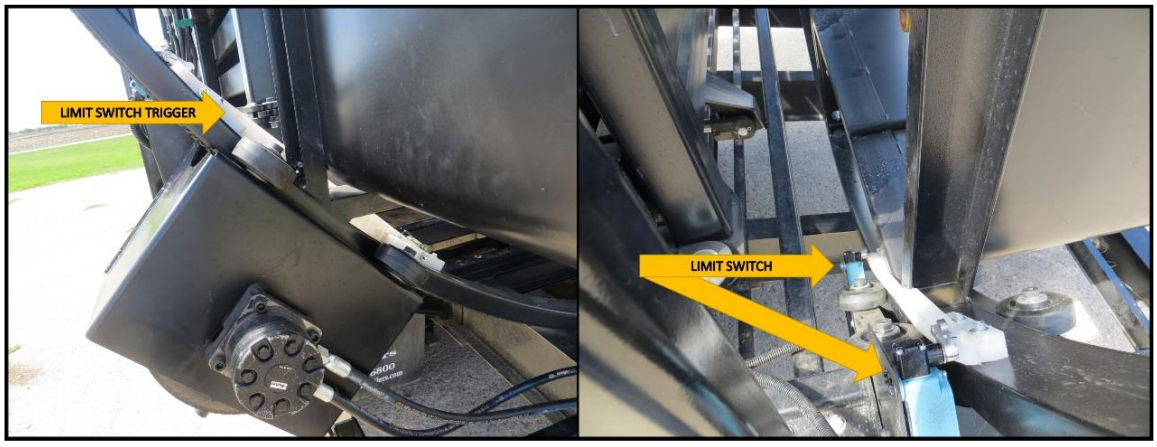

Figure 8.7: Hoop locating system with limit switches and UHMW plastic trigger

The two switch design allowed for a braking period of the rotation of the hoop. When the hoop was rotating and came back around to the home position, the first switch was triggered "on" by the plastic track. This started the braking period. The track was made in such a way that the first switch remained in the "on" position. Then when the hoop reached the exact home position, the second switch was triggered "on." The length of the trigger on the plastic track was just long enough for both switches to be triggered at the same time. If the hoop would overshoot the home position, the first switch would go to "off" and the hoop would not be considered "home."

8.2 Control Program Logic

With the full electrical circuit complete, the controls of the machine could be developed. Manual control could be completed with the switch box, however, an automated

control system was also developed for future use. The automated system design followed the modes laid for earlier: compaction, extrusion, and rotation modes. In addition, it used the three plunger system in sequential fashion.

8.2.1 Control Logic Flagged Points

A number of logical points were flagged for control. Table 8.1 explains these factors. They were used to actuate the signals that are sent to the valves. Sometimes they were used to completely turn on or off a signal, other times they were used to vary a control signal. Eventually, these flagged points facilitated system checks for safety and functionality.

Table 8.1: Listing of flagged points used in control program logic

Logical Flags	Description
Mode_Compress	In compression mode (either doors closed or regular)
Mode_Extrude	In extrude mode to clean out module from compaction chamber
Mode_Rotate	Silage bag hoop is rotating for packaging
L1_Full	Both ultrasonic distance sensors for level 1 covered
L2_Full	Both ultrasonic distance sensors for level 2 covered
L3_Full	Both ultrasonic distance sensors for level 3 covered
D_Closed	All four doors in the closed position
D_Open	All four door in the open position
D_Comp	All four doors at distances equal to those corresponding to the angles for compaction
P1_Ret	Plunger 1 fully retracted
P1_Ext	Plunger 1 fully extended
P1_MaxComp	Plunger 1 at maximum distance or pressure during compaction
P1_MaxCompDC	Plunger 1 at maximum distance or pressure during compaction with the doors closed (pressure reduced)
P2_Ret	Plunger 2 fully retracted
P2_Ext	Plunger 2 fully extended
P2_MaxComp	Plunger 2 at maximum distance or pressure during compaction
P2_MaxCompDC	Plunger 3 at maximum distance or pressure during compaction with the doors closed (pressure reduced)
P3_Ret	Plunger 3 fully retracted
P3_Ext	Plunger 3 fully extended
P3_MaxComp	Plunger 3 at maximum distance or pressure during compaction
P3_MaxCompDC	Plunger 3 at maximum distance or pressure during compaction with the doors closed (pressure reduced)
H_Home	Hoop in the home position (both limit switches triggered)

8.2.2 Control Program Flowcharts

Upon startup, the machine was in compaction mode with the doors closed. There were two different levels of compaction mode, one with the doors closed and one with the doors open. Figure 8.8 shows the logic flowchart with doors closed in compaction mode.

The number of cycles with the doors closed could be adjusted in the program, and to start, the value was set to three. This means the plungers cycled in and out three times before the program entered the regular compaction mode. The plunger cycle began when the level sensors were triggered. The max compression cutoffs for the plungers included a two-fold logic. First, the pressure read by the Danfoss pressure transmitters could not be over the threshold value. As a safety, a maximum allowable distance travelled was also include in the logic. This way, the plungers could not travel far enough to reach the door hinges while in compaction mode. Therefore, the only time the plungers travelled into the door area was during extrude mode. This meant that the initial automated control design was based around equal pressures on each plunger section of the compressed module, and the distances were simply used as a safety shutoff.

Figure 8.9 shows the flowchart for the next section of the control program. This contains the compaction mode with the doors open to their desired angles (as set by the compaction chamber pressure model). This began once the desired number of cycles with the doors closed was complete. With the doors open to their respective angles, the plungers cycled out and back as many times as necessary to create a full module. This factor was set by the operator. When the operator felt the module was complete, the “Extrude” switch on the control switch box was pressed. This notified the program that the user would like to package and complete the module after the next compaction cycle.

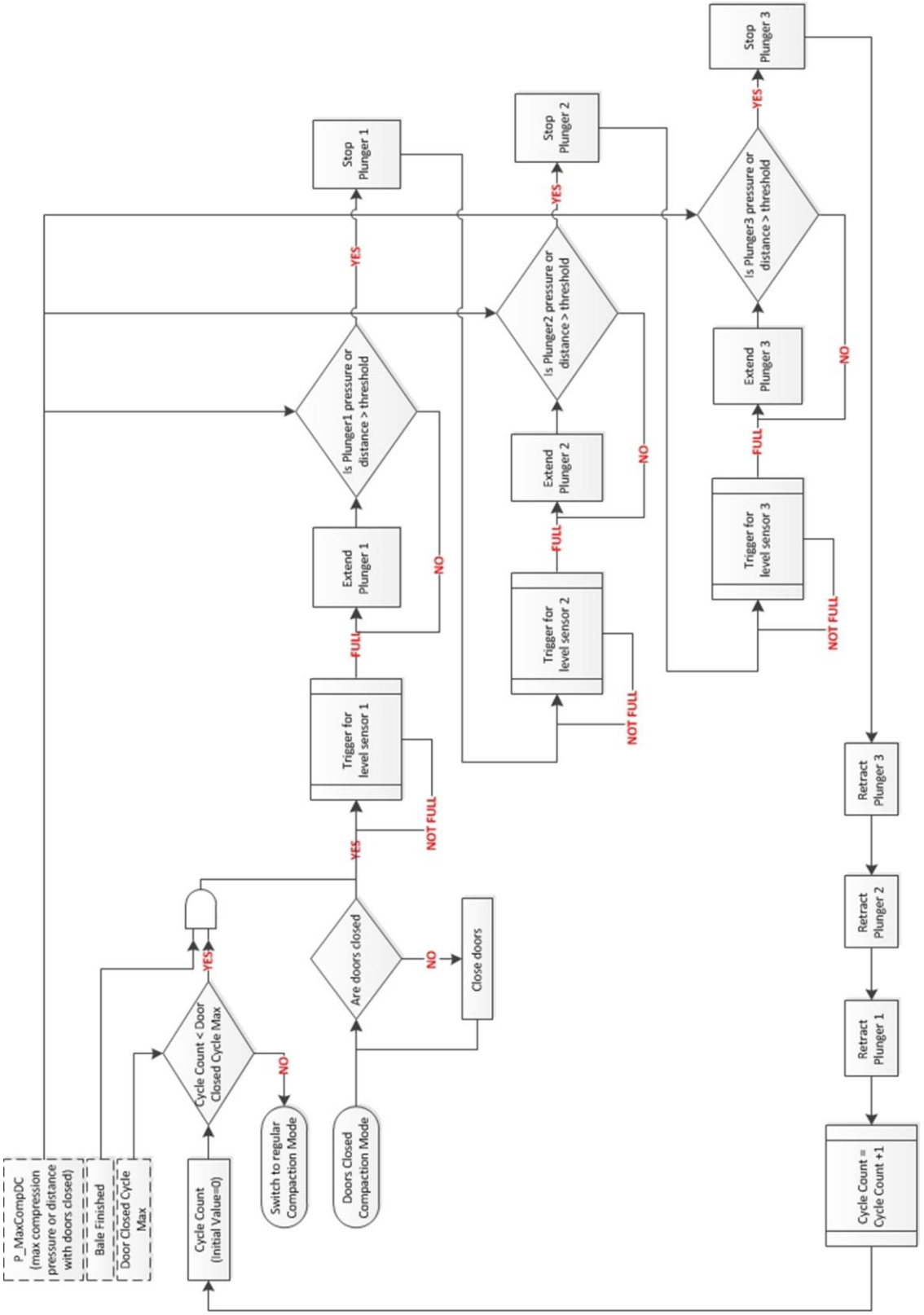

Figure 8.8: Control logic flowchart for compaction mode with the doors closed

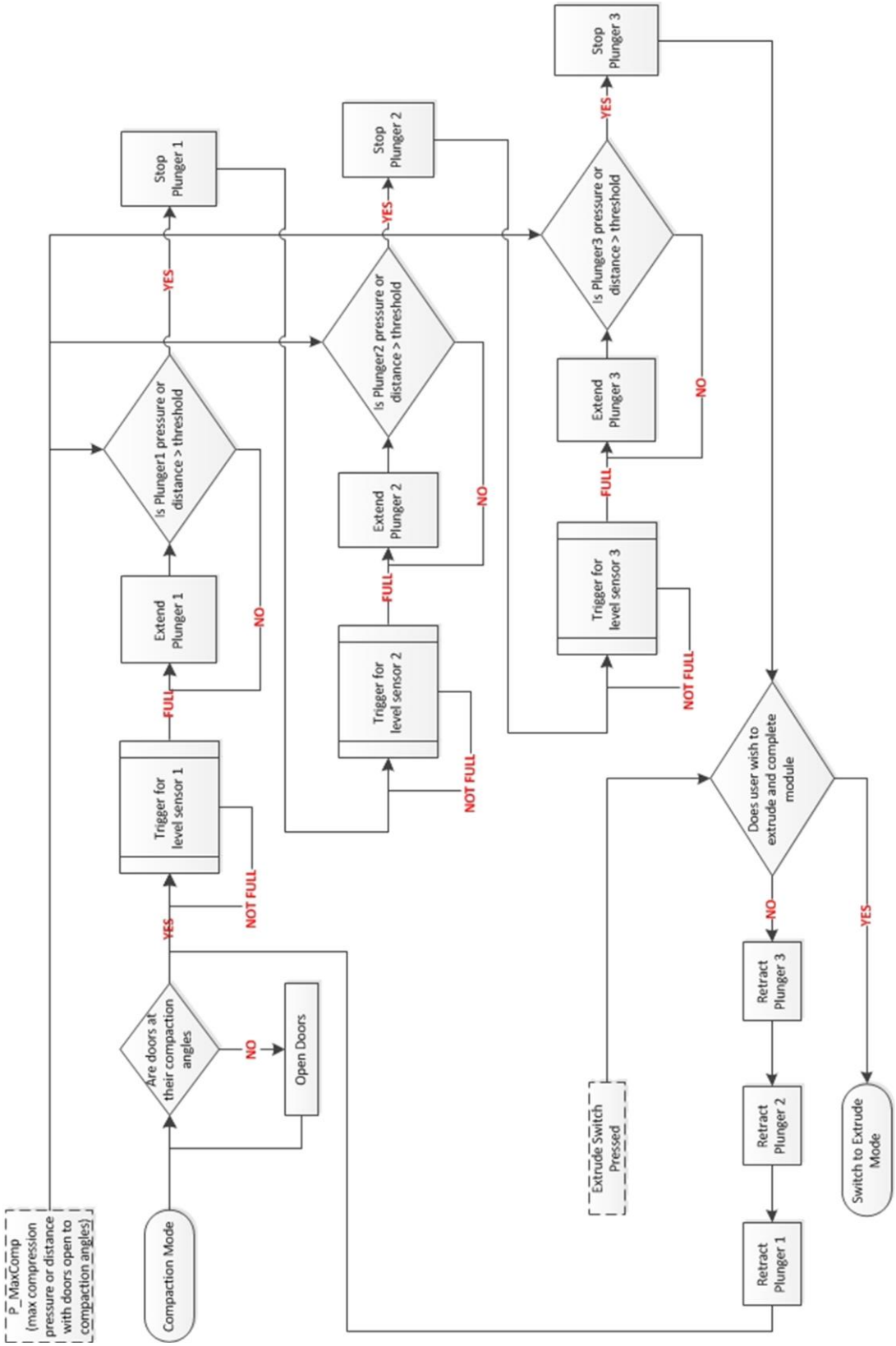

Figure 8.9: Control logic flowchart for compaction mode with the doors open to compaction angles

If the program entered the extrude mode, all three plungers would still be at their distances where compression was completed. Then, the doors were not allowed to open unless the silage bag hoop was it the home position. If these two are true, the door cylinders retracted to open the doors, starting with the left and right (outside) pair. Once both sets of doors were completely open, the middle plunger extended to extrude the module and completely clean out the compaction chamber (Figure 8.10). Once the chamber was cleared, all three plungers retracted and the doors closed again. Now, the compaction mode could begin again with the doors closed.

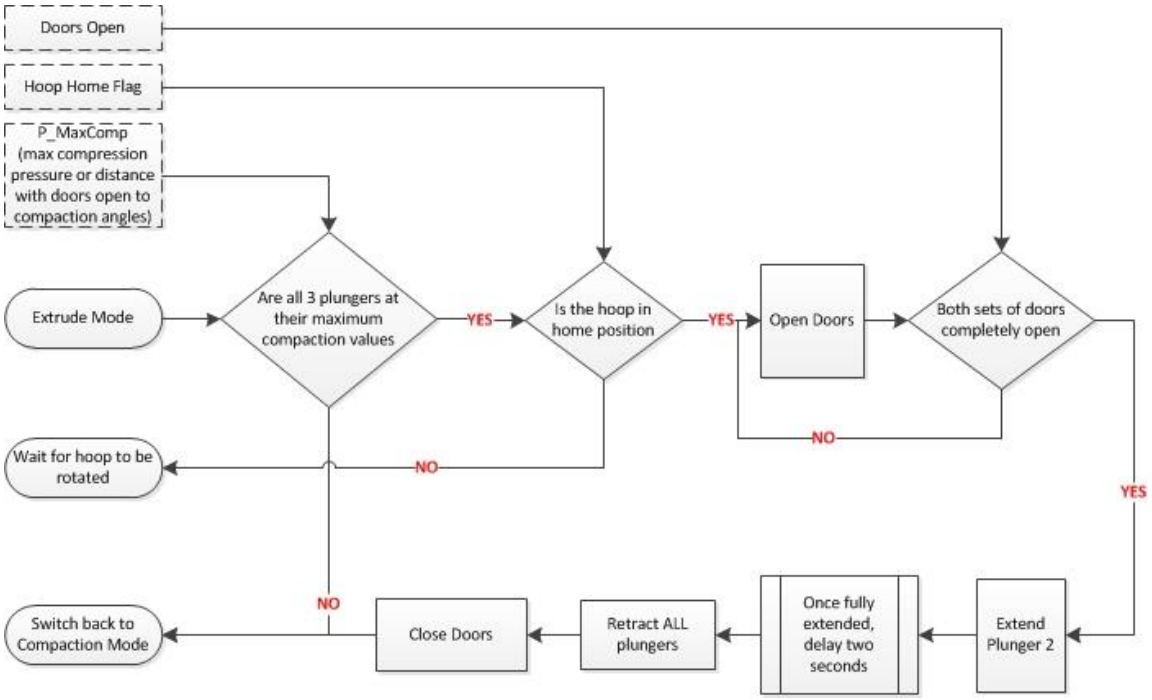

Figure 8.10: Control logic flowchart for extrude mode

Finally, when the hoop spun, the program was in rotate mode. Rotate mode took place during compaction with the doors closed. This way, multiple machine functions occurred simultaneously. In rotate mode, the program checked that the doors remained fully

closed. The logic allowed the hoop to rotate three times. On the third rotation, when the plastic track triggered the first limit switch, the control signal to the valve reduced the flow and slowed the rotation. Then, when the second limit switch was triggered, the hoop stopped in place. The silage bag could now be twisted tightly and was ready for sealing. The hoop remained in place and the cycle began again with a new module. The doors were allowed to open again as soon as the door closed cycle count reached the maximum value as stated previously.

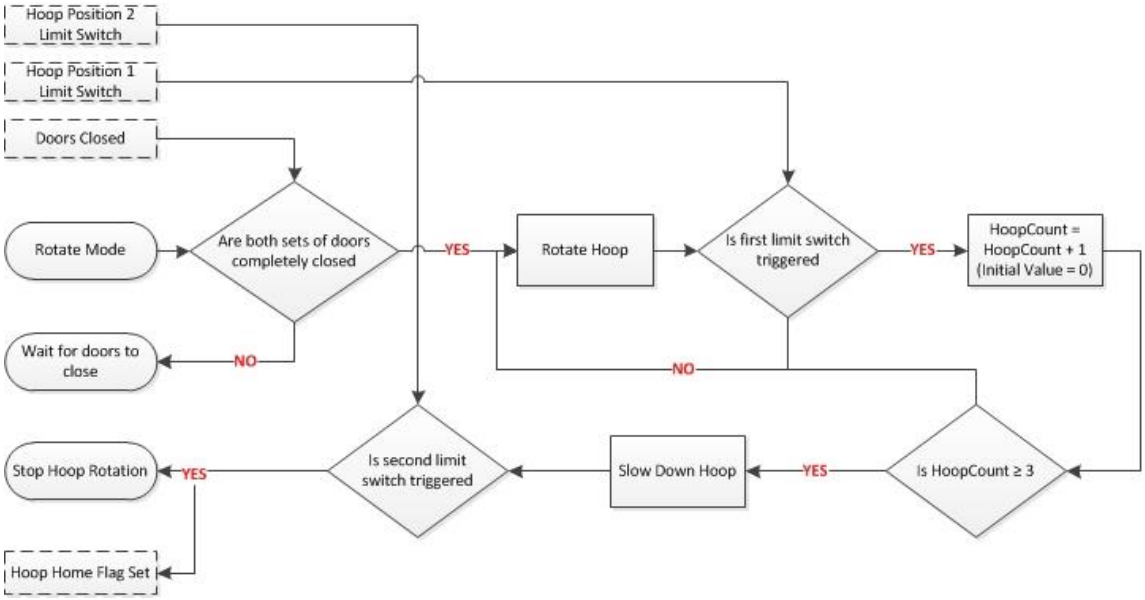

Figure 8.11: Control logic flowchart for rotate mode

8.2.3 Control Checkpoint Equations

The flagged points introduced earlier were used to develop a system of checkpoints for the automated program. With safety a big concern, these checkpoints allowed for more seamless operation of the machine. The checkpoints were established so that if any of the control logic was untrue, the machine would simply stop all movement and wait until either

the conditions were satisfied or the operator has taken over manual control. The checkpoint was placed in the PLUS+1 control program as a final Boolean switch directly before the current value to the valve module was set. Each work function required its own set of control checkpoint equations. The product of sums method was used to create a final checkpoint switch in the PLUS+1 program. With the sequential nature of the control flowcharts, it was necessary to make sure each logical flag was verified before valves can be actuated. The logical flags in section 8.2.1 were assigned identities for these equations. The equations also provided shutoffs for ambiguous situations. This way, the plungers were only allowed to extend or retract exactly when needed, and the control program would not send any signal to the valves if these conditions were not met.

Table 8.2: Logical flags for control checkpoints of plungers, doors, and hoop

Logical Flag	Identity
Plunger retracted	X1
Plunger at max compression point	X2
Plunger extended	X3
Doors closed	X4
Doors at compression angle	X5
Doors open	X6
Hoop Home	X7
Compaction Mode	X8
Extrude Mode	X9
Rotate Mode	X10

The plungers required checkpoint equations for both extension and retraction. The extension of the plungers depended on the ten different logical flags above. The following equations represent the simplified control checkpoints for plunger extend and retract. These two signal check equations ensured that the plungers did not crash into the doors or compact the material with too much force, and they also checked that the plunger was travelling the correct distance based on the mode they machine was operating in.

$$PlungerExtendCheck = X_6X_7\overline{X_8}X_9\overline{X_{10}} + \overline{X_2}X_4X_8\overline{X_9} + \overline{X_2}X_7X_8\overline{X_9X_{10}} \quad \text{Equation 8.3}$$

$$PlungerRetractCheck = X_4X_8\overline{X_9} + X_7X_8\overline{X_9X_{10}} + X_6X_7\overline{X_8}X_9\overline{X_{10}} \quad \text{Equation 8.4}$$

The door control checkpoints required slightly more detail with the two-paired door system. Additional logical flags had to be added to ensure that the two sets of doors did not crash into each other. Those additional points and their identities are found in Table 8.3.

Table 8.3: Additional logical flags for individual door control checkpoints

Additional Logical Flags	Identity
Top/Bottom door closed	X11
Top/Bottom door at compression angle	X12
Top/Bottom door open	X13
Left/Right door closed	X14
Left/Right at compression angle	X15
Left/Right door open	X16

The two outermost doors, left and right, had the simplest control checkpoints for opening, regardless of the mode. They required the hoop to be stationary and in the home position before moving. The top and bottom doors could not open until the left and right doors opened both in extrude and compaction mode.

$$LR\ Door\ Open\ Check = X_7X_8\overline{X_9X_{10}} + X_7\overline{X_8}X_9\overline{X_{10}} + X_7X_8X_9\overline{X_{10}} \quad \text{Equation 8.5}$$

$$TB\ Door\ Open\ Check$$

$$= X_7X_8\overline{X_9X_{10}X_{12}}X_{15} + X_7X_8\overline{X_9X_{10}}X_{16} + X_7\overline{X_8}X_9\overline{X_{10}}X_{16} \quad \text{Equation 8.6}$$

$$+ X_7\overline{X_8X_9X_{10}}X_{16} + X_7\overline{X_8X_9X_{10}X_{12}}X_{15}$$

The checkpoint equations for the doors closing were also rather complex. The equations assured that the doors could not close on each other or while the plungers were

extruded. The top and bottom doors must be closed before the left and right doors were allowed to.

$$TB\ Door\ Close\ Check$$
$$= X_1X_8\overline{X_9X_{10}X_{14}} + X_1X_7\overline{X_8}X_9\overline{X_{10}X_{14}} + X_1X_7\overline{X_8X_9X_{10}X_{14}} \quad \text{Equation 8.7}$$

$$LR\ Door\ Close\ Check$$
$$= X_7X_8\overline{X_9X_{10}}X_{11}\overline{X_{12}X_{13}} + X_7X_8\overline{X_9X_{10}}X_{12}\overline{X_{13}X_{15}}$$
$$+ X_7\overline{X_8}X_9\overline{X_{10}}X_{11}\overline{X_{12}X_{13}} + X_7\overline{X_8X_9X_{10}}X_{11}\overline{X_{12}X_{13}} \quad \text{Equation 8.8}$$
$$+ X_7\overline{X_8X_9X_{10}}X_{12}\overline{X_{13}X_{15}}$$

The rotate signal checkpoint was by far the simplest one of all. The hoop could rotate as long as the doors remained closed and the program was not in the extrude mode.

$$Rotate\ Check = X_4\overline{X_9} \quad \text{Equation 8.5}$$

With all of these safeguards in place, the PLUS+1 control program delivered a much more robust process for manipulating the work functions of the machine. Graphical views of the truth table equations shown here can be found in the Appendix.

8.2.3 Data Logging

The last portion of the electrical and control system involved data logging. In order to understand the details of how the machine was operating as well as provide lasting data, the HEM Data Mini Logger was utilized. The data logger recorded all of the logical flagged points that have been mentioned here. Also, the logger registered the raw data for the sensors. This included plunger pressures and distances and door pressures and distances. This data was eventually used to verify the compaction chamber pressure model created.

Power to the data logger came from the main power bus coming into the electrical box. A MicroSD card inside the logger stored the data. As stated, the logger received messages over the CAN bus network. The J1939 protocol was used in case the machine will be integrated in the future with other equipment. In order to package the messages, the PLUS+1 program contained code to claim an address as well as assign PGN numbers (Parameter Group Numbers). Data was packed into five unique CAN messages and transmitted to the logger. A program called DawnEdit was used to set up a database for the CAN messages. DawnEdit created a configuration file for the data logger that must be uploaded upon first use. This configuration file set the logger to only record specific CAN messages, in this case the five messages sent from the PLUS+1 controllers. Once the machine was run, the MicroSD card was inserted into a computer and the DawnEdit program decoded the CAN messages into useful data and converted the file to a .csv file which could then be used in programs such as Microsoft Excel.

CHAPTER 9: FABRICATION, ASSEMBLY, AND PRELIMINARY FINDINGS

Welding of components was completed by Quality Manufacturing, in Urbandale, Iowa, including all major steel frames, plungers, doors, and hoop. The entire machine fabrication was completed at the Iowa State Agricultural Engineering and Agronomy Farm in Boone, Iowa. The machine was built onto a 7 m deck-over Kaufman trailer with a pintle hitch (Kaufman Trailers, Beaver City, NE). The tandem axle trailer is rated for 10,200 kg with an 5.5 m flat deck and 1.5 m dove tail. Stake pocket sleeves welded to the bottom frame of the compaction chamber slid into the side rails of the trailer and were pinned. The hinge between the compaction chamber and the doors was placed at the start of the sloped dove tail, and the floor boards on the dovetail were removed to provide room for the hoop to spin. The front section of the trailer was used to mount all of the hydraulic drive components including the PTO pump, hydraulic reservoirs, filters, and control valves, as well as the electrical control box. Drop-leg jacks mounted on each front corner of the trailer deck could swing down for stability during testing.

9.1 Main Assembly

With the bottom frame mounted to the trailer, the side frames were bolted together next. From there, the trusses, front cross members, and plungers were placed in. The hydraulic compaction cylinders slid in from the sides. Finally, top frame including the hopper and conveyor assembly finished the initial compaction chamber. Next, the two sets of doors and door cylinders were mounted, followed by the stationary hoop structure and tire assemblies. The two piece hoop assembly started by placing the bottom half on the bottom

two drive tires and bolting on the top half. The hoop was then adjusted into place. Finally, all other hydraulic components and sensors were mounted. Hoses and wiring harnesses were routed through clamps and secured.

Figure 9.1: Large module builder prototype with all structural, hydraulic, and electrical components

9.2 Finished Module Platform

As the module was formed, it extruded from the rear of the machine. Therefore, some type of platform must be added to hold the finished module. In order to create a surface that will not tear the silage bag or disrupt the module, roller beds were used. Removing the ramps from the trailer left mounting points for a frame. A steel bed frame with roller beds bolted on top was fastened to the frame on the rear edge of the trailer. Two hydraulic cylinders rotated the roller bed frame up or down. The range of motion of the

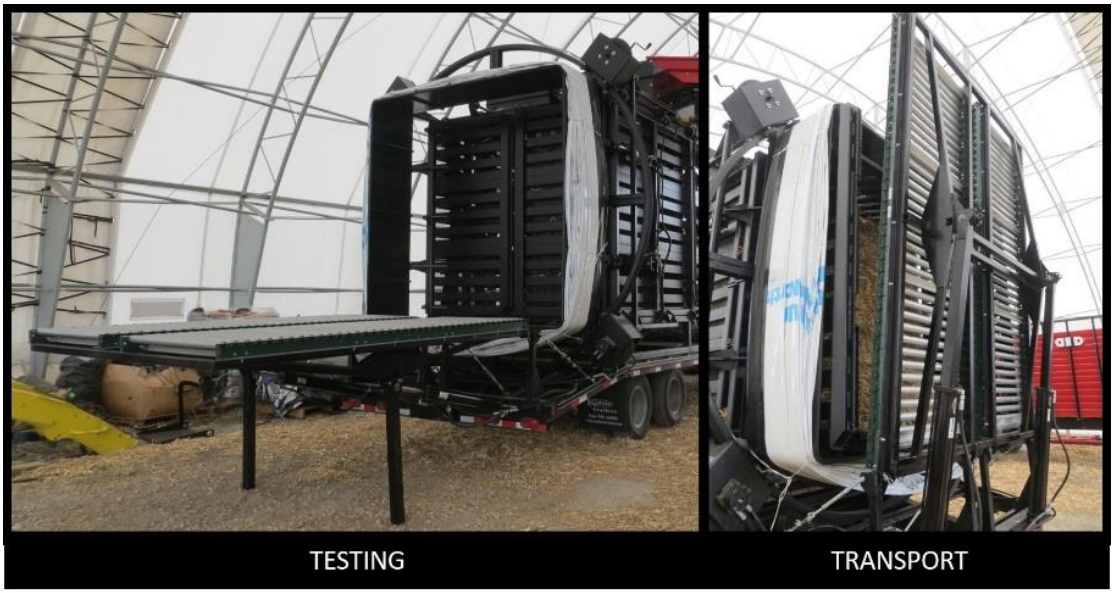

Figure 9.2: Finished module platform in both testing and transport positions

roller bed platform was from the ground to nearly vertical. The vertical position could be used for transport. During transport, cylinder stops swing into place to prevent the bed from falling down. Conversely, these same stops provided stands to keep the platform level as the module was extruded from the chamber.

9.3 Preliminary Findings and Modifications

With a working prototype machine, the focus shifted to trial runs of the machine. Initially, some loose stover was compacted to understand the basics of the operations. Most of the functions of the large module builder seemed to be fairly acceptable. However, some small issues were targeted to be fixed before data was collected.

9.3.1 Support for Plunger Face

The trial runs completed with the doors closed led to alignment issues of the plunger face. The hydraulic cylinder pins at the plunger end of the cylinder are oriented in the horizontal direction, with the axis of rotation in such a way that the plunger face can rotate. During the development stage, it was assumed that the track and floor structures on each plunger set would provide enough strength to hold the plungers from rotating. When loose material is loaded into the machine and compaction chamber is not completely full, the pile is larger at the bottom and smaller at the top. This gradient in material caused the top edge of each plunger to lead the bottom edge when compacting. Therefore, additional steel reinforcement was added to the upper and lower tracks. Also, a steel plate with square tubing reinforcement was added to tie the upper track to the lower track more securely (Figure 9.3). This strengthening was enough to prevent the plunger face rotation.

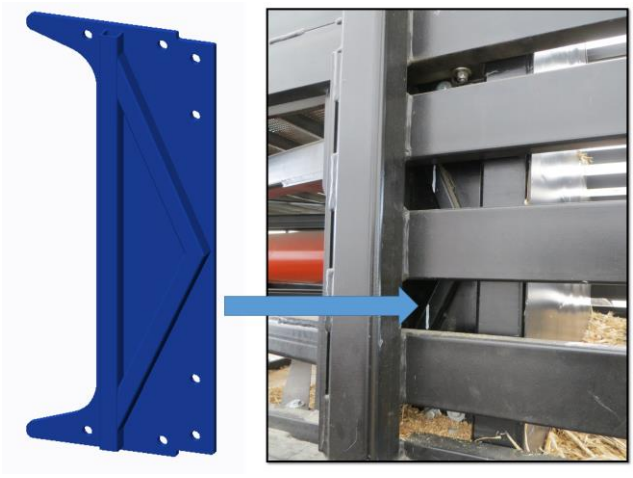

Figure 9.3: Support frame for to keep plunger from rotating

9.3.2 Outside Door Edge Support

Figure 9.4: Support tube added to edge of outer doors

In addition, when the material was pushed against the closed doors some deformation occurred in the door frame itself. The compacted material attempted to force the inside set of doors to open. This stress caused the outside doors to bow along the center edges where the left and right doors meet. The hydraulic cylinder force provided was sufficient to hold back the material, however, the door structure itself was lacking in strength along this edge. The door frame would bow the most in the sections where the c-channel tracks met one another. The solution was to place an extra length of tubing matching the dimensions of the rectangular slats along the edges of the outside doors.

9.3.3 Compaction Chamber Expanded Metal

With the trial runs, the stover would compact relatively well, and then have a significant amount of spring-back, meaning it would creep back towards the plungers after the plungers were retracted. To add more friction, expanded metal was added, to line the entire inside surface of the compaction chamber, from the initial frame to the rear edge of the doors. The c-channel tracks were left open so the plungers could travel through. This expanded metal provided a surface with a

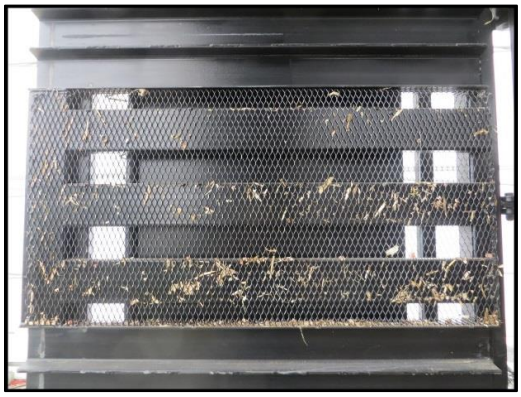

Figure 9.5: Expanded metal welded to inside of left door

much higher coefficient of friction for the stover to slide past. The addition of the expanded metal considerably reduced the spring-back of the compacted material, and results in higher densities.

9.3.4 Silage Bag Retainer and Ramp

During initial testing, an attempt was made to extrude the compacted material and package it. The bag was tied off and the module extruded. While doing this, the entire silage bag started to slide off the square portion of the hoop frame, rather than unfold. Also, on the bottom side, the bag would sag down. The frame member on the hoop between the circular rolled tubing and the square section was used to mount supports for the silage bag. On the bottom of the hoop, a small welded shelf is bolted to this support. On top surface of that shelf, half-inch thick UHMW plastic protects the bag from tearing. For the top retainer, a similar style support was used, but also included a small plastic overhang which capped the folded up portion of the bag and held it onto the hoop (Figure 9.6).

In addition, the gap between the door outlet and the roller bed frame allowed for the material and silage bag both to fall down. This would cause the entire module to stop

Figure 9.6: Silage bag retainer mounted to rotating hoop

Figure 9.7: Ramp to bridge gap between door outlet and roller bed

moving on the bottom, but continue moving on the top. A steel frame with a slight ramp on the front was built and covered in the same 1.3 cm thick UHMW plastic (Figure 9.7). This assembly provided a bridge for the module to be extruded onto the finish module platform as well as a method for keeping the bag situated on the hoop.

CHAPTER 10: METHODS AND MATERIALS

With these adjustments made, initial testing of the machine could be completed. For this research, the goals of testing the prototype machine include determining the achievable density of a large square module as well as verifying the scaled up compaction chamber pressure model derived from Afzalinia and Roberge (2008). Testing was completed during - the spring of 2014 at the Iowa State University Agricultural Engineering and Agronomy Farm in Boone, Iowa.

10.1 Testing Materials and Equipment

Since the prototype was testing in the springtime, previously baled corn stover provided the loose material. Large square bales 0.9 by 1.2 by 2.4 m were cut apart and broken up to serve as the loose stover. The bales had been stored either inside or under cover and had minimal damage and rotting. The bales originated from a single pass harvest system and consisted mostly of stalks and leaves from the corn plant. The material was dry with an average moisture content of 11.7%.

Figure 10.1: Sample of loose stover used for testing

Testing was completed in a stationary position. The large module builder prototype was attached to an 8310R John Deere tractor, and the PTO shaft connected. The loose material was held in a Meyer forage wagon, pulled by a 7215 John Deere tractor. The forage wagon has both front and rear discharge capabilities. The existing large square bales were broken up and placed in the forage wagon. The wagon is equipped with weigh bars and a scale to measure the weight of the loose material entering the large module builder prototype.

In order to carry the material from the forage wagon to the hopper of the large module builder, a Logan Fill Pro Planter Filler was used. The planter filler originates from the potato industry. It contains a 76 cm

wide chevron patterned belt, and a five foot tip-down extension on the end of the belt. The loading hopper on the planter filler was placed directly beneath the side discharge at the front of the forage wagon. Modified lifting linkages added approximately an extra 0.6 m of height to the planter filler. This way, the 1.5 m tip-down extension could be placed over top of the module builder hopper in order to place material in the center of the feed

Figure 10.2: Test location setup for large module builder prototype

conveyor belts.

10.2 Testing Procedure

Since the machine had never been run before, this testing utilized the manual mode operation, meaning that all functions were controlled through the use of the switch box and the corresponding data recorded. This was deemed acceptable to prove the limits of the machine as well as establish a starting point for future work and further control development. Upon startup of the machine, the initial weight of the forage wagon was recorded and the tractor PTO speed was set to 700 rpm. This equates to a maximum flow rate from the pump of about 87 lpm. The flow was kept at this value simply to assure that no damage would occur to the prototype during the initial testing.

Two different treatments were included in the testing procedure in order to determine the effects of the door angle as well as determine the side wall pressures. Treatment 1 involved fully opening the doors after the initial small module was complete. Treatment 2 opened the doors as well, but stopped them at the compaction angles. For both treatments, the building the module began with the doors completely closed. Three repetitions were completed with each treatment, for a total of six full modules completed.

The testing procedure began with the doors closed. Then material was conveyed up and into the hopper. The feed system was run continuously until the initial compaction chamber was as full of loose material as possible. Occasionally, the top two plungers would be extended to more fully fill the top outer corners of the chamber. Care was taken not to compact the material, but simply move it out of the way. This space was then filled with additional loose material. When the compaction chamber was full, the feed system was

turned off and the weight of material loaded into the machine recorded. For cycle number one, the plungers were extended then one at a time, starting with the bottom plunger. The plunger was stopped in place once the doors were observed to bow slightly under the pressure. The middle plunger followed, stopping again when the doors began to deform. Finally, the top plunger was extended in the same fashion. The plungers were then retracted sequentially, starting with the bottom. The small scale test stand presented earlier suggested that this sequential method produced a more even and stable module face, and the testing completed with the full scale prototype reinforced this observation.

The forage wagon, planter filler, and feed conveyors were started up again and additional loose material placed into the compaction chamber in the space left between the already compacted material and the plunger faces. Now, with an existing compacted module face, the volume to fill with loose material did not require cycling the top two plungers to fill the chamber. The plunger extension and retraction procedure was followed in the same way as cycle number one. At the end of cycle number two, the initial compaction chamber (with doors closed) was completely full of compacted material. The module face was nearly even with the end of the throat opening in the top frame.

10.2.1 Treatment 1: Fully Open Doors

The following procedures are where the two treatments differ. For Treatment 1, the doors were fully opened, and the existing module remained unmoved. The compaction chamber was filled again with loose material. For the remainder of the compaction cycles, all three plungers were extended simultaneously. The plungers were then stopped at a distance 7.6 cm past the end of the throat opening. This causes the loose material to be

compacted, and the full module to move slightly into the door section. The retraction of the plungers, however, was still done sequentially. Once the plungers were retracted, the filling process and plunger cycles continued until the rear of the compacted module reached the outer edge of the doors. This was considered to be a full compacted large module. With the weight of material loaded into the machine for each cycle, the full weight of the module can be known. In addition, the volume of the module is known from the physical measurements. This way, the density was calculated. Also, data logged during the duration of the test run provides pressure and distance values for the system.

10.2.2 Treatment 2: Angled Doors

Treatment 2 involved holding the compaction angles of the top, left, and right doors. Once the initial small module was created, the left and right doors were opened first, stopping at an angle of 6.5 degrees. The top and bottom opened next, with the top door stopped at 6.5 degrees as well, and the bottom opened completely. The filling and plunger procedure was carried out exactly as in Treatment 1. At the end of each cycle, the pressure produced by compaction pushed the doors out slightly, lessening the compaction angle. Once the plungers retracted completely, this door distance was recorded and the top, left, and right doors returned to the correct measurements.

10.2.3 Other Testing Procedure Considerations

During module formation, the rear face of the module did not stay together throughout the entire process. As the module was compacted from the front, flakes of compacted material often fell off the back and dropped onto the finished module platform or the ground. Tarps laid out on the ground accumulated any stover that fell off of the finished

module platform. At the end of each module repetition, this dropped material was collected, placed back into the Meyer forage wagon, and weighed. This weight of dropped material was subtracted from the total weight of material that was loaded into the large module builder, producing an accurate final weight of each module. After this process was complete, the module compaction chamber was completely cleaned out of all stover and the doors were closed, ready for the next repetition. In addition, material availability constraints required the loose material to be run through the large module builder twice. Each batch of loose stover was used to produce one module from Treatment 1 and one module from Treatment 2.

CHAPTER 11: RESULTS AND DISCUSSION

Data analysis included multiple aspects of the testing procedure. First of all, simply looking at the graphs of each sensor reading for pressures and distances provided insight into what was occurring in the system. From there, important factors could be identified, such as where pressure spikes occur, lags between plungers, and effects of the compaction pressure on the doors. Also, the overall performance of the prototype was compared between the two treatments with the doors fully open or set at the 6.5 degree compaction angles.

With this data available, calculations for the density of each completed module as well as the pressure levels produced in creating the module were found. The density data was compared to common baling methods. The pressure data was used to analyze the forces placed on the system. Finally, additional testing trials completed provided observational data for machine functions other than strictly the compaction of the module.

The data logged by the HEM Mini Logger delivered a very clear picture of the status of the machine at each point along the testing. Figure 11.1 shows one full module replication for Treatment 1 with the doors opening fully before the third plunger cycle.

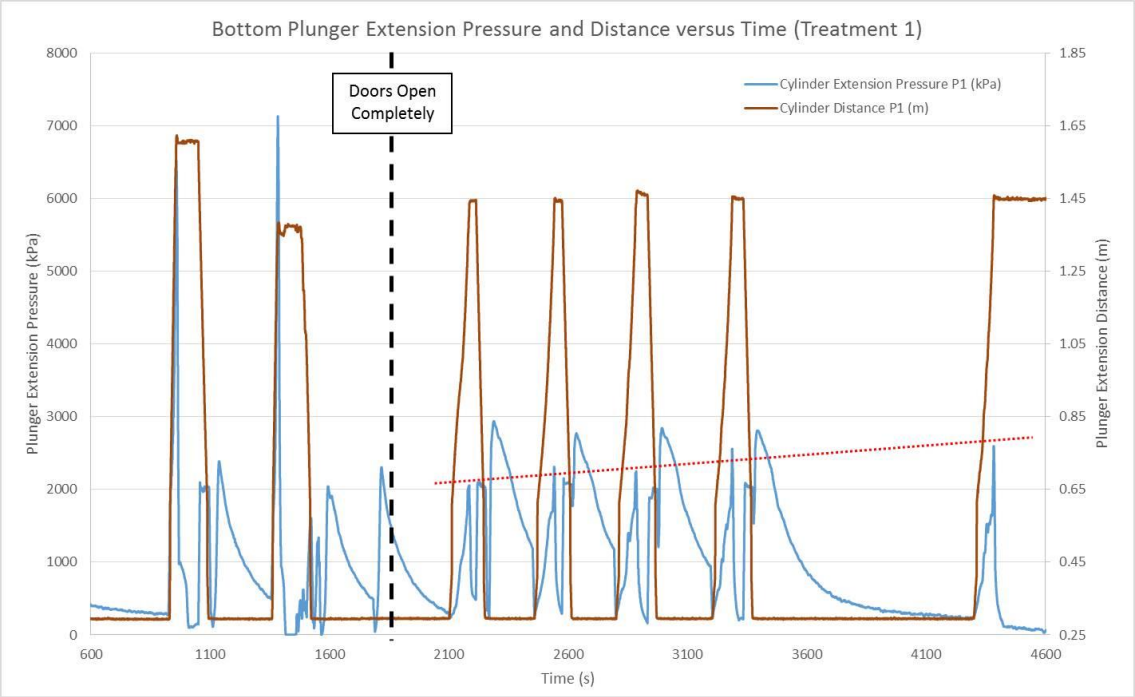

Figure 11.1: Graph of bottom plunger extension pressure and distance over time for Treatment 1 with doors opening fully

The graph is simplified to show the bottom plunger information only. This way the pressure spikes can be analyzed more easily for the moment. The first aspect to note is that the pressure spikes occurred very quickly, especially in the first two cycles where the doors were closed. As the material compresses in the small final portion, the pressure required to complete that compaction rises quickly. The next aspect of interest is in the second portion of the graph, where the doors were open. The pressure spikes, just before the plungers stop each time, increased slightly over the course of the five cycles, as denoted by the dotted red line. It is assumed that equal amounts of loose material were fed into the machine each cycle. Therefore, higher pressures were required to compact the same amount of material. This provides support in part to the compaction chamber pressure model derived, which shows that as more material is compacted in the chamber, the back pressure decreases due to the added friction on each side of the module.

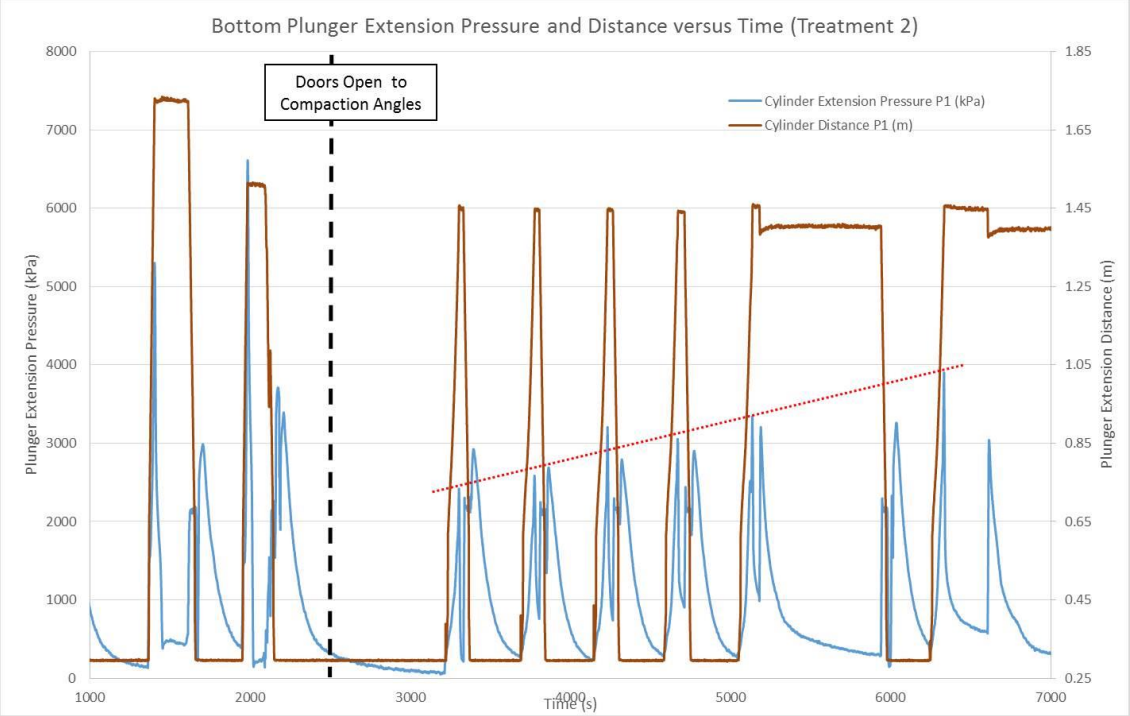

Figure 11.2: Graph of bottom plunger extension pressure and distance over time for Treatment 2 with doors open to 6.5 degree compaction angles

Similar trends were seen for Treatment 2, with the doors open to compaction angles. With the doors held at an angle, the plunger pressure required to complete the cycle increased. Not only did each individual spike increase, but the rate at which they grew also increased. This can be seen by the fact that the dotted red line has a steeper slope. The last plunger cycle to create a full module saw a pressure spike of nearly 4,000 kPa for the angled door scenario, whereas the last cycle for the open doors was only about 2,700 kPa. Graphs of the door pressure provide additional information. When plotted with the plunger travel, the door pressure was found to increase with each cycle. Figure 11.3 shows the same module as in Figure 11.2 however the door pressures are plotted rather than the plunger pressure. The graph only contains the portion with the doors open to their compaction angles.

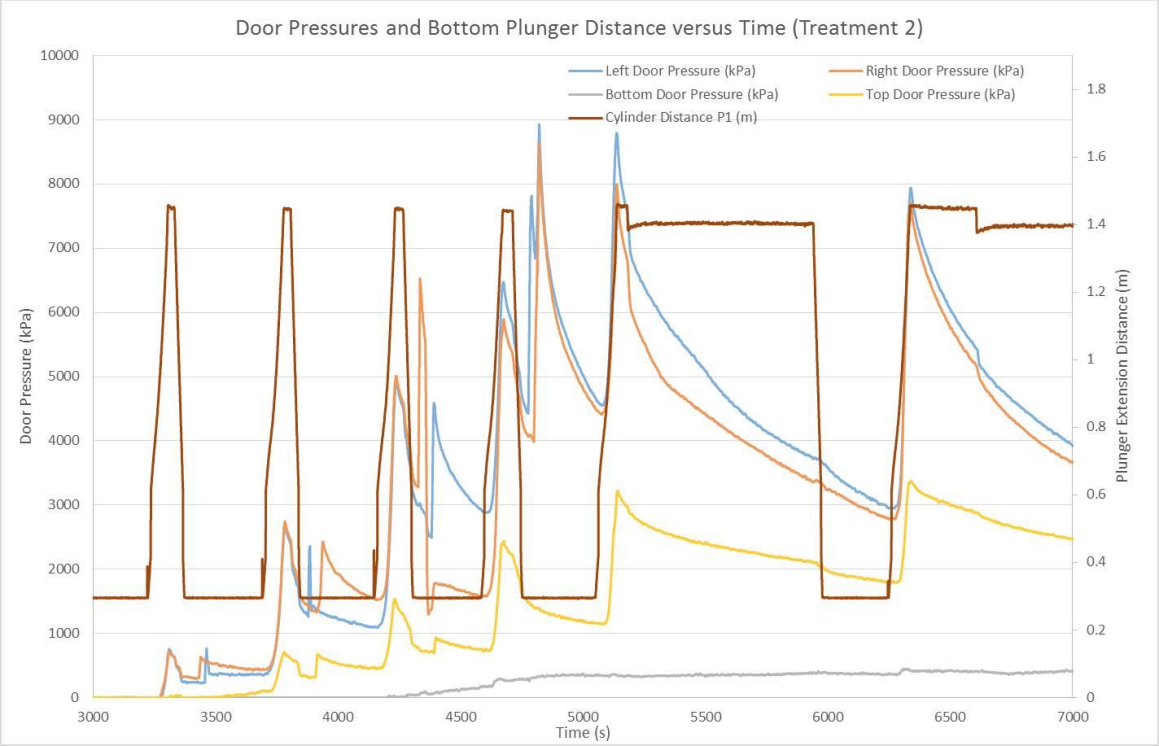

Figure 11.3: Graph of door pressures and bottom plunger distance over time for Treatment 2 with doors open to 6.5 degree compaction angles

It should be noted that the door pressure spikes when the plungers were fully retracted originated from returning the doors to the correct compaction angles, as they would drift open slightly with each plunger cycle. The compaction spikes, however, followed a relatively constant trend upward over time. The left and right doors showed the largest pressures. This can be explained by the fact that all three plungers were pushing on the side doors. The top door still saw pressure spikes of a lower value, but only the top plunger was effectively pushing on this door. The bottom door was completely flat, explaining the nearly constant pressure. Again, with the equal amounts of loose material fed in for each plunger cycle, the increases in plunger and door system pressures led to the result that the module became increasingly dense as length of compacted material increased in the chamber.

11.1 Module Density

The first objective of testing the prototype machine involved determining the achievable densities of the modules created. To start, the volume of the finished module for each treatment had to be found. This was completed through the help of two CAD models evaluated for volume. The volume for the open door condition and the angled door condition were found to be 11.4 m^3 and 10.8 m^3 respectively.

Figure 11.4: CAD models used to find true volume of finished modules for both Treatment 1 (left) and Treatment 2 (right)

Each module's final weight was calculated after subtracting the dropped material, then the density was calculated. Table 11.1 shows all six modules, their corresponding final weights, and their densities.

Table 11.1: Results for full module weights and densities for both open and angled door treatments

Open Doors (Treatment 1)			Angled Doors (Treatment 2)		
Module #	Module Weight (kg)	Module Density (kg/cubic m)	Module #	Module Weight (kg)	Module Density (kg/cubic m)
2	1,374	121.1	1	1,669	154.8
4	1,361	119.9	2	1,447	134.2
6	1,352	119.1	3	1,751	162.3
Average	**1,362**	**120.0**	**Average**	**1,622**	**150.4**
Standard Deviation	**11**	**1.0**	**Standard Deviation**	**157**	**14.6**

11.1.1 Module Density Discussion

The average densities are acceptable for initial prototype development. The control case with the doors open was able to compact the stover to nearly 120 kg/m^3, with a standard deviation of 1. The angled door case increased that density by about twenty-five percent to 150.4 kg/m^3, with a standard deviation of 14.6. Even with the larger standard deviation, the density can be expected to be greater with the angled doors. The density of the angled door modules compares respectably to some common baling methods, with a much larger package size. Large square baling methods average somewhere in the 160 to 192 kg/m^3 range. The densities achieved with the large module builder were somewhat lower than this range. However, due to the fact that this data was the first round of tests for this prototype machine, it can be expected that with some modifications, the achievable density will be increased. In addition, the concept of angling the doors was proven to significantly increase the final module density.

11.2 Compaction Chamber Pressure Model Validation

In order to validate the compaction chamber pressure model, three different data points from each module were evaluated. When the doors were closed, the recorded door pressure data can be used to calculate the back pressure, P_x, produced by the module. Also, at the full module point, or the last cycle, the back pressure can be assumed to be equal to zero. An attempt was made to validate the model for P_x with these three points from each module repetition.

The first two cycles of each treatment were conducted exactly the same with the doors completely closed. Therefore each of these data points was evaluated in the same

manner. The distance of each plunger was recorded by the data logger. Accounting for the deadband distance of the sensor, the length traveled by each plunger was calculated. Then the three plunger distances were averaged. This average was used to find the compacted stover length, L_c, for each cycle. The extension pressure, P_p, of each plunger was noted at the point when all three plungers had reached their compaction distance, and the force applied, F_p, by each was calculated. The effective cy-linder extension area, A_p, for each cylinder is 153 cm^2.

$$F_p = P_p * (A_p * 2) \qquad \textbf{Equation 11.1}$$

The total force applied by all three plungers was assumed to create a uniform pressure load on the module face. The module face has a width, W_m, and a height, H_m. In this way, the average module face pressure, P_f, produced by the plungers was evaluated.

$$P_f = (F_{p1} + F_{p2} + F_{p3}) * (W_m * H_m) \qquad \textbf{Equation 11.2}$$

With the average module face pressure, the derived model for back pressure is evaluated at the length found from the plunger distance data. This produces a predicted value for the back pressure, $P_{x\_predicted}$, in the initial module compaction chamber (with doors closed). The closed door situation was simplified with some assumptions. The module face pressure load was assumed to be acting on the top and bottom (inside) doors. For the left and right doors (outside) the resistive forces from the door cylinders were assumed to be acting on the top and bottom door equally, at a point in the center of the module. The simplified free body diagrams above explain these assumptions. The bottom door is identical to the top door, and the left door is identical to the right door.

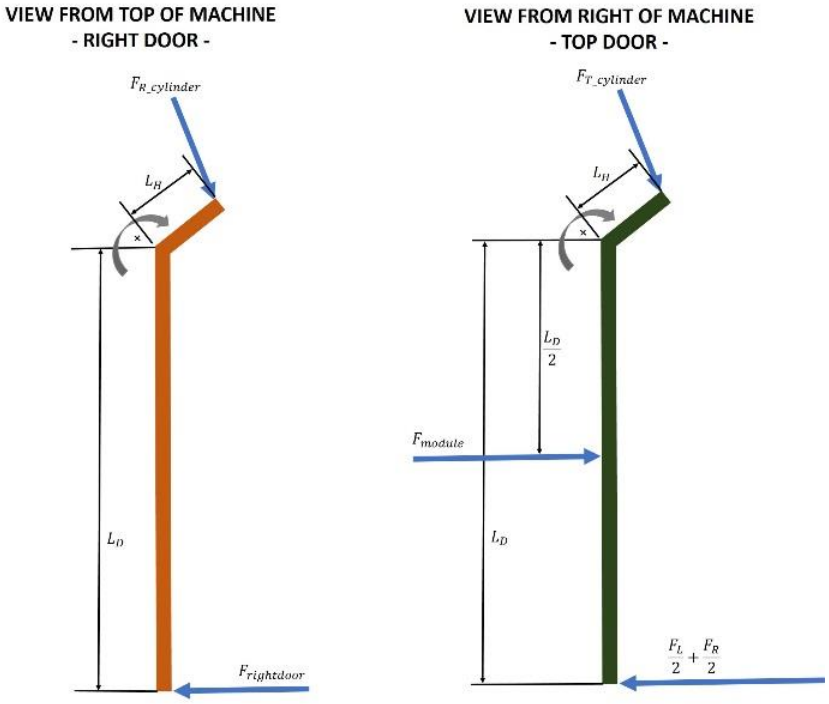

Figure 11.5: Free-body diagrams of top and right door

Then, the data from the door cylinders provided measurements of the pressure loads on each door. At the same data point where the plunger pressures were evaluated, the door pressures, P_d, were also pulled from the data set. The effective cylinder extension area for the door cylinders, A_d, is 70 cm^2. With this way, the force exerted by each door was calculated.

$$F_d = P_d * (A_d * 2) \qquad \textbf{Equation 11.3}$$

Utilizing the torque produced by the outside door cylinders and applying it as a force equally distributed between the top and bottom door, the following equation represents the summation of torques for each of the inside doors. In this equation, the desired variable is the force exerted by the module.

$$\sum M = 0 = \left[\left(\frac{F_L + F_R}{2}\right) * L_D\right] + \left(F_{T\_cylinder} * L_H\right) - \left(F_{module} * \frac{L}{2}\right) \quad \textbf{Equation 11.4}$$

$$F_{T\_module} = (F_L + F_R) + 2F_T\left(\frac{L_H}{L_D}\right) \quad \textbf{Equation 11.5}$$

$$F_{B\_module} = (F_L + F_R) + 2F_B\left(\frac{L_H}{L_D}\right) \quad \textbf{Equation 11.6}$$

This measured module force was then used to calculate pressure, $P_{x\_calculated}$.

$$P_{x\_calculated} = \left(F_{T\_module} + F_{B\_module}\right) * W_m * H_m \quad \textbf{Equation 11.7}$$

Evaluation of these parameters at each of the door closed cycles produced twelve data points. In addition, another six data points could be derived from the final plunger cycle of each module. The back pressure, P_x, for both the open and angled door cases was assumed to be equal to zero during the last plunger cycle. Again, by utilizing the recorded plunger distances travelled, a full module length was recorded. This compacted material length was input into the pressure model with the correct door angles to create a predicted back pressure. This predicted back pressure during the final cycle was then compared to the actual back pressure assumed to be zero.

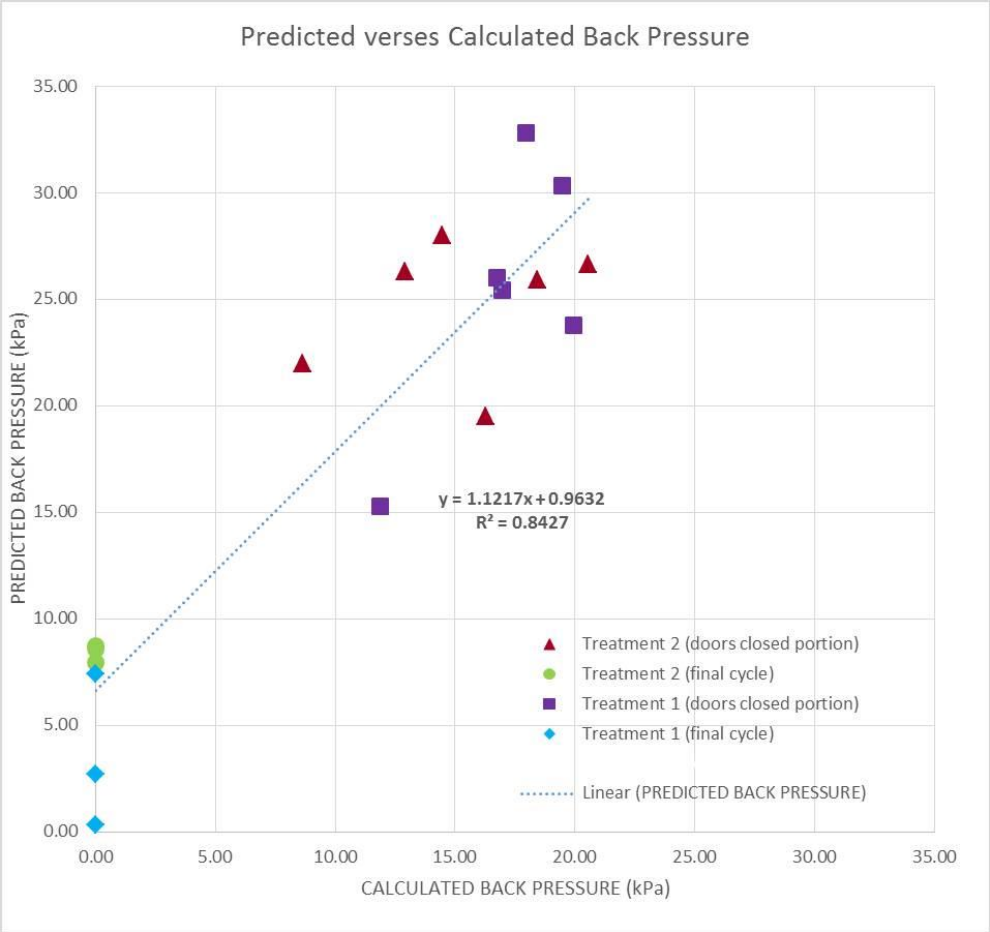

The results of the full eighteen data points are found in Figure 11.6. The graph was broken out by each treatment and also whether the doors were open or closed at the time of the data point. A linear regression line fit to the full data set produces an equation with a slope of 1.1217 and an offset of 0.9632. The linear regression line has an R-squared value of 0.8427.

11.2.1 Compaction Chamber Pressure Model Discussion

This research supported the model to predict back pressure in the module chamber. Although further testing with additional data points would be needed to fully validate the model, the data seems to follow the right trend. The slope of the regression line was found to

be 1.1217. If the model perfectly predicted the calculated pressures, this value would be equal to one. However, with variances in experimental data and this small data set, the testing completed here defends the model. There was not enough data to conclude any significant differences between the two treatments in terms of compaction chamber pressures. The regression line also accounts for 84% of the variability in the data set. This value was acceptable for now, but would hope to increase with further testing and data.

11.3 Observational Results

During the testing phase, additional observations were made about the overall machine functionality. Some of these observations included material compaction characteristics, formation of flakes, feed system issues, and packaging system trials. To begin, the material compaction before and after the installation of the expanded metal proved to be significantly different. Not only did the rough surface provide much better densification properties, but more importantly, it retained the material from falling back down off of the compacted face. With such a large surface area, this was very important for the integrity of the module.

Figure 11.7: Difference in module face quality before and after addition of expanded metal inside compaction chamber

Multiple compaction characteristics were observed. The most notable of these was the formation of large flakes, similar to those found in conventional large square bales. The flakes formed with each plunger compaction cycle, and definitive segments could be seen from one flake to the next. This flake-like formation was carried from top to bottom of the module. The overall flake was somewhat segmented between each plunger. However, there did appear to be some material compaction overlap between plunger sections, especially between the bottom and middle plungers.

Figure 11.8: Flake formation within compacted large module

This factor was mostly seen during cleanout of the compaction chamber. For example, the two photos show flake divisions. The flakes would fall or be pulled off of the module in large portions, and remain together until dropped back into the forage wagon.

11.3.1 Feed System Observations

Next, many different aspects were noted about the feed system and its impact on the filling of the machine. The hopper and conveyor system seemed to function enough to fill the compaction chamber, however there were some issues. First of all, the layout of the hopper and throat opening made it difficult to fill the top outer corners of the compaction

chamber. This meant that often times the top plunger had slightly less material in its section than the other two plungers. Furthermore, the rear edge of the throat did not have any type of cutting mechanism. Material often became trapped or pinched between the plunger face and the edge of the throat. This would cause the top plunger to lag behind the other two.

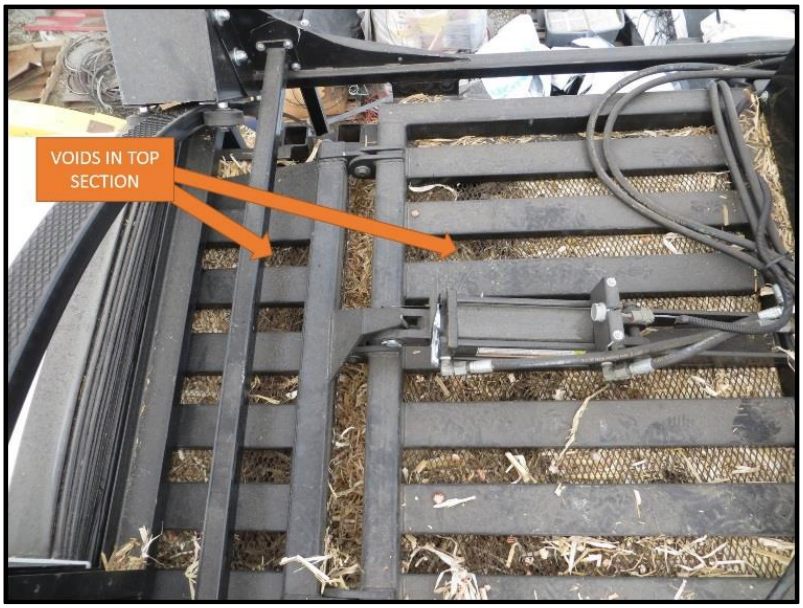

Figure 11.9: Effect of lagging top plunger from pinch point at end of throat opening

When this happened, the bottom two plungers would be shut off and the top would have to catch up. Between the under-filling of the chamber and the pulsing of the top plunger, stratification was seen to form in the top compacted section of the module. In addition, this section was always the first to fall once the module was extruded from the chamber, leading to the conclusion that it was not as dense.

11.3.2 Packaging System Observations

The quantifiable data for the scope of this project involves the compaction chamber itself. However, some examination of the packaging system was also completed. With a

module in the chamber, the silage bag was pulled out and sealed. For the trial run purposes, the simplest way to seal the bag was with two wood boards. The bag was pulled away from the hoop and the sides folded into the middle. Next, the bottom flap was folded around one of the boards. The top flap was placed into the fold and the board was rolled until tight against the module face. Then a second board served as a clamp. Wood screws held the two boards with the silage bag tight.

Figure 11.10: Sealed silage bag with wooden boards

Once the seal was complete, the plungers extended to extrude the module from the chamber. Upon first movement, the sealed bag and full module seemed to exit the chamber cleanly and still compacted. After about 1.2 m of the module was extruded from the chamber, the top, rear-most flake fell away from the module face.

Upon inspection, two factors were likely to have caused this issue. The first of these two was the gap between the doors and the finished module platform. A UHMW plastic ramp and table bridge the gap. However, as seen in the photo, higher resistance on the

Figure 11.11: Module extrusion issue with falling flakes

bottom of the module face allowed the top section to overrun the bottom section. Also, as previous photos have shown, the top plunger section was not as well formed as the bottom two, and therefore could not withstand the movement.

Another aspect of these findings was that the silage bag was significantly larger than the module being extruded from the chamber. With the current door and hoop design constraints, the smallest possible sized silage bag was used, however this still meant that there was about a 10 cm gap between the bag and the compacted module on the left and right sides. Despite these issues, the module sides remained flat inside of the silage bag, providing encouragement that this method could be viable in the future with further development.

CHAPTER 12: CONCLUSIONS AND RECOMMENDATIONS

Overall, the performance of the machine proved to be positive. Without the issues of attempting to package the material, the full modules generally remained intact upon extrusion from the compaction chamber. With additional work towards the silage bag portion of the machine, it is reasonable to say that a solution to compacting and packaging biomass in a single step could be possible with this type of machine design. In addition, the structure of the prototype machine was unharmed during testing and functioned well. Hydraulically and electrically, no major issues arose. Compaction capabilities were found to be comparable to other commonly used methods, with an average density of 151 kg/m^3 when the doors were held at an angle, which was 25% greater than the density with the doors fully open.

Figure 12.1: Large module builder machine with full module in chamber

In addition, the predictions for pressure within the compaction chamber nearly followed a one-to-one relationship with the calculated pressures found from the sensor data. A regression line fit to the data showed a slope of 1.12 and an R-squared of 0.82.

The hydraulic forces for compaction proved to be much lower than the maximum design constraints. This means that with some small modifications, opportunities exist to push this prototype further to increase densities. The models derived here for pressures in the compaction chamber are proven to be sufficient enough to predict the pressure profile in the compaction chamber, and can be expanded upon for further analysis.

Figure 12.2: Upright side face of compacted module

12.3 Initial Machine Recommendations

Some recommendations can be set forth for future improvement of the large module builder machine. Although the fundamentals were proven through this research, the machine is not capable of competing with current practices at the moment. To start with, some structural issues should be considered:

- Strengthening the door structure at the hinge points

- Add support at plunger end of grain bin flooring to prevent it from dipping down and packing stover
- Possibly further strengthening plunger rotation support frames and finding a better way to tie the upper and lower plunger tracks to each other

In addition, many of the compaction and density issues may be able to be solved by examining the design of the hopper and feed system:

- Attack pinch point problem at end of throat opening
    - Possibly place knife edge on end of throat and plunger
- Change conveyor design to incorporate cleated belts for better material flow
- Explore problem of filling evenly and out to the top corners of the compaction chamber
- Investigate issue of material settling more tightly at the bottom of the chamber than the top due to the length of fall of the material and gravity
    - Possibly design a pre-packing system from the top of the machine

With these initial recommendations and remedies, the module builder could undergo further testing and analysis. The experiments completed here could be replicated with much more data to fully validate the compaction chamber pressure model, as well as increase the achievable density.

12.4 Future Work Recommendations

Further into the future of the large module builder, some additional insight may help produce a marketable product. Some considerations include:

- Research on cycle times and efficiency in the field
- Explore possibility of other methods to actuate plungers
    - Possibly smaller cylinders, or even a scissor type design
    - Transition compaction and extrusion into two different stages to reduce size and cost of compaction cylinders
- Research to determine best possible packaging material and method
    - Design a closer fit between the bag hoop and the doors to lessen gap between module and packaging material
    - Possibly place packaging system after door section
- Investigate sealing possibilities for bag to determine if anaerobic storage is possible
- Move machine to more field-ready design: lighter, lower to the ground, and different axle/tire options

This research was completed to provide a prototype machine to produce a large square module of corn stover. The large square module is four times the size of one conventional large square bale. This would provide more efficient logistic and cost models for the biomass and biofuel industries. The concept and design of this large module builder was based on numerous calculations and analyses, which led to a working prototype. The prototype testing yielded encouraging results for both density of the module as well as predicting the pressures seen inside the compaction chamber of a machine of this size. Overall, the development, fabrication, and testing of this large module builder machine could provide a new outlook on these types of systems in the future.

APPENDIX

Table A-1: Large Module Builder hydraulic component bill of materials

Hydraulic System Components				
Component	Manufacturer	Part #	Quantity	Description
PTO Driveshaft	Waltersheid	1-3720-K	1	Driveline between tractor and pump
Driveline Bearing	Zero-Max	915-24	1	Overhung Load Adaptor
Hydraulic Pump	Danfoss		1	Series 45 axial piston pump
Hydraulic Reservoir	Buyers	9-8068	2	Main hydraulic reservoirs
Plunger Control Valve	Danfoss		1	PVG 32 valve assembly (3)
Door Control Valve	Danfoss		1	PVG 32 valve assembly (4)
Motors Control Valve	Danfoss		1	PVG 32 valve assembly (4)
Hoop Drive Motor	Parker	TL0170U080AAAA	2	Hydraulic Wheel Motor
Plunger Cylinder	Prince	PMC-54-1310-TGCT	6	Telescopic, double-acting hydraulic cylinder
Door Cylinder	Lynx	40LH10-150	8	Double acting hydraulic cylinder

Table A-122: Large Module Builder electrical component bill of materials

Electrical System Components				
Component	Manufacturer	Part #	Quantity	Description
Controller 1	Danfoss	MC050-022	1	Danfoss 50-pin microcontroller
Controller 2	Danfoss	MC050-010	1	Danfoss 50-pin microcontroller
Fuse Panel	Cooper-Bussman	15303-3-2-7	1	10-fuse, 3-relay bussed panel
Pressure Sensor	Danfoss	MBS1250	10	Heavy Duty Pressure Transmitter
Door/Level Distance Sensor	MaxBotix	MB7367	10	High Resolution Compact Ultrasonic Range Finder
Plunger Distance Sensor	Maxbotix	MB7369	3	High Resolution Ultrasonic Range Finder
Hoop Position Switch	Honeywell	SZL-WLC-A-N	2	General purpose limit switch

Table A-3: Door hinge strength calculations

INPUTS		
Bale Pressure	60	psi
Full bale force	552960	lbs
Number of bolts/side	5	
Total bolts	20	
Force/bolt	27648	lbs
BOLT SHEAR		
Bolt dia	0.625	in
Shear area (threads)	0.205887416	in2
Grade of bolt	5	
Tensile strength	120000	psi
Shear strength	72000	psi
Double Shear	29647.78792	lbs
BEARING STRENGTH		
Fu	58000	psi
Outer dia	3	
Lc	1.16	in
db	0.68	in
t	0.5	in
Ab	0.363168111	
Rn	40368	lbs
Bearing strength	30276	lbs
TEAR OUT		
At	0.41	in2
Tear out force	47560	lbs
FAILURE POINT	29647.78792	
FACTOR OF SAFETY	1.072330292	

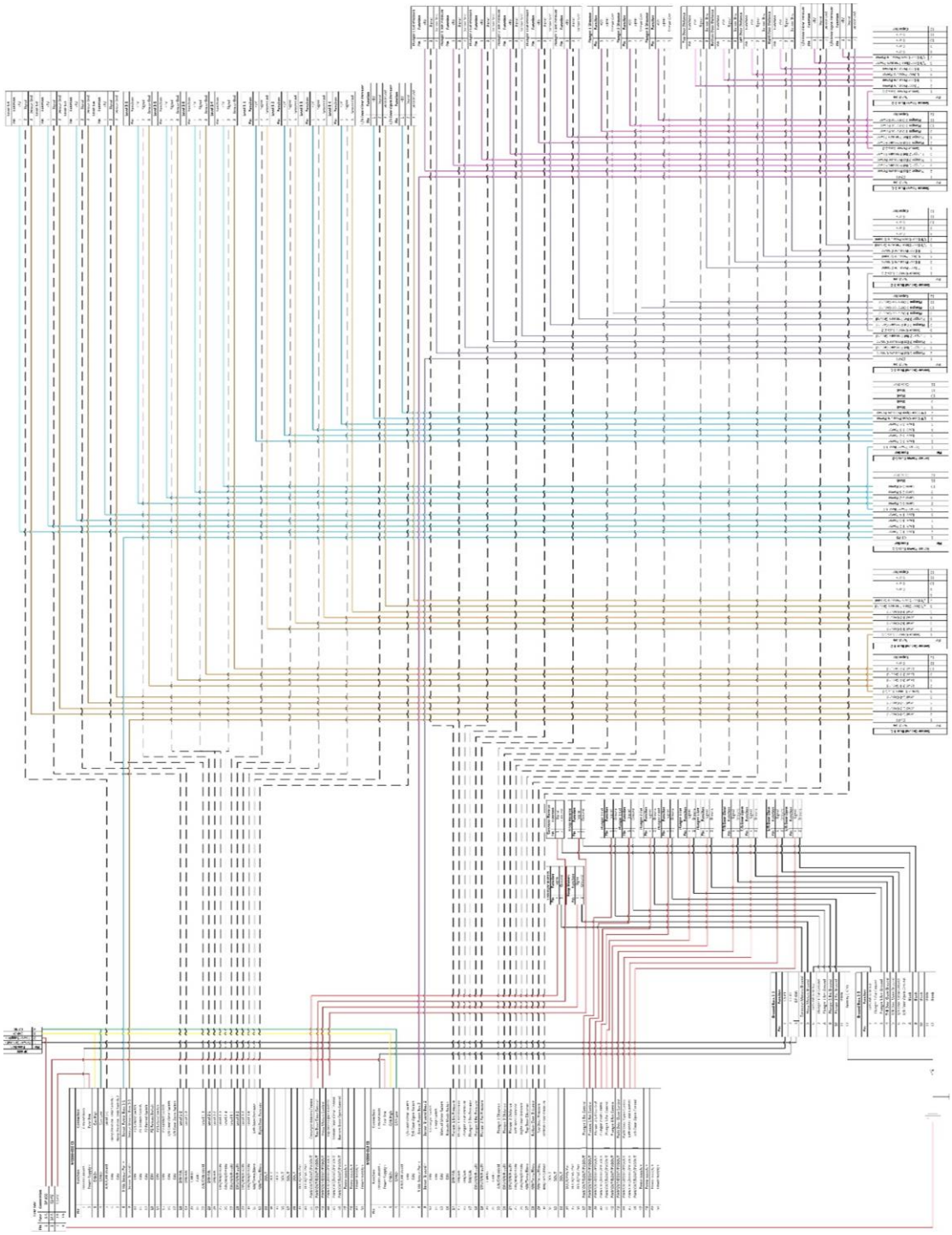

Figure A-1: Large Module Builder complete wiring diagram

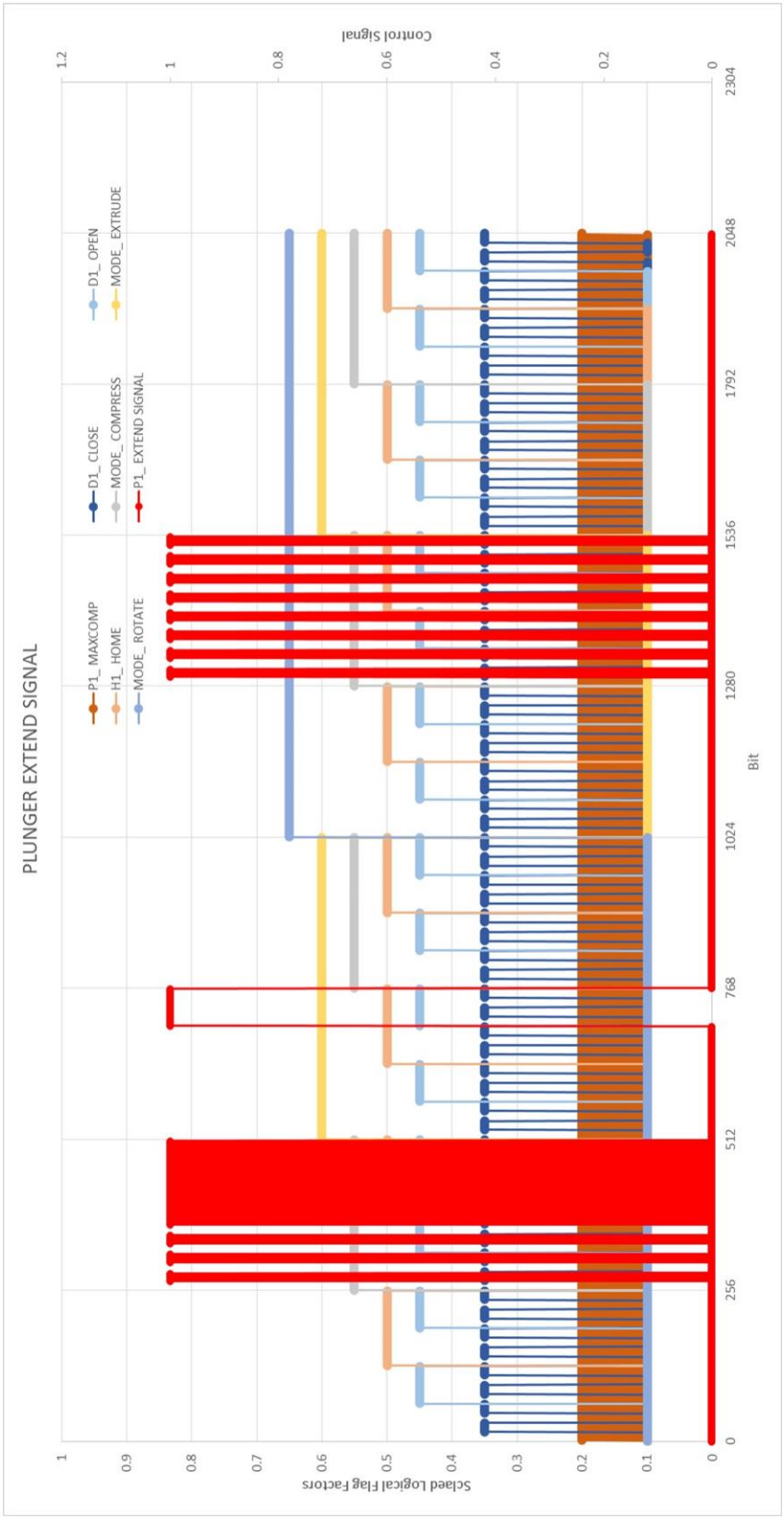

Figure A-2: Graphical overview of plunger extend control signal

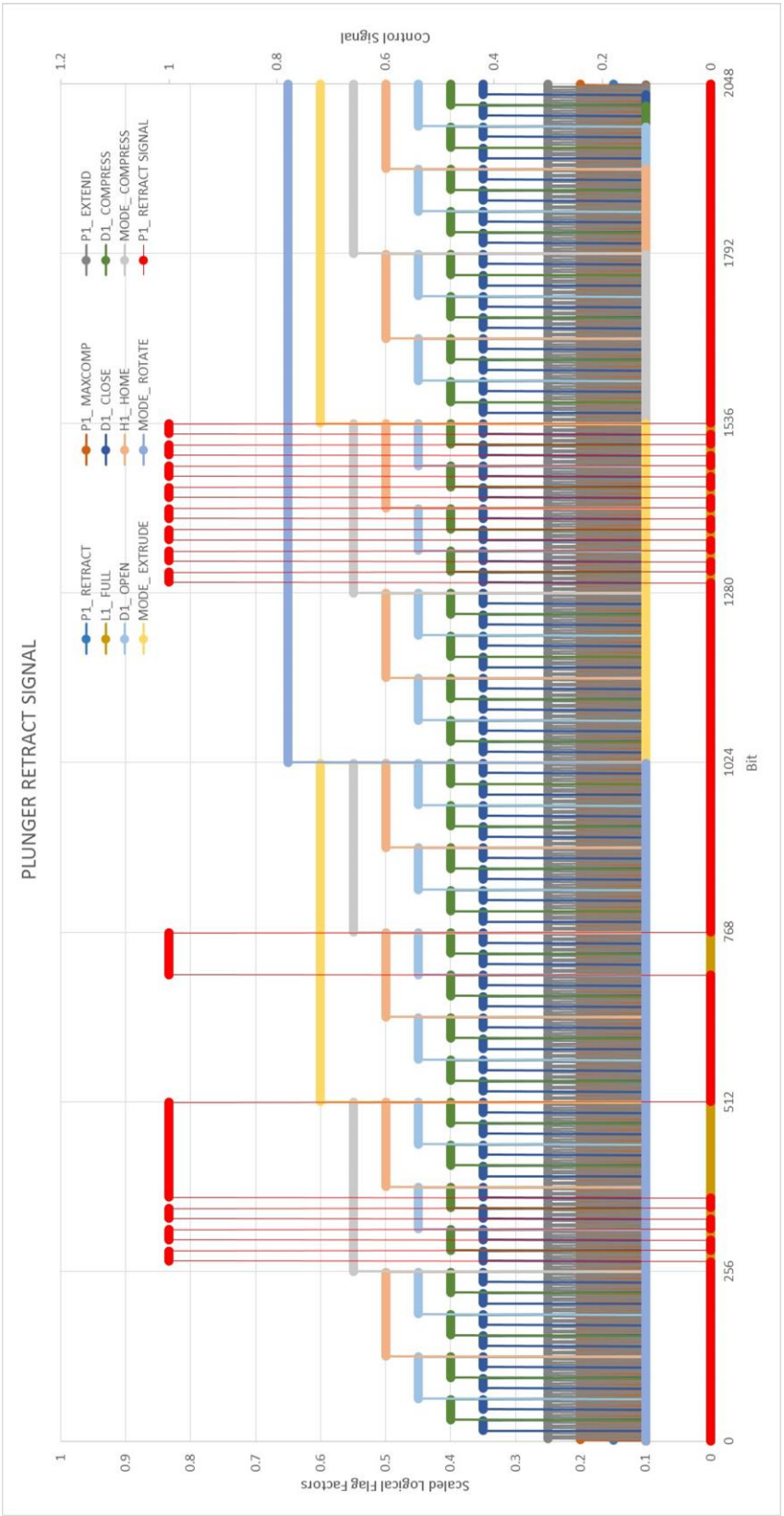

Figure A-3: Graphical overview of plunger retract control signal

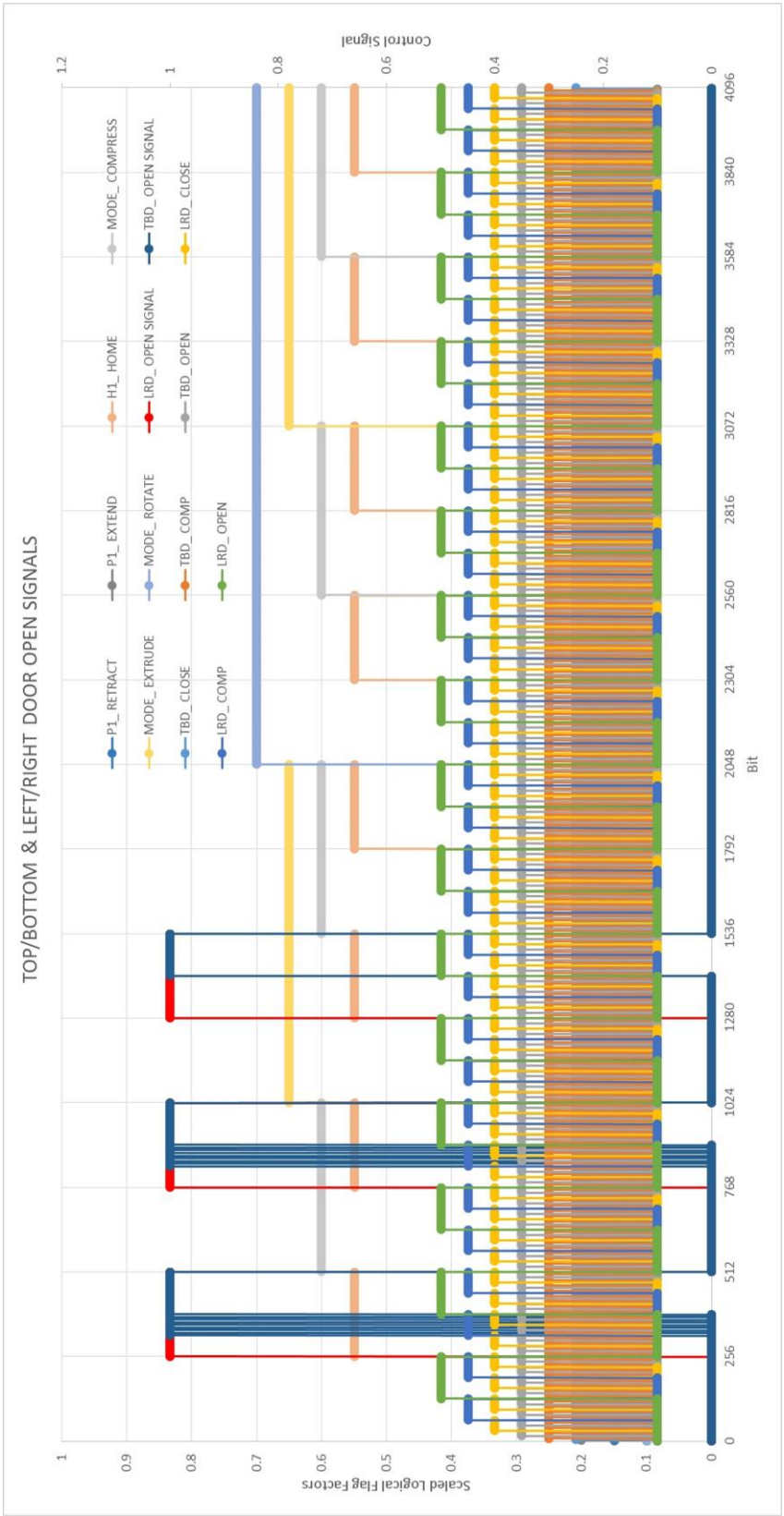

Figure A-4: Graphical overview of top/bottom and left/right door

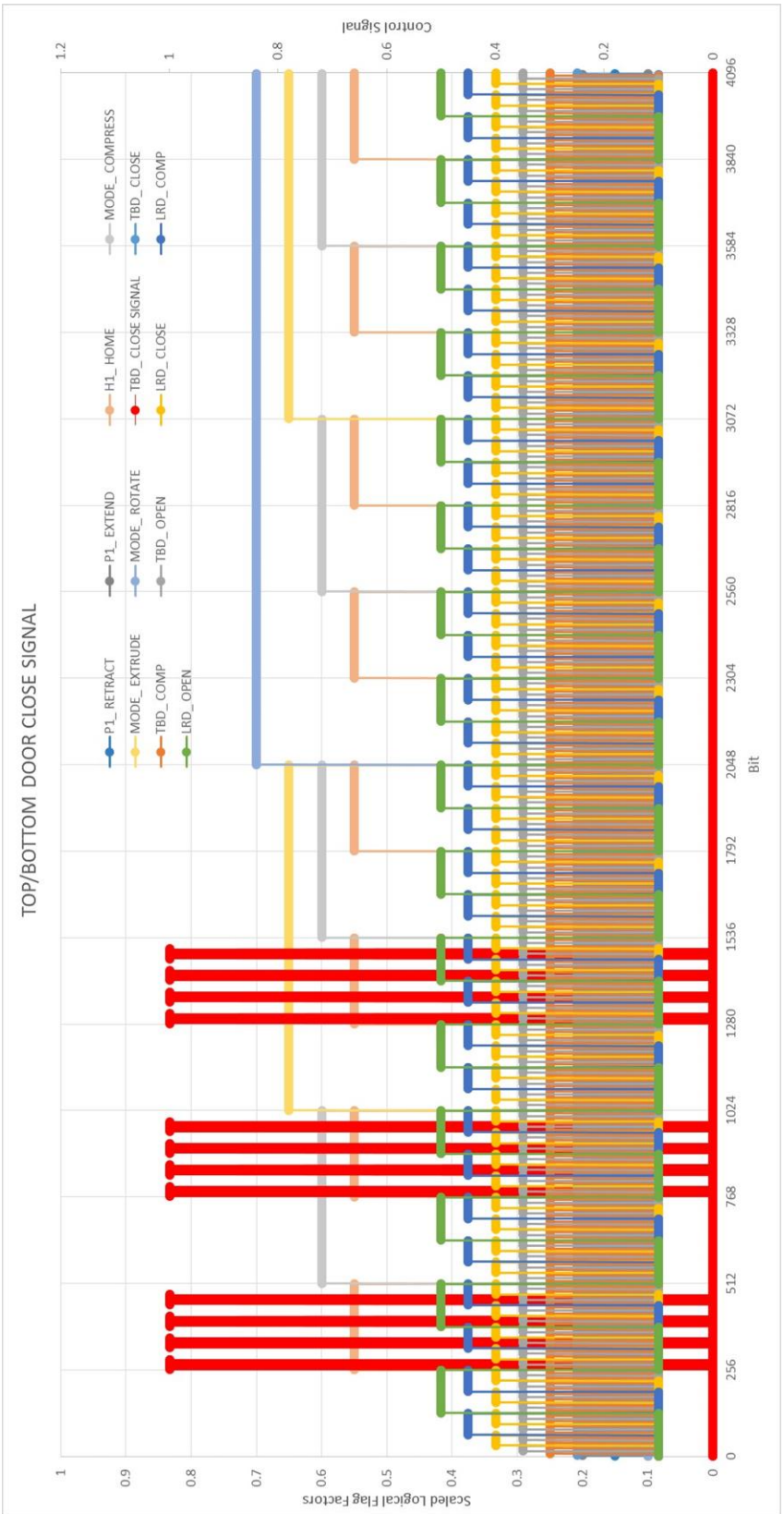

Figure A-5: Graphical overview of top and bottom door close control signals

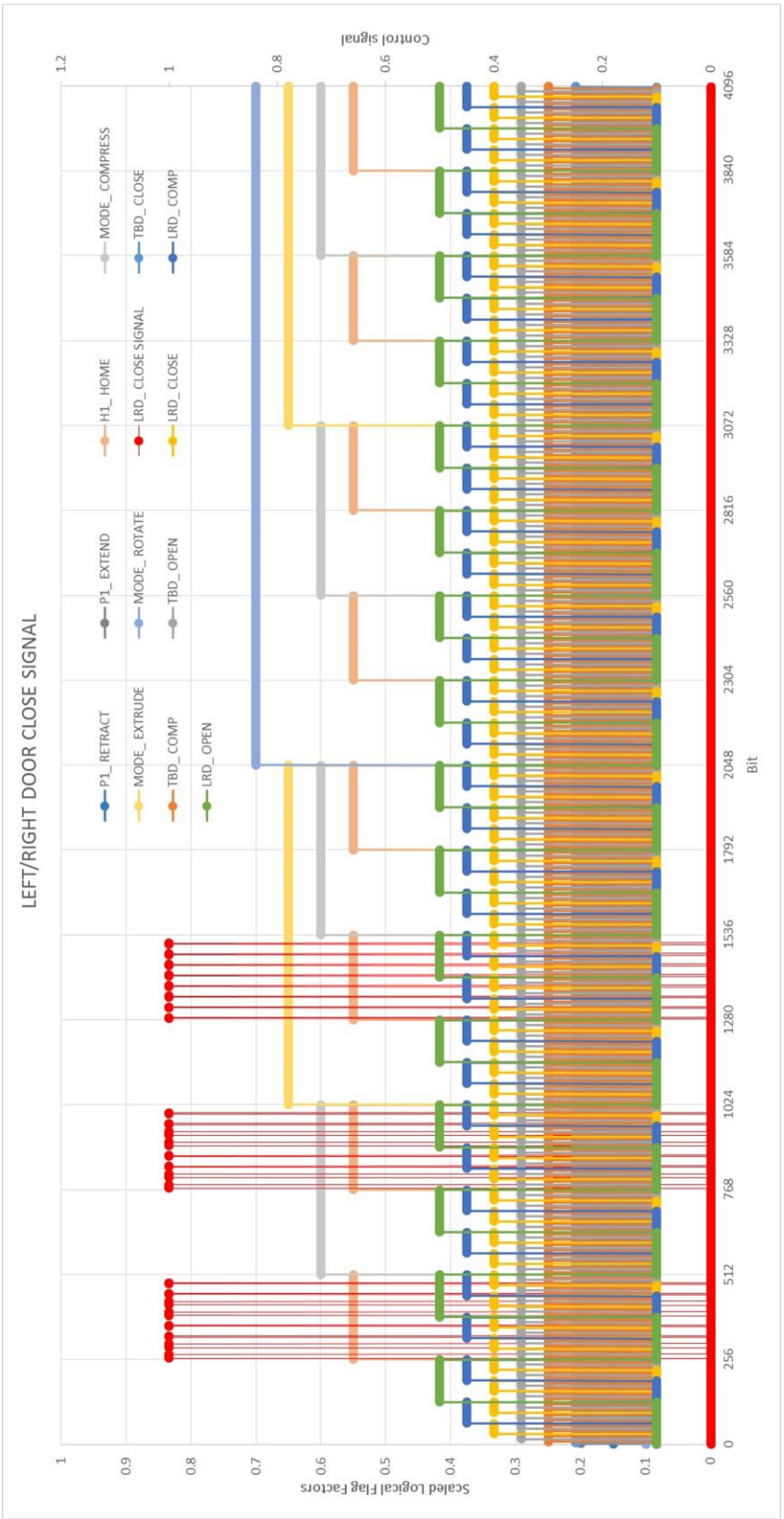

Figure A-6: Graphical overview of left and right door close control signals

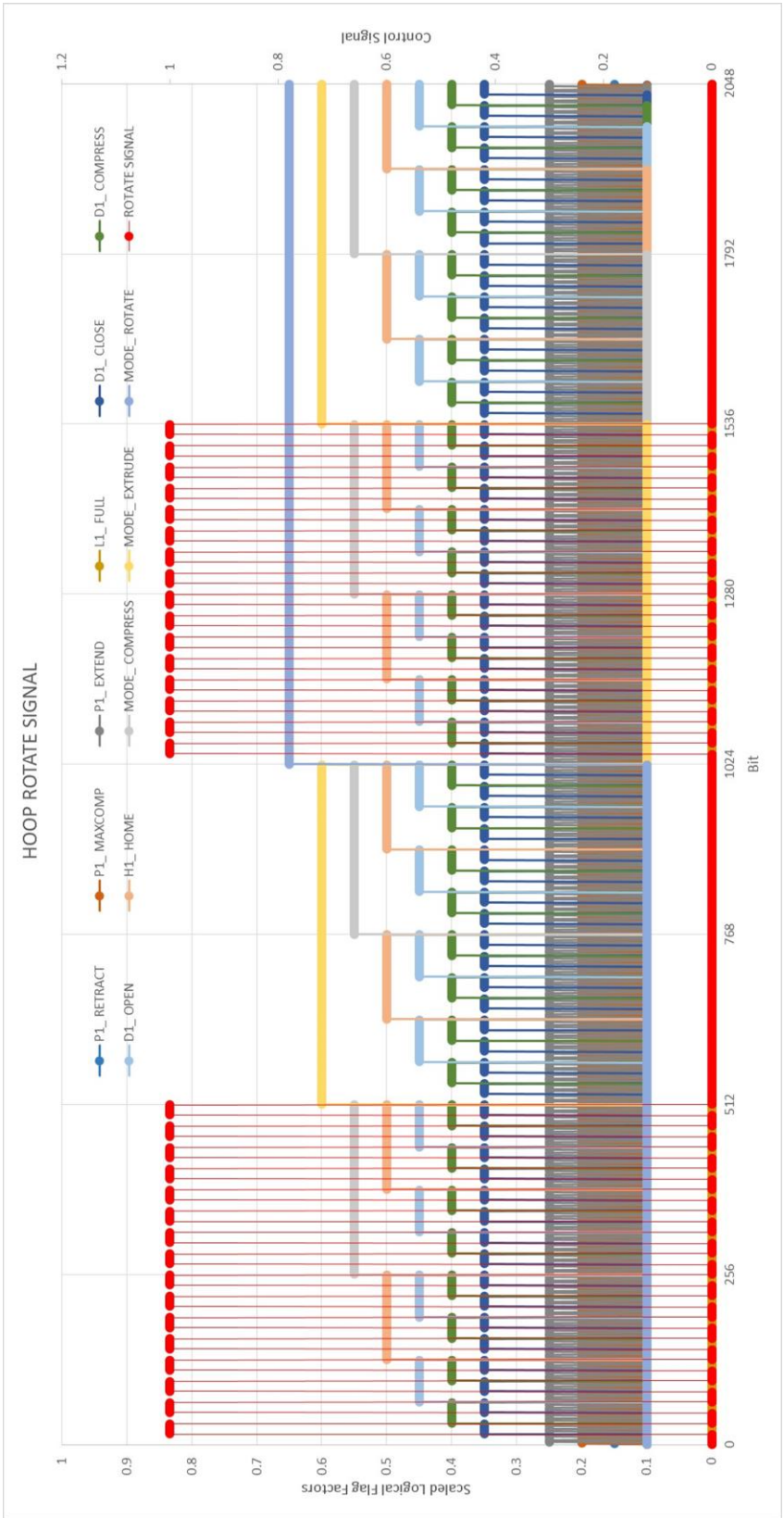

Figure A-7: Graphical overview packaging hoop rotation signal

REFERENCES

Afzalinia, S., & Roberge, M. 2008. Modeling of pressure distribution inside the compression chamber of a large square baler. Transactions of the ASABE, 51(4), 1143-1152.

Chevanan, N., Womac, A. R., Bitra, V. S., Igathinathane, C., Yang, Y. T., Miu, P. I., & Sokhansanj, S. 2010. Bulk density and compaction behavior of knife mill chopped switchgrass, wheat straw, and corn stover. Bioresource technology, 101(1), 207-214.

Glassner, D., Hettenhaus, J., & Schechinger, T. 1998, October. Corn stover collection project. In *BioEnergy'98—Expanding Bioenergy Partnerships: Proceedings* (Vol. 2, pp. 1100-1110).

Graham, R. L., Nelson, R., Sheehan, J., Perlack, R. D., & Wright, L. L. 2007. Current and potential US corn stover supplies. *Agronomy Journal*, *99*(1), 1-11.

Huggins, D. R., Karow, R. S., Collins, H. P., & Ransom, J. K. 2011. Introduction: evaluating long-term impacts of harvesting crop residues on soil quality. *Agronomy journal*, *103*(1), 230-233.

Karlen, D. L., Birrell, S. J., & Hess, J. R. 2011. A five-year assessment of corn stover harvest in central Iowa, USA. *Soil and Tillage Research*, *115*, 47-55.

Lizotte, P. L., & Savoie, P. 2011. Spring harvest of corn stover. *Applied Engineering in Agriculture*, *27*(5), 697.

Mani, S., Tabil, L. G., & Sokhansanj, S. 2004. Mechanical properties of corn stover grind. Transactions of the ASAE, 47(6), 1983-1990.

Morey, R. V., Kaliyan, N., Tiffany, D. G., & Schmidt, D. R. 2010. A Corn Stover Supply Logistics System.

National Agricultural Statistics Service. 2013. Crop Progress and Condition: Corn in Iowa, ' 2013. U.S. Department of Agriculture. Available at www.nass.usda.gov/Charts_ and_Maps/Crop_Progress_&_Condition/2013/IA_2013.pdf. Accessed 19 June 2014.

National Research Council (US). Committee on Economic and Environmental Impacts of Increasing Biofuels Production. 2011. *Renewable Fuel Standard: Potential Economic and Environmental Effects of US Biofuel Policy*. National Academies Press.

Perlack, R. D., & Turhollow, A. F. 2002. Assessment of options for the collection, handling, and transport of corn stover. *ORNL/TM-2002/44, Report to the US Department of Energy, Office of Energy Efficiency and Renewable Energy, Biomass Program, http://bioenergy. ornl. gov/pdfs/ornltm-200244. pdf(9 April 2010).*

Prewitt, R. M., Montross, M. D., Shearer, S. A., Stombaugh, T. S., Higgins, S. F., McNeill, S. G., & Sokhansanj, S. 2007. Corn stover availability and collection efficiency using typical hay equipment. *Transactions of the ASABE*,*50*(3), 705-711.

Shinners, K. J., Adsit, G. S., Binversie, B. N., Digman, M. F., Muck, R. E., & Weimer, P. J. 2007. Single-pass, split-stream harvest of corn grain and stover.*Trans. ASABE*, *50*(2), 355-363.

Shinners, K. J., Binversie, B. N., Muck, R. E., & Weimer, P. J. 2007. Comparison of wet and dry corn stover harvest and storage. *Biomass and Bioenergy*, *31*(4), 211-221.

Sokhansanj, S., & Turhollow, A. F. 2004. Biomass densification-cubing operations and costs for corn stover. *Applied Engineering in Agriculture*, *20*(4), 495-502.

Suh, K., & Suh, S. 2010. Economic and environmental implications of corn stover densification options for biofuel in Minnesota. *Transactions of the ASABE*, *53*(4), 1183-1192.

Suh, K., Suh, S., Walseth, B., Bae, J., & Barker, R. 2011. Optimal corn stover logistics for biofuel production: A case in Minnesota. *Transactions of the ASABE*, *54*(1), 229-238.

Sultana, A., & Kumar, A. 2011. Optimal configuration and combination of multiple lignocellulosic biomass feedstocks delivery to a biorefinery. *Bioresource technology*, *102*(21), 9947-9956.

Tyndall, J. C., Berg, E. J., & Colletti, J. P. 2011. Corn stover as a biofuel feedstock in Iowa's bio-economy: an Iowa farmer survey. *Biomass and bioenergy*, *35*(4), 1485-1495.

U.S. Department of Energy. 2013. U.S. Production, Consumption, and Trade of Ethanol. Energy Efficiency and Renewable Energy: Alternative Fuels Data Center. Available at www.afdc.energy.gov/data/10323. Accessed 19 June 2014.

U.S. Department of Energy. *US billion-ton update: biomass supply for a bioenergy and bioproducts industry*. Energy Efficiency and Renewable Energy: Office of the Biomass Program. Oak Ridge National Laboratory, 2011.

Webster, Keith. 2011. Single-pass corn stover harvest system productivity and cost analysis. MS thesis. Ames, Iowa: Iowa State University, Department of Ag Engineering.

Zhou, B., Ileleji, K. E., & Ejeta, G. 2008. Physical property relationships of bulk corn stover particles. Transactions of the ASABE, 51(2), 581-590.